
UNIVERSITÀ DEGLI STUDI DI PALERMO

Dottorato in Scienze Fisiche
Dipartimento di Fisica e Chimica – Emilio Segrè
Settore Scientifico Disciplinare FIS/03

# Non-Hermiticity in Quantum Physics

IL DOTTORE
**FEDERICO ROCCATI**

IL COORDINATORE
**Prof. GIUSEPPE LAZZARA**

IL TUTOR
**Prof. FRANCESCO CICCARELLO**

IL CO-TUTOR
**Prof. FABIO BAGARELLO**

CICLO XXXIV
ANNO CONSEGUIMENTO TITOLO – 2022

*To my friends*

*A grandi difetti corrispondono grandi margini di miglioramento*
M.C.

*Lc 5:5*

# List of Publications

This dissertation is based on the references highlighted with an asterisk.

1. F. Roccati, A. Purkayastha, G. M. Palma, F. Ciccarello "Quantum correlations in a generalised gain-loss system" (submitted)

2. F. Roccati, B. Militello, E. Fiordilino, R. Iaria, L. Burderi, T. Di Salvo, F. Ciccarello "Quantum correlations beyond entanglement in a classical channel model of gravity" (submitted)

3. F. Roccati, G. M. Palma, F. Bagarello, F. Ciccarello "Non-Hermiticity and master equations" (submitted)

4. *F. Roccati, S. Lorenzo, G. M. Palma, G. Calajò, A. Carollo, F. Ciccarello "Exotic interactions mediated by a non-Hermitian photonic bath" (submitted)

5. F. Roccati. "Non-Hermitian skin effect as an impurity problem". Phys. Rev. A 104, 022215 (2021)

6. *F. Roccati, S. Lorenzo, G. M. Palma, G. T. Landi, M. Brunelli, F. Ciccarello. "Quantum correlations in PT-symmetric systems". Quantum Science and Technology 6.2 (2021): 025005.

7. F. Bagarello, F. Gargano, and F. Roccati. "Modeling epidemics through ladder operators". Chaos, Solitons & Fractals 140, 110193

8. F. Bagarello, F. Gargano, and F. Roccati. "Some remarks on few recent results on the damped quantum harmonic oscillator". Annals of Physics 414, 168091

9. *F. Bagarello, F. Gargano, and F. Roccati. "Tridiagonality, supersymmetry and non self-adjoint Hamiltonians". Journal of Physics A: Mathematical and Theoretical 52.35 (2019): 355203.

10. *F. Bagarello, F. Gargano, and F. Roccati. "A no-go result for the quantum damped harmonic oscillator". Physics Letters A (2019)

# Abstract

The field of non-Hermitian Physics has attracted great attention over the last 23years, both from the in the physical and mathematical communities. From the physical point of view, non-Hermiticity was regarded as a phenomenological tool to describe open quantum systems. Besides this, the rising interest in this field comes especially from the possible exploitation of *exceptional points* for quantum technologies, and from the exotic topology arising in periodic non-Hermitian systems, connected to the so called *non-Hermitian skin effect*. From the mathematical point of view, the range of possible topics to investigate has been wide open, as dropping an hypothesis of a theory makes the mathematician wonder what keeps holding true and what is lost. This dissertation wishes to be a contribution to both lines of research. In the first part, after a minimal introduction, we mainly discuss exotic behaviors at the exceptional point of two very different but realistic quantum systems: a gain-loss open system and a waveguide QED setup. The second part is devoted to a more mathematical approach to non self-adjoint operators inpired by quantum mechanics: the problem of quantization of a dissipative system is considered, and the construction of a class of non self-adjoint Hamiltonians is developed.

# Contents

# Part I

# Non-Hermitian effects in quantum optics

# Chapter 1

# Introduction

In this chapter we discuss the minimal ingredients necessary to deal with non-Hermitian Hamiltonians from a physical standpoint. We introduce non-Hermiticity as a deviation from Hermitian Hamiltonians, highlighting what is lost (and what is gained!). We then discuss the role of $\mathcal{PT}$ symmetry in this field, the notion of exceptional points and present one implementation of $\mathcal{PT}$ symmetry in classical optics.

## 1.1 Hermiticity and non-Hermiticity in (quantum) physics

One of the postulates of quantum mechanics is that physical observables are described by self-adjoint[1] operators acting on the state space, i.e. a Hilbert space [1]. The reason is at least twofold:

($i$) measurements outcomes, i.e. the eigenvalues of an observable, must be real numbers and Hermiticity is a sufficient condition:

$$a \langle\psi|\psi\rangle = \langle\psi|\mathcal{A}\psi\rangle = \langle\mathcal{A}\psi|\psi\rangle = a^* \langle\psi|\psi\rangle \tag{1.1}$$

where $\mathcal{A} = \mathcal{A}^\dagger$ is an observable, satisfying the eigenequation $\mathcal{A}|\psi\rangle = a|\psi\rangle$

($ii$) the eigentates corresponding to different measurement outcomes are distinguishable, i.e. orthogonal, and form a complete set:

$$a_2 \langle\psi_1|\psi_2\rangle = \langle\psi_1|\mathcal{A}\psi_2\rangle = \langle\mathcal{A}\psi_1|\psi_2\rangle = a_1 \langle\psi_1|\psi_2\rangle \Rightarrow \langle\psi_1|\psi_2\rangle = 0 \tag{1.2}$$

and

$$\mathbb{1} = \sum_n \frac{|\psi_n\rangle\langle\psi_n|}{\langle\psi_n|\psi_n\rangle} \tag{1.3}$$

where $a_1 \neq a_2$ and $\mathcal{A}|\psi_n\rangle = a_n|\psi_n\rangle$.

When applied to the Hamiltonian operator $H$, the requirement of Hermiticity combined with the Schrödinger equation imply that the *full* evolution must be unitary. This, in particular, results in the conservation of the wavefunction norm [1]:

$$|\langle\psi_t|\psi_t\rangle|^2 = |\langle\psi_0| U^\dagger U |\psi_0\rangle|^2 = |\langle\psi_0|\psi_0\rangle|^2 \tag{1.4}$$

where $|\psi_0\rangle$ is the initial state and $U = e^{-iHt}$ is the evolution operator for a time independent Hamiltonian $H$ ($\hbar = 1$ throughout). Therefore, *Hermiticity* (of the Hamiltonian at least) appears a key assumption to describe *closed* quantum systems.

[1] In most physical contexts one usually uses the term *Hermitian*, having in mind the matrix representation of the operator. As it will not make any substantial difference, we will loosely use the terms *self-adjoint* and *Hermitian* interchangeably, despite these two concepts are not mathematically equivalent.

However, no realistic physical system can be isolated from its external environment. This is even more compelling for quantum systems, as the act of measurement itself (i.e. the interaction with an element of the environment) projects the state of the system onto an (or superposition of) eigenstate(s) of the measured observable corresponding to the measurement outcome. Being a projection, the act of measurement cannot be a unitary operation and therefore does not conserve probability. It is thus natural to wonder whether, dropping the assumption of Hermiticity, it is possible to describe, at least *effectively*, the dynamics of *open* quantum systems [2,3].

This question is a possible way of introducing the field of *non-Hermitian (quantum) physics*, a research area that has attracted great attention per se, beyond the initial motivations [4–6].

The topic of non-Hermitian physics can be tackled from two different perspectives: on the one hand, non-Hermiticity can be regarded as an *effective* description of an open system, which nonetheless shows interesting intrinsic features (e.g. appearance of exceptional points [7,8], non-Hermitian skin effect [4], etc.), under the constraint that the full microscopic Hamiltonian is always Hermitian. On the other hand, a more mathematically-oriented research line, which was triggered by the idea that Hermiticity could be replaced by a symmetry assumption ($\mathcal{PT}$ symmetry [9]), is assuming that the *full* Hamiltonian of the system is generally non-Hermitian and on this basis either constructing the formalism of *bi-orthogonal* quantum mechanics [10], or trying to somehow redefine the Hilbert space so that the Hamiltonian becomes Hermitian[2] [11], or finally investigating the mathematical framework of non self-adjoint physically-inspired operators [12].

In this first part of the thesis we will focus on the first, more physical, approach. the second part is devoted to some topics regarding mathematical properties of non self-adjoint operators inspired by quantum mechanics. Before discussing the relation between the Lindblad master equation approach and non-Hermitian Hamiltonians for the description of open (Markovian) quantum dynamics (Sec. 3), we present in the next section the role of $\mathcal{PT}$ symmetry as this was a starting point of this literature and most importantly because a variety of platforms (especially in optics) implementing $\mathcal{PT}$ symmetry have been experimentally realized. Extensive review papers fully dedicated to non-Hermitian physics recently appeared such as Refs. [4–6], to which we refer the interested reader.

## 1.2 Non-Hermiticity, $\mathcal{PT}$ symmetry and Exceptional Points

The recent history of non-Hermitian physics starts from the observation that some physically-inspired *Hamiltonians* display real spectra of eigenvalues despite being non-Hermitian[3]. The prototypical example is the non-Hermitian Hamiltonian initially proposed by Bender [9]

$$H = p^2 - (ix)^N. \tag{1.5}$$

This *Hamiltonian* has a discrete and positive spectrum for $N \geq 2$, see Fig. 1.1, and for $N > 2$ is not self-adjoint[4]. This property, first supported numerically and then proved mathematically [13], suggested the idea that occurrence of a real spectrum is related to the invariance of $H$ in Eq. (1.5) under both *parity* $\mathcal{P}$ and *time reversal* $\mathcal{T}$, as represented by the equation $[H, \mathcal{PT}] = 0$.

Operators satisfying this property are called $\mathcal{PT}$-symmetric. Note that the explicit form of $\mathcal{P}$ and $\mathcal{T}$ depends on the specific model: e.g., for a continuous case as in Eq. (1.5) they are defined as $\mathcal{P} : \{p, x\} \to \{-p, -x\}$ and $\mathcal{T} : i \to -i$.

[2] The concept of Hermiticity relies on the chosen inner product in the Hilbert space, which is of course not unique.

[3] It worth recalling that Hermiticity is only a sufficient condition for the spectrum to be real.

[4] Except for even $N$.

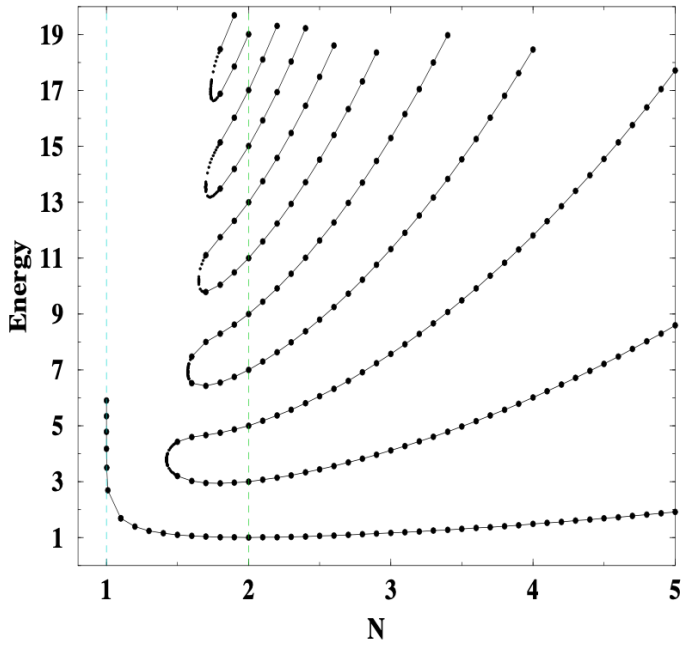


Figure 1.1: Spectrum of $H$ in Eq. (1.5) as a function of $N$. If $N \geq 2$ it is purely real, while purely complex for $N \leq 1$ [9]. Reprinted by permission from the American Physical Society: Physical Review Letters [9], license number RNP/21/NOV/047110 (1998).

Let us observe that, contrarily to what one is usually accustomed to in (Hermitian) quantum mechanics, the commutation relation $[H, \mathcal{PT}] = 0$ does not imply that $H$ and $\mathcal{PT}$ have a common basis of eigenstates. Indeed this holds true if both commuting operators are Hermitian which is not the case here since $\mathcal{PT}$ is anti-Hermitian [1].

This points to the existence of two distinct $\mathcal{PT}$-symmetric phases: an *unbroken* phase when $H$ and $\mathcal{PT}$ do possess a common basis of eigenstates, and a *broken* $\mathcal{PT}$-symmetric phase when they do not [14].

A typical *discrete* realization of $\mathcal{PT}$-symmetric Hamiltonians are *gain-loss* systems, which we will discuss later in more details, especially because it is the scenario where $\mathcal{PT}$-symmetry breaking (from unbroken to broken) through the so called *exceptional point* has been observed in classical optics [15].

### 1.2.1 Gain-loss systems

We report next a very general (apparently unrelated) discussion based on [16] in order to pedagogically introduce the topic. Consider two boxes whose contents (e.g., energy, matter, etc.) are labeled by continuous (generally complex) variables $G$ and $L$. Suppose these two boxes are exchanging their content at rate $g$ and that the $G$ box is continuously filled (*gain*) from the outside with rate $\gamma$, while $L$ is leaking (*loss*) into the environment at the same rate $\gamma$, see Fig. 1.2.

As gain and loss rate are balanced (same rates), this ideal system is indeed $\mathcal{PT}$-symmetric: exchanging $G$ and $L$ (parity) and reversing the arrows in Fig. 1.2 (time reversal) leaves the entire system invariant.

If we want to quantitatively describe the dynamics of such a system, one way is to write the dynamical equations for $G$ and $L$: $\dot{G} = \gamma G - igL$ and $\dot{L} = -\gamma L - igG$ (the $\pi/2$ phase in the coupling is not necessary, but we keep it for the sake of argument). These equations can be cast into a *Schrödinger-like* equation $i\dot{\psi} = \mathcal{H}\psi$ where $\psi = (G, L)^T$ and

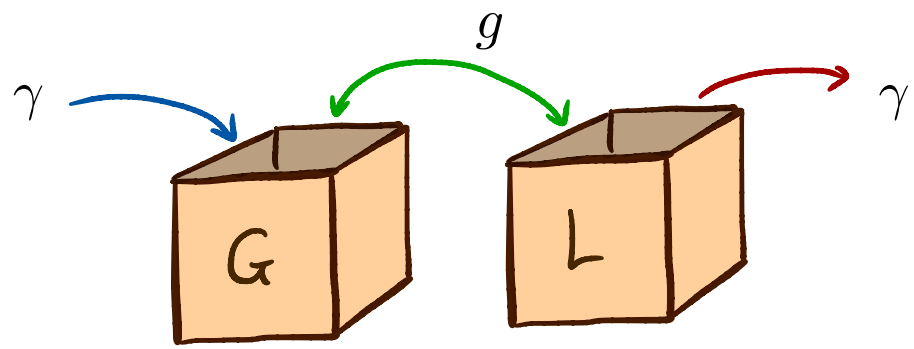


Figure 1.2: Sketch of a general gain-loss system.

the *Hamiltonian* reads

$$\mathcal{H} = \begin{pmatrix} i\gamma & g \\ g & -i\gamma \end{pmatrix}. \tag{1.6}$$

$\mathcal{PT}$ symmetry is then more manifest as

$$\mathcal{P} = \begin{pmatrix} 0 & 1 \\ 1 & 0 \end{pmatrix} \tag{1.7}$$

and $\mathcal{T}$ is complex conjugation, hence $[\mathcal{H}, \mathcal{PT}] = 0$.

The vector $\psi$ is not a state of a quantum system, nevertheless the analogy with the Schrödinger equation is not fully out of context. Indeed, as for any system of coupled differential equations, the solution can be written[5] as $\psi_t = \sum_{j=\pm} c_j \varphi_j e^{-i\lambda_j t}$, where $\varphi_j$ are eigenvectors of $\mathcal{H}$ corresponding to the eigenvalues $\lambda_j$, and $c_j$ are coefficients.

As for the Bender's Hamiltonian in Eq. (1.5), one can either suppose that a Schrödinger equation $i\dot{\psi} = \mathcal{H}\psi$ with $\mathcal{H}$ as in Eq. (1.6) makes sense in some suitably defined Hilbert space, or that $\mathcal{H}$ is an *effective* Hamiltonian.

Let us now examine the eigenvectors and eigenvalues of $\mathcal{H}$. Its eigenvalues are $\lambda_\pm = \pm\sqrt{g^2 - \gamma^2}$ with corresponding eigenvectors

$$\varphi_\pm = \begin{pmatrix} i\gamma + \lambda_\pm \\ g \end{pmatrix}. \tag{1.8}$$

A few observations are in order:

- we can consider the parameter $\gamma$ as the degree of non-Hermiticity since $H$ is Hermitian if and only if $\gamma = 0$,
- for any non-zero $\gamma$ the eigenstates are not orthogonal[6],
- for $\gamma < g$ ($\gamma > g$) eigenvalues are real (imaginary) and $\mathcal{PT}$ symmetry is unbroken (broken). Indeed if $\gamma < g$ the eigenstates $\varphi_\pm$ are eigenstates of both $\mathcal{H}$ and $\mathcal{PT}$, while if $\gamma > g$ they are eigenstates only of $H$.

### 1.2.2 Exceptional points

The critical value $\gamma = g$ found previously deserves special attention. At this point, not only the eigenvalues are degenerate (as it can occur for Hermitian operators), but even the eigenvectors are *coincident* ("coalesce").

This point of non-Hermitian degeneracy is called an *exceptional point* (EP): at an EP of order $n$ (in the case of Eq. (1.6) we have $n = 2$), $n$ eigenvalues *together with the*

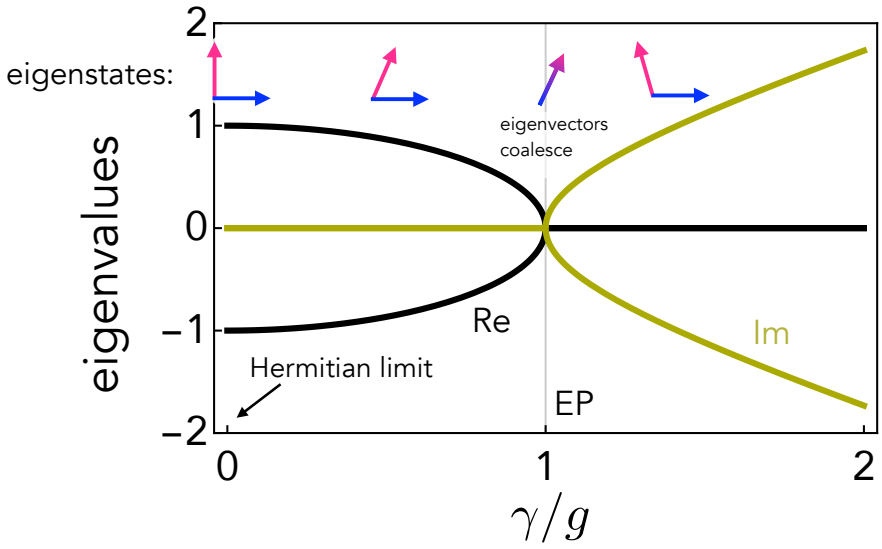


Figure 1.3: Spectrum of $\mathcal{H}$ in Eq. (1.6) as a function of $\gamma/g$. Eigenvalues are real (imaginary) in $\mathcal{PT}$ unbroken (broken) phase $\gamma < g$ ($\gamma > g$), and coincide at EP. Eigenvectors are pictorially represented so as to highlight their orthogonality in the Hermitian limit and coalescence at the EP.

*corresponding eigenstates* coalesce [14,17,18]. Most remarkably, this entails that at an EP the Hamiltonian becomes defective (diagonalizability is lost), that is its eigenstates do *not* span the entire Hilbert space (the identity is not resolved).

Exceptional points and the corresponding $\mathcal{PT}$ symmetry breaking transition received great attention in recent years, and one of the main current interests in this field is the potential exploitation of critical behaviors near EPs in quantum systems. For instance: enhancing mode splitting between counter-propagating whispering gallery modes in nanophotonics [8], EP-based sensors [19], and critical behavior of quantum correlations near EPs [20].

We want to stress that EPs are *not* a prerogative of $\mathcal{PT}$ symmetry as they can appear for general non-Hermitian operators. A simple example is the case that our two boxes are not subject to gain or loss, yet the coupling is non-reciprocal:

$$\mathcal{H}' = \begin{pmatrix} 0 & g_1 \\ g_2 & 0 \end{pmatrix}. \tag{1.9}$$

with $g_2 \neq g_1^*$. At $g_2 = 0$, the eigenvalues and eigenvectors coalesce despite $[\mathcal{H}', \mathcal{PT}] \neq 0$.

Finally we want to mention that, even in $\mathcal{PT}$-symmetric systems, there can appear EPs that are not associated with $\mathcal{PT}$ symmetry breaking transition [21].

### 1.2.3 An optical implementation of $\mathcal{PT}$ symmetry

One of the first implementations of $\mathcal{PT}$ symmetry was realized in classical optics [15], as briefly described next. The starting observation is the paraxial equation of diffraction

$$i\frac{\partial E}{\partial z} + \frac{1}{2k}\frac{\partial^2 E}{\partial x^2} + k_0[n_R(x) + in_I(x)]E = 0, \tag{1.10}$$

describing the propagation along the $z$ direction of the electric field envelope $E$ of an optical beam.

[5] Provided that $\mathcal{H}$ is diagonalizable
[6] With respect to the standard inner product in $\mathbb{C}^2$.

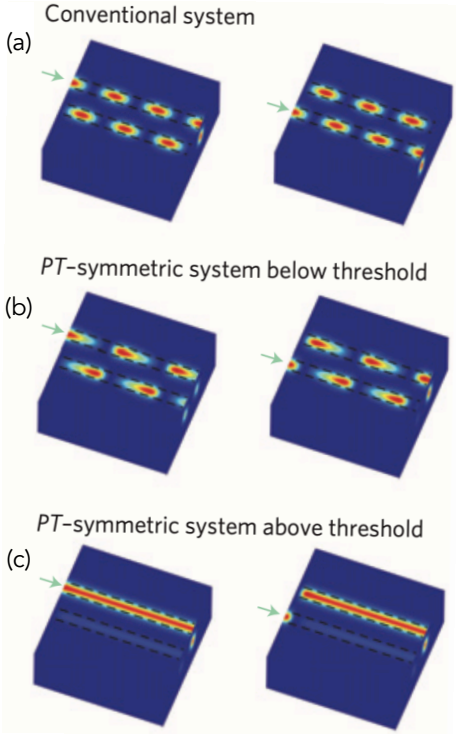


Figure 1.4: Propagation of light in coupled waveguides following Eq. (1.11). Left (Right): input in waveguide 1 (2). (a): Hermitian limit $\gamma = 0$. (b): Unbroken $\mathcal{PT}$ symmetry $\gamma < g$. (c): Broken $\mathcal{PT}$ symmetry $\gamma > g$ [15]. Adapted by permission from Springer Nature Customer Service Centre GmbH: Springer Nature, Nature Physics [15], license number 5198080479690 (2010).

This can be regarded as an effective Schrödinger equation with a complex potential. Here $k_0$ ($k$) is the wave number in the vacuum (substrate), the $x$ direction is transversal to $z$ and $n_{R/I}(x)$ are the real/imaginary part of the refracting index, playing the role of an optical potential.

By judiciously setting them so that $n_R(x)$ is even and $n_I(x)$ is odd, Eq. (1.10) has the form of a Schrödinger equation with a $\mathcal{PT}$-symmetric potential, in the spirit of Bender's Hamiltonian (1.5).

Furthermore, under these assumptions, by using the coupled-mode approach [15], the propagation of the electric field envelopes $E_1$ and $E_2$ in two coupled waveguides, the first being optically pumped (gain), the second experiencing the same amount of loss, is given by

$$i\frac{d}{dz}\begin{pmatrix} E_1 \\ E_2 \end{pmatrix} = \begin{pmatrix} i\gamma & g \\ g & -i\gamma \end{pmatrix}\begin{pmatrix} E_1 \\ E_2 \end{pmatrix}. \tag{1.11}$$

This implements a gain-loss system, Eq. (1.6) with all the properties outlined earlier. The $\mathcal{PT}$-symmetric transition at the EP has been experimentally observed as light propagation strongly depends on the $\mathcal{PT}$ phase, unbroken or broken. In the former, the optical wave propagates jumping back and forth between the waveguides somewhat in a Hermitian-like fashion. In the latter, only light injected in the pumped channel survives irrespective of the initial input, see Fig. 1.4.

### 1.2.4 Passive - $\mathcal{PT}$ symmetry

The *Hamiltonian* of a balanced gain-loss system is probably the most typical way of introducing $\mathcal{PT}$ symmetry breaking at EPs. However, implementing such a system

can raise some issues. On the one hand, a gain like the one previously considered is an approximation holding up to not too long times (to avoid insurgence of non-linearities) [22]. On the other hand it is nonsensical when working ab initio with nonlinear systems (such as a two-level atom).

However, most of the above phenomena (appearance of EPs, different dynamical behaviors below and above EP, etc.) still hold true in fully dissipative systems (no gain whatsoever), for instance when one introduces *non-uniform* losses.

As an instance, consider again a pair of coupled waveguides under the coupled-mode approach. If they experience a different amount of loss then the *Hamiltonian* reads

$$\mathcal{H} = \begin{pmatrix} -i\gamma_1 & g \\ g & -i\gamma_2 \end{pmatrix}. \tag{1.12}$$

The corresponding spectrum and eigenstates are

$$\lambda_\pm = -i\Gamma_+ \pm \sqrt{g^2 - \Gamma_-^2}\,, \qquad \varphi_\pm = \begin{pmatrix} \lambda_\pm + i\gamma_2 \\ g \end{pmatrix} \tag{1.13}$$

where $2\Gamma_\pm = \gamma_2 \pm \gamma_1$.

Despite losing $\mathcal{PT}$ symmetry ($[\mathcal{H}, \mathcal{PT}] \neq 0$), there still is an EP at $\Gamma_- = g$ separating two dynamical dissipative phases, an *underdamped* one ($\Gamma_- < g$) and an *overdamped* one ($\Gamma_- > g$).

The connection with $\mathcal{PT}$ symmetry is manifest once we notice that by making a complex global shift on the balanced gain-loss Hamintonian $\mathcal{H}$ in Eq. (1.6)

$$\mathcal{H} \to \mathcal{H} - i\gamma\mathbb{1} = \begin{pmatrix} 0 & g \\ g & -2i\gamma \end{pmatrix} \tag{1.14}$$

one gets a passive-$\mathcal{PT}$-symmetric Hamiltonian with only one local loss and no gain. This operation shifts the spectrum to the lower half of complex plane, without altering the eigenvectors. Therefore, the key point of these so called *passive-$\mathcal{PT}$-symmetric* systems [23] is that we have $\mathrm{Im}(\lambda_\pm^p) \leq 0$ avoiding any amplification process, but still inheriting features of $\mathcal{PT}$-symmetric systems [24].

# Chapter 2

# Open quantum systems and non-Hermiticity

In this chapter we describe the connection between the treatments of open quantum systems through a Markovian master equation and through a non-Hermitian Hamiltonian. First, we introduce the standard tool of Lindblad master equation for open Markovian quantum dynamics. In particular this is connected to non-Hermitian effective Hamiltonians, and how they arise, specifically from a mean-field approach.

## 2.1 Open Markovian quantum dynamics

The evolution of closed quantum systems is governed by the Schrödinger equation

$$i\frac{\mathrm{d}}{\mathrm{d}t}\left|\Psi_t\right\rangle = H\left|\Psi_t\right\rangle \ , \tag{2.1}$$

where $|\Psi_t\rangle$ is the state of the whole system at time $t$ living in the total Hilbert space $\mathcal{H}$, and $H$ is the (Hermitian) Hamiltonian of the full system acting on $\mathcal{H}$.

By *open* quantum system, we mean one that is interacting with an *environment* so that the full dynamics of system and environment is unitary [25]. This separation of system $S$ and environment $E$ corresponds to a bipartition of the Hibert space, $\mathcal{H} = \mathcal{H}_S \otimes \mathcal{H}_E$, with $\mathcal{H}_S$ ($\mathcal{H}_E$) the system's (environment's) Hilbert space.

When dealing with composite systems, the description of physical states through *kets* (or wave functions) as in Eq. (2.1) is no longer complete. Indeed, just to make an example, if $\psi(x_1, x_2)$ is the wave function of two particles, there is no way to infer from it a well-defined wavefunction of the first particle only [26] (unless the joint state is factorized).

The most general description of physical states is indeed through *density operators* instead of kets, allowing in particular an appropriate description of *subsystems* [27]. More concretely, if $|\Psi_t\rangle$ is the state of $S+E$ at time $t$, then the corresponding density operator is given by $\rho_t = |\Psi_t\rangle\langle\Psi_t|$ and the ones representing $S$ and $E$ are obtained by tracing out $E$ and $S$ as $\rho_{S(E)} = \mathrm{Tr}_{E(S)}\,\rho$, respectively.

In the language of density operators, the Schrödinger equation turns into the *von Neumann equation*

$$\dot{\rho}_t = -i[H, \rho_t]. \tag{2.2}$$

Although containing the same amount of information as Eq. (2.1) for the full $S+E$ dynamics, the density-matrix formalism allows to (at least formally) write the reduced dynamical equation for the system (or environment) only, that is

$$\dot{\rho}_S = -i\,\mathrm{Tr}_E[H, \rho_t]. \tag{2.3}$$

At this level, this equation is not closed in $\rho_S$ (i.e., it is not a so called master equation). However, under the assumptions that

(*i*) $\rho_t \approx \rho_S(t) \otimes \rho_E$, i.e. the *Born approximation*,

(*ii*) the time scale over which the state of the system varies appreciably is large compared to the time scale over which the environment correlation functions decay (*Markov approximation*),

(*iii*) the *rotating-wave approximation* for system-environment interaction holds,

the master equation for $S$ can be written as [25]

$$\dot{\rho}_S = -i[H_S, \rho_S] + \mathcal{D}(\rho_S) \tag{2.4}$$

where $H_S$ is the free Hamiltonian of the system and the *dissipator* reads

$$\mathcal{D}(\rho_S) = \sum_i \Gamma_i \left( \hat{L}_i \rho_S \hat{L}_i^\dagger - \frac{1}{2}\{\hat{L}_i^\dagger \hat{L}_i, \rho_S\} \right) \tag{2.5}$$

where $\{\hat{L}_i\}$ are the so called *jump* operators acting on $\mathcal{H}_S$ and the rates $\{\Gamma_i\}$ are positive.

Equation (2.4) is called GKSL (Gorini -Kossakowski-Sudarshan-Lindblad) or simply *Lindblad master equation* and describes the dynamics of an open quantum system interacting with an environment, under the previously discussed assumptions. A large variety of physical systems are well-described by such an equation.

In the following, we will discuss some paradigmatic instances showing the connection between the previously discussed non-Hermitian physics with the Lindblad master equation.

## 2.2 Atom decay: Lindblad versus non-Hermitian approach

A minimal model for atomic decay is that of a two-level system (the atom) interacting with a zero temperature thermal reservoir [25]. The two-level approximation works in every situation where only the transition between two levels is significant and all others can be neglected.

We call these two levels $|g\rangle$ and $|e\rangle$ standing for *ground* and *excited* state, respectively, whose respective energies are $\omega_g = 0$ and $\omega_e$. The free Hamiltonian of the atom thus reads $H_S = \omega_e |e\rangle\langle e|$. In order to study atomic decay we will consider $|e\rangle$ as the initial state of the system.

### 2.2.1 Decay of a two-level system: master equation description

First, we describe atomic decay through the Lindblad master equation as in [25, 28]. Coupling the atom to the quantized radiation field through the electric-dipole approximation and rotating-wave approximation, and assuming the field to be in a zero temperature thermal state (vacuum), the master equation (2.4) in this case reads

$$\dot{\rho} = -i[H_S, \rho] + \Gamma \left( \sigma_- \rho \sigma_+ - \frac{1}{2}\{\sigma_+ \sigma_-, \rho\} \right) \tag{2.6}$$

where $\rho$ is the state of the two-level system, $\sigma_- = |g\rangle\langle e|$ is the jump operator, $\sigma_+ = \sigma_-^\dagger$ and $\Gamma > 0$.

In the $\{|e\rangle, |g\rangle\}$ basis the state is represented by

$$\rho = \begin{pmatrix} \rho_{ee} & \rho_{eg} \\ \rho_{ge} & \rho_{gg} \end{pmatrix}, \tag{2.7}$$

where $\rho_{ij} = \langle i|\,\rho\,|j\rangle$, $\rho_{ee(gg)}$ is the *population* of the excited (ground) state and $\rho_{eg,ge}$ are the *coherences*. The solution of Eq. (2.6) is then

$$\rho_t = \begin{pmatrix} e^{-\Gamma t} & 0 \\ 0 & 1-e^{-\Gamma t} \end{pmatrix} \tag{2.8}$$

and correctly captures the fact that, starting from the excited state, population is irreversibly transferred to the ground state: $\rho_0 = |e\rangle\langle e| \to \rho_\infty = |g\rangle\langle g|$. Accordingly, the probability of finding the system in the excited (ground) state exponentially approaches 0 (1), see Fig. 2.1.

### 2.2.2 Decay of a two-level system: non-Hermitian description

A second more phenomenological approach to the instability of a state, which is typical in non-Hermitian physics (see e.g. Ref. [1]) can be formulated as follows.

One can solve the Schrödinger equation corresponding to the free atomic Hamiltonian $H_S = \omega_e|e\rangle\langle e|$ getting $|\psi_t\rangle = e^{-i\omega_e t}\,|e\rangle$ and then introduce an *ad hoc* complex shift through the replacement $\omega_e \to \omega_e - i\Gamma/2$ so that $p_e = |\langle\psi_t|e\rangle|^2 = e^{-\Gamma t}$. This shift can of course be made at the Hamiltonian level $H_S \to (\omega_e - i\Gamma/2)\,|e\rangle\langle e|$, so as to introduce a non-Hermitian Hamiltonian from the beginning.

Such approach correctly reproduces the probability $p_e$ of finding the two-level system in the excited state, however note that $p_g = |\langle\psi_t|g\rangle|^2 = 0$ at any time $t$. This highlights how the non-Hermitian description is only an *effective* one, compared to the Lindblad master equation. The latter indeed is a completely positive trace-preserving dynamics, while the former is not, as witnessed in particular by the non-conservation of the norm $|\langle\psi_t|\psi_t\rangle|^2 = e^{-\Gamma t}$. Note that the Lindblad master equation (2.6) correctly predicts that when the excited-state probability decays the ground-state population grows accordingly. The latter effect is instead absent in the non-Hermitian Hamiltonian description which only predicts excited-state decay, without ground-state population growth, see Fig. 2.1.

### 2.2.3 Connection between master equation and non-Hermitian approach

The general connection between the two approaches can be made more transparent by rearranging terms in the Linblad master equation (2.4) (subscript $S$ is omitted) as

$$\begin{aligned} \dot\rho &= -i[H,\rho] + \sum_i \Gamma_i \left(\hat L_i \rho \hat L_i^\dagger - \frac{1}{2}\{\hat L_i^\dagger \hat L_i, \rho\}\right) \\ &= -i\left(H_{\rm eff}\,\rho - \rho H_{\rm eff}^\dagger\right) + \sum_i \Gamma_i \hat L_i \rho \hat L_i^\dagger\,. \end{aligned} \tag{2.9}$$

Here,

$$H_{\rm eff} = H - \frac{i}{2}\sum_i \Gamma_i \hat L_i^\dagger \hat L_i \tag{2.10}$$

is the effective non-Hermitian Hamiltonian. Dropping *quantum jumps* [last sum in Eq. (2.9)] one gets

$$\dot\rho = -i\left(H_{\rm eff}\rho - \rho H_{\rm eff}^\dagger\right) \tag{2.11}$$

which is equivalent to working with a non-Hermitian Hamiltonian from the beginning [6]. Observe that, being $H_{\rm eff}$ non-Hermitian, Eq. (2.1) implies $\frac{\rm d}{{\rm d}t}\langle\Psi_t| = iH_{\rm eff}^\dagger\langle\Psi_t|$ so that Eq. (2.11) follows.

Of course discarding quantum jumps is as phenomenological as introducing a complex shift in the energy, and it can be regarded as a *semiclassical limit* of the full quantum

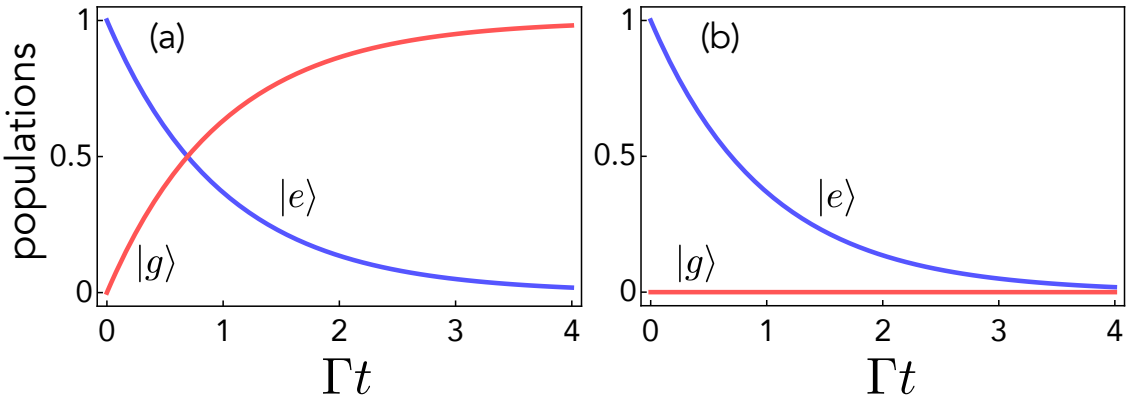


Figure 2.1: Populations of excited and ground state of a two-level system according to the Lindbladian (a) and the phenomenological non-Hermitian description (b).

dynamics [29]. Furthermore, the non-Hermitian Hamiltonian $H_{\text{eff}}$ emerges when dealing with quantum trajectories and post-selection [29].

In the formalism of quantum trajectories, the state of the system is described by a stochastic wave function. For trajectories where no quantum jumps occur, the system evolves according to $H_{\text{eff}}$. On the other hand if a jump occurs, the state abruptly changes due to the term $\sum_i \Gamma_i L_i \rho L_i^\dagger$. The Lindblad master equation (2.4) can be regarded as an average over infinitely many trajectories, i.e. many experimental realizations.

Finally, in order to illustrate the connection between Lindbladian and non-Hermitian Hamiltonian for the previously introduced decay of a two-level system we can rewrite Eq. (2.6) as

$$\dot{\rho} = -i\left[(\omega_e - i\Gamma/2)\,|e\rangle\langle e|\,\rho - \rho(\omega_e + i\Gamma/2)\,|e\rangle\langle e|\right] + \Gamma\sigma_-\rho\sigma_+\,. \tag{2.12}$$

Except for the quantum jump term $\Gamma\sigma_-\rho\sigma_+$, this is equivalent to working with the non-Hermitian Hamiltonian $(\omega_e - i\Gamma/2)\,|e\rangle\langle e|$.

## 2.3 Non-Hermitian mean-field dynamics from Lindblad equation

In this section we want to show an alternative method to derive non-Hermitian *effective* Hamiltonians from a full Lindbladian dynamics.

Consider a quantum system made of $N$ identical bosonic modes $\hat{a}_i$ ($[\hat{a}_i, \hat{a}_j^\dagger] = \delta_{ij}$) coherently exchanging excitations through the quadratic Hamiltonian

$$H = \sum_{i\neq j}(g_{ij}\hat{a}_i^\dagger\hat{a}_j + \text{H.c.}) \tag{2.13}$$

where all of them are generally subject to local dissipation and incoherent pumping so that the full Lindblad master equation reads

$$\dot{\rho} = -i[H,\rho] + \sum_i \gamma_i\mathcal{D}[\hat{a}_i]\rho + \Gamma_i\mathcal{D}[\hat{a}_i^\dagger]\rho. \tag{2.14}$$

where

$$\mathcal{D}[\hat{A}]\rho = \hat{A}\rho\hat{A}^\dagger - \{\hat{A}^\dagger\hat{A},\rho\}/2 \tag{2.15}$$

and $\gamma_i, \Gamma_i > 0$. We assumed a rotating frame so as to eliminate the free Hamiltonian term $\omega_0\sum_j \hat{a}_j^\dagger\hat{a}_j$, with $\omega_0$ the frequency of each oscillator.

We will restrict to the relevant class of *Gaussian states*, i.e. those states whose characteristic function is Gaussian [30]. These states are completely determined by the mean-field vector

$$\psi = (\alpha_1, \dots, \alpha_N)^T , \tag{2.16}$$

with $\alpha_i = \langle \hat{a}_i \rangle$, and covariance matrix

$$\sigma_{ij} = \langle \hat{A}_i \hat{A}_j + \hat{A}_j \hat{A}_i \rangle - 2\langle \hat{A}_i \rangle \langle \hat{A}_j \rangle , \tag{2.17}$$

where[1] $\hat{A}_i = (\hat{a}_1, \dots, \hat{a}_N, \hat{a}_1^\dagger, \dots, \hat{a}_N^\dagger)$ [31].

For the Lindbladian in Eq. (2.14) the mean-field dynamics is given by

$$i\dot{\psi} = \mathcal{H}\psi \tag{2.18}$$

with

$$\mathcal{H} = i(\mathcal{G} - \mathcal{L}) + \mathcal{C} \tag{2.19}$$

where $\mathcal{G} = \mathrm{diag}(\Gamma_1, \dots, \Gamma_N)$, $\mathcal{L} = \mathrm{diag}(\gamma_1, \dots, \gamma_N)$ and $\mathcal{C}_{ij} = g_{ij}$.

The mean-field dynamics is then a Schrödinger-like equation with a non-Hermitian *Hamiltonian* which, as previously discussed, despite having nothing genuinely quantum, can possess unconventional features like exceptional points or $\mathcal{PT}$ symmetry.

A specific instance of such non-Hermitian mean-field dynamics coming from a Lindbladian master equation is a gain-loss system [20]. This is a pair of quantum harmonic oscillators labeled by $G$ and $L$, whose joint state evolves in time according to the Lindblad master equation

$$\dot{\rho} = -i[g(\hat{a}_L^\dagger \hat{a}_G + \text{H.c.}), \rho] + 2\gamma_L \, \mathcal{D}[\hat{a}_L]\rho + 2\gamma_G \, \mathcal{D}[\hat{a}_G^\dagger]\rho \tag{2.20}$$

which is a particular instance of Eq. (2.14).

Besides the coupling Hamiltonian describing a coherent energy exchange at rate $g$ between the modes, the dissipators describe a local incoherent interaction with a local environment: the one on $G$ pumps energy into the system with characteristic rate $\gamma_G$ (gain) while that on $L$ absorbs energy with rate $\gamma_L$ (loss).

This system can be implemented in a variety of ways [14], including coupled waveguides [15], microcavities [32] and in double-quantum-dot circuit QED setups [22]. As for the general case of $N$ modes, from Eq. (2.20) it follows that the evolution of the mean-field vector $\psi = (\langle \hat{a}_L \rangle, \langle \hat{a}_G \rangle)^T$ is governed by the Schrödinger-like equation $i\dot{\psi} = \mathcal{H}\psi$ with

$$\mathcal{H} = \begin{pmatrix} -i\gamma_L & g \\ g & i\gamma_G \end{pmatrix} , \tag{2.21}$$

which is exactly the non-Hermitian Hamiltonian in Eq. (1.6) with generally different gain and loss rate, and a particular instance of Eq. (2.19). If gain and loss are balanced ($\gamma_L = \gamma_G = \gamma$), $\mathcal{H}$ is $\mathcal{PT}$-symmetric. Equations analogous to (2.20) for the full-quantum description of $\mathcal{PT}$-symmetric systems can be found also e.g. in Refs. [22, 33, 34].

[1] Both mean-field vector and covariance matrix can be written in terms of position and momentum variables. Here we stick to the representation with ladder operators.

# Chapter 3

# Quantum correlations in non-Hermitian systems

In this chapter, starting from the mean-field dynamics outlined in Sec. 2.3, we will take a step further and study the full quantum dynamics of the gain-loss system described by the master equation (2.20). This allows to investigate quantum correlations and we will show how the EP stands out as a critical point for them. This result can be seen as a *quantum* signature of the EP as it separates between asymptotic survival and vanishing of quantum correlations beyond the usual spectral separation of unbroken (real eigenvalues) and broken (complex eigenvalues) phases.

## 3.1 Introduction

To date the most studies on gain-loss dynamics as (2.20), pictorially described in Fig. 3.1, adopted a classical description (based on Maxwell's equations in all-optical setups) as we outlined in Sec. 1.2, thus discarding quantum noise. Recent works yet showed that a full quantum treatment (beyond mean field) may have major consequences [35–38], but the exploration of this quantum regime is still at an early stage [37, 39–48]. With regard to the potential exploitation of $\mathcal{PT}$-symmetric systems for quantum technologies, a major obstacle is that gain and loss inevitably introduce quantum noise, which is detrimental for quantum coherent phenomena—most importantly for entanglement [49]. In particular, the incoherent pumping acting as a gain is not customary in quantum optics settings [50]. This issue even motivated recent proposals to employ parametric driving in place of gain/loss to effectively model non-Hermitian systems [38, 51].

Notwithstanding, in the last 20years, "cheaper" quantum resources have been discovered, putting lighter constraints on the necessary amount of quantum coherence. Among these is quantum *discord*, a type of quantum correlations (QCs) occurring even without entanglement [52, 53]. This extended paradigm of QCs has received great attention for its potential of yielding a quantum advantage in noisy environments [54]. Notably, a recent work reported the first experimental detection of such a form of QCs [55] in an anti-$\mathcal{PT}$-symmetric system featuring similarities with the setup in Fig. 3.1. However, the existence of a general connection between $\mathcal{PT}$ symmetry and QCs dynamics is yet unknown.

In this chapter we provide a detailed study of total and quantum correlations in the gain-loss setup in Fig. 3.1. A connection emerges between $\mathcal{PT}$ symmetry breaking and the long-time behavior of both total and QCs: these are found to have different scalings in the $\mathcal{PT}$-broken/unbroken phase and at the EP. This is proven analytically and the underlying mechanism explained in detail through entropic arguments. In particular, breaking of $\mathcal{PT}$ symmetry is accompanied by the appearance of finite stationary discord. These results provide a new characterization of phases with unbroken/broken $\mathcal{PT}$ symmetry in terms of

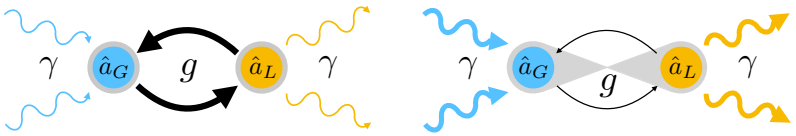


Figure 3.1: A pair of quantum oscillators $G$ and $L$ undergoing a coherent exchange energy with rate $g$. On top of that, mode $G$ ($L$) is subject to a local gain (loss) with rate $\gamma$. The mean-field dynamics is described by the $\mathcal{PT}$-symmetric Hamiltonian in Eq. (2.21) with $\gamma_G = \gamma_L = \gamma$. (Left): when $\mathcal{PT}$ symmetry is preserved ($\gamma < g$), after some time they will share only classical correlations (gray halos are not connected). (Right): $\mathcal{PT}$ symmetry breaking ($\gamma > g$) is instead accompanied by stationary quantum correlations (gray halos are connected).

the asymptotic behavior of correlations, whose knowledge requires accounting for the full quantum nature of the field.

## 3.2 Second-moment dynamics

As the mean-field dynamics has been discussed in Sec. 2.3, we focus here on the second-moment dynamics. These describe completely the joint state of the two oscillators as the dynamics in Eq. (2.20) is Gaussian preserving and we will only consider initial Gaussian states [30, 56].

The two oscillators have an associated quantum uncertainty described by a $4 \times 4$ covariance matrix. Introducing quadratures

$$\hat{x}_n = \tfrac{1}{\sqrt{2}}(\hat{a}_n + \hat{a}_n^\dagger) \tag{3.1}$$

$$\hat{p}_n = \tfrac{i}{\sqrt{2}}(\hat{a}_n^\dagger - \hat{a}_n) \tag{3.2}$$

(with $n = G, L$), we define the covariance matrix as in Eq. (2.17) with $\hat{A}_i = (\hat{x}_L, \hat{p}_L, \hat{x}_G, \hat{p}_G)$ [31]. Following a standard recipe [31], the master equation (2.20) implies a Lyapunov equation for the covariance matrix:

$$\dot{\sigma} = Y\sigma + \sigma\, Y^T + 4D \tag{3.3}$$

with

$$Y = \begin{pmatrix} -\gamma_L & 0 & 0 & g \\ 0 & -\gamma_L & -g & 0 \\ 0 & g & \gamma_G & 0 \\ -g & 0 & 0 & \gamma_G \end{pmatrix} \tag{3.4}$$

and $D = \frac{1}{2}\,\mathrm{diag}(\gamma_L, \gamma_L, \gamma_G, \gamma_G)$.

On the $\mathcal{PT}$ line excluding the EP, that is for $\gamma_L = \gamma_G = \gamma \neq g$, the solution of Eq. (3.3) under the initial condition $\sigma(0) = \mathbb{1}_2 \otimes \mathbb{1}_2$ (product of coherent states) reads

$$\begin{aligned}
\sigma_{11}(t) = \sigma_{22}(t) &= \frac{\gamma g^2 \sinh(2\Omega t)}{\Omega^3} - \frac{2\gamma g^2 t}{\Omega^2} + 1\,, \\
\sigma_{14}(t) = -\sigma_{23}(t) &= -\frac{\gamma g}{\Omega^2} + \frac{\gamma^2 g \sinh(2\Omega t)}{\Omega^3} - \frac{2\gamma^2 g t}{\Omega^2} + \frac{\gamma g \cosh(2t\Omega)}{\Omega^2}\,, \\
\sigma_{33}(t) = \sigma_{44}(t) &= -\frac{\gamma^2 + 2\gamma g^2 t + g^2}{\Omega^2} + \frac{2\gamma^2 \cosh(2\Omega t)}{\Omega^2} + \frac{\gamma\left(\gamma^2 + \Omega^2\right)\sinh(2\Omega t)}{\Omega^3}\,,
\end{aligned}$$

where

$$\Omega = \sqrt{\gamma^2 - g^2} \tag{3.5}$$

and all the remaining matrix entries vanish.

The covarance matrix of a single mode coherent state is $\mathbb{1}_2$, that is the same of the vacuum state, because it contains only the noise of the vacuum, indeed

$$\langle 0|\,\hat{\mathcal{O}}^2\,|0\rangle = \langle\alpha|\,\hat{\mathcal{O}}^2\,|\alpha\rangle - (\langle\alpha|\,\hat{\mathcal{O}}\,|\alpha\rangle)^2 \tag{3.6}$$

for $\hat{\mathcal{O}} = \hat{x}, \hat{p}$.

In the unbroken phase, $\Omega = i\sqrt{g^2-\gamma^2}$ and hyperbolic functions are turned into oscillating functions of $\sqrt{g^2-\gamma^2}\,t$. At the EP $\gamma = g$ the solution reads

$$\sigma_{11}(t) = \sigma_{22}(t) = \frac{4g^3t^3}{3} + 1, \quad \sigma_{33}(t) = \sigma_{44}(t) = \frac{4g^3t^3}{3} + 4g^2t^2 + 4gt + 1,$$

$$\sigma_{14}(t) = -\sigma_{23}(t) = \frac{4g^3t^3}{3} + 2g^2t^2\,,$$

with all the remaining matrix entries being zero. Although exact analytical solution of Eq. (3.3) for unbalanced gain-loss rates can be found, their expressions are not reported here since these are lengthy and uninformative.

As this will be relevant for the following discussion, we compute the mean energy of joint and reduced states from the covariance matrix as $E = \mathrm{Tr}\,\sigma$ and $E_{L(G)} = \mathrm{Tr}\,\sigma_{L(G)}$, respectively. On the $\mathcal{PT}$ line and in the long-time limit, they scale as

$$E_{\mathrm{UP}}(t) \approx \frac{8g^2\gamma}{g^2-\gamma^2}\,t\,, \quad E_{L,\mathrm{UP}}(t) \approx \frac{1}{2}\,E_{\mathrm{UP}}(t)\,, \tag{3.7}$$

$$E_{\mathrm{EP}}(t) \approx \frac{16g^3}{3}t^3\,, \quad E_{L,\mathrm{EP}}(t) \approx \frac{1}{2}\,E_{\mathrm{EP}}(t)\,, \tag{3.8}$$

$$E_{\mathrm{BP}}(t) \approx \frac{2\gamma^2\,(\gamma+\Omega)}{\Omega^3}\,e^{2\Omega t}\,, \quad E_{L,\mathrm{BP}}(t) \approx \frac{g^2\gamma}{2\gamma^2(\gamma+\Omega)}\,E_{\mathrm{BP}}(t)\,, \tag{3.9}$$

where UP and BP stand for unbroken and broken $\mathcal{PT}$ symmetry, respectively.

## 3.3 Correlation measures

A measure of the *total* amount of correlations between $\hat{a}_G$ and $\hat{a}_L$ is provided by the mutual information

$$\mathcal{I} = S_G + S_L - S\,, \tag{3.10}$$

that is the difference between the sum of local entropies

$$S_{L(G)} = -\mathrm{Tr}(\rho_{L(G)}\log\rho_{L(G)})\,, \tag{3.11}$$

with $\rho_{L(G)} = \mathrm{Tr}_{G(L)}\rho$, and the entropy of the joint system $S = -\mathrm{Tr}(\rho\log\rho)$ [49, 57]. It follows that $\mathcal{I} = 0$ if and only if $\rho = \rho_L \otimes \rho_G$. The amount of QCs is instead measured by the so-called *quantum discord* [52–54]

$$\mathcal{D}_{LG} = S_G - S + \min_{\hat{G}_k} \sum_k p_k S(\rho_{L|k})\,, \tag{3.12}$$

where minimization is over all possible quantum measurements $\{\hat{G}_k\}$ made on subsystem $G$. A measurement outcome indexed by $k$ collapses the joint system onto

$$\rho_{L|k} = \mathrm{Tr}_G(\hat{G}_k\rho)/p_k\,, \tag{3.13}$$

with probability $p_k$. Let us observe that discord is in general asymmetric[1], i.e., $\mathcal{D}_{LG} \neq \mathcal{D}_{GL}$, which is the typical case for our system [see Fig. 3.2]. The difference $\mathcal{I} - \mathcal{D}_{LG}$ represents the maximum amount of information that can be extracted about $L$ only performing local measurements on $G$. For this reason, discord captures QCs *beyond* entanglement, as it is in general nonzero for separable states [54]. Therefore, correlations between the modes are completely classical only if both $\mathcal{D}_{LG}$ and $\mathcal{D}_{GL}$ vanish.

In the case of Gaussian states, the optimization in (3.12) can be restricted to *Gaussian* measurements (Gaussian discord) [58], yielding a closed-form, although cumbersome, expression for $\mathcal{D}$ [59, 60]. In order to provide a simpler analytic formula we replace the von Neumann entropy by the *Rényi-2* entropy $S(\varrho) = -\log \mathrm{Tr}(\varrho^2)$ in each expression [61]. For Gaussian states, it has been shown that the choice of Rényi-2 entropy leads to well-behaved correlation measures [62]. Nevertheless, we numerically checked that all of the results (in particular asymptotic scalings) are qualitatively unaffected if von Neumann entropy is used instead. The fact that discord detects QCs more general than entanglement is condensed in a simple property: states such that $\mathcal{D} > \log 2$ are entangled ($\log 2 \to 1$ if von Neumann entropy is used) [60].

One of the main advantages of Gaussian states is that all the previously discussed correlations can be readily calculated through the covariance matrix, especially in terms of the Rényi-2 entropy. The general form of $\sigma$ generated by Eq. (3.3) with an initial product of coherent state features $2 \times 2$ blocks

$$\sigma = \begin{pmatrix} L & C \\ C^{\mathrm{T}} & G \end{pmatrix}, \tag{3.14}$$

where $L = \mathrm{diag}(\sigma_{11}, \sigma_{22})$, $G = \mathrm{diag}(\sigma_{33}, \sigma_{44})$ and

$$C = \begin{pmatrix} 0 & \sigma_{14} \\ \sigma_{23} & 0 \end{pmatrix} \tag{3.15}$$

describe uncertainties affecting the local fields $L$ and $G$ and cross-correlations, respectively. While von Neumann entropy requires the knowledge of the symplectic eigenvalues of $\sigma$, the Rényi-2 entropy for Gaussian states is simply given by

$$S(\sigma) = \frac{1}{2} \ln |\sigma| , \tag{3.16}$$

with $|\sigma| \equiv \det(\sigma)$. The entropies of the reduced states of $L$ and $G$ are similarly obtained as $S(L)$ and $S(G)$.

## 3.4 Correlations dynamics for balanced gain and loss

We consider here the dynamics of correlations when each oscillator $n = L, G$ starts in a coherent state

$$|\alpha_n\rangle = e^{(\alpha \hat{a}_n^\dagger - \alpha^* \hat{a}_n)} |0\rangle \ . \tag{3.17}$$

The initial covariance matrix is thus simply $\sigma_0 = \mathbb{1}_4$. The covariance matrix evolves through (3.3) and we can then compute the time evolution of both correlation measures $\mathcal{I}$ and $\mathcal{D}$, for which we can obtain exact and compact expressions.

Before going on with quantum discord, a comment about entanglement, as this is generally the longstanding measure of QCs. We verified that it is indeed always zero in our dynamics. As mentioned earlier, discord detects QCs more general than entanglement. For Gaussian discord, this is condensed in a simple property: Gaussian states with $\mathcal{D} > \log 2$

[1] Parity is a minimal requirements for symmetric discord.

(1 with von Neumann entropy) are entangled. In our setup, discord never goes beyond this threshold (see Fig. 3.2) and we checked that the state is never entangled as $\tilde{\nu}_- > 1$ at any time ($\tilde{\nu}_-$ is the smallest symplectic eigenvalue of the partially transposed covariance matrix [60]). Besides these analytical results, absence of entanglement at any given time is justified by the fact that the coupling Hamiltonian acts like a beam-splitter, and therefore cannot entangle coherent states, and that the two gain/loss channels are local.

Coming back to quantum discord, (3.12) admits a global minimum for all possible parameter values, corresponding to a phase-insensitive (heterodyne) measurement. Intuitively, this property can be related to the absence of any coherent drive: the dynamics in (2.20) is $U(1)$-symmetry-preserving and therefore favors the conditioning of phase-insensitive measurements over phase-sensitive ones; this in turn makes the latter suboptimal for the generation of QCs.

Fig. 3.2 shows the typical time behavior of mutual information $\mathcal{I}$ (a) and discord $\mathcal{D}$ (b) in the UP (green line), at the EP (blue) and in the BP (red). Correlations, including QCs, are created on a typical time scale $\tau$ of the order of $\sim g^{-1}$ or less. and stationary QCs occur only when the dynamics is unstable, as we will shortly discuss. It is therefore important from an experimental point of view to compute the *transient time* $\tau$, namely the time it takes for QCs to reach a relevant percentage of their asymptotic value. We focus here on the $\mathcal{PT}$ line in broken phase and define $\tau_{LG}$ as that time satisfying $\mathcal{D}_{LG}(\tau_{LG}) = 90\%\,\mathcal{D}_{LG}(\infty)$, with an analogous definition for $\tau_{GL}$. From Fig. 3.3, we see that both $\tau$'s are of the order of $g^{-1}$. We numerically checked that this holds true besides the $\mathcal{PT}$-broken phase whenever asymptotic discord is finite. As discussed in the following, *transient* generation of QCs is common in noise-driven multipartite systems. In the long-time limit, instead, correlations show a peculiar behavior, which we next analyze for each phase.

In the UP, $\mathcal{I}$ approaches a finite value while exhibiting secondary oscillations at frequency $2\sqrt{g^2-\gamma^2}$, while discord slowly decays until it vanishes. Their asymptotic expressions are given by

$$\mathcal{I} \approx \log\left(\frac{g^2}{g^2-\gamma^2}\right), \qquad \mathcal{D}_{LG}, \mathcal{D}_{GL} \approx \frac{\gamma}{2g^2 t}\,, \tag{3.18}$$

(throughout the symbol $\approx$ indicates the long-time limit) showing that quantum discord displays a power-law decay in this phase. Therefore, in the UP asymptotic correlations are *completely classical*, i.e., they do not involve any quantum superposition. This may seem to contradict the well-known property that Gaussian states such that $\mathcal{I} = 0$ are all and only those with zero discord [60]. That property yet holds for systems with bounded mean energy, while the present dynamics is *unstable* on the whole $\mathcal{PT}$ line.

When $\mathcal{PT}$ symmetry is broken instead, the behavior of long-time correlations changes drastically. Mutual information now increases linearly as $\mathcal{I} \approx 2\Omega\, t$, while QCs tend to a finite value given by

$$\mathcal{D}_{LG} \approx \log\left(\frac{\gamma(\gamma+\Omega)+g^2}{2\gamma^2}\right), \quad \mathcal{D}_{GL} \approx \log\left(\frac{\gamma(3\gamma+\Omega)-g^2}{2\gamma^2}\right). \tag{3.19}$$

Thus in the BP *stationary* QCs are established, despite the noisy action of gain/loss and the dynamics being unstable. Jointly taken, Eqs. (3.18) and (3.19) show that the nature of asymptotic correlations is different in the two phases. In each phase, stationary finite correlations occur, but these are purely classical in the UP (where $\mathcal{I}$ converges, while $\mathcal{D} \to 0$) and purely quantum in the BP.

Finally, a critical behavior occurs at the EP with the correlations scaling as

$$\mathcal{I} \approx \log\left(\frac{4g^2}{3}t^2\right), \quad \mathcal{D}_{LG}, \mathcal{D}_{GL} \approx \frac{1}{gt}. \tag{3.20}$$

Thus, while discord scales as in the UP phase (yet with a different pre-factor, cf. (3.18)), the growth of mutual information is now logarithmic. Remarkably, the EP is the only

point on the $\mathcal{PT}$ line such that $\mathcal{I} \to \infty$, $\mathcal{D} \to 0$ (purely classical and diverging correlations). Thus, for balanced gain and loss, the EP can be regarded as the *most classical* configuration of the system.

Fig. 3.2(c) shows the long-time QCs on the $\mathcal{PT}$ line. In the BP, $\mathcal{D}_{GL}(\infty)$ monotonically grows with $\gamma$ asymptotically approaching the entanglement threshold, while $\mathcal{D}_{LG}(\infty)$ takes a maximum followed by a long-tail decay. A critical behavior occurs at the EP (on the boundary between regions of zero and non-zero discord) since

$$\mathcal{D} \sim (\gamma/g - 1)^{\frac{1}{2}} \tag{3.21}$$

for $\gamma > g$ while

$$\mathcal{D} = 0 \tag{3.22}$$

for $\gamma \leq g$.

All the results and plots in Fig. 3.2 are for an initial coherent state (covariance matrix $\sigma_0 = \mathbb{1}_4$). Yet, we gathered numerical evidence that mutual information and discord exhibit analogous long-time behaviors if different (Gaussian) initial states are chosen. This is illustrated in Fig. 3.4 where we set $\gamma_G = \gamma_L = \gamma$ ($\mathcal{PT}$ line) and plot mutual information and $\mathcal{D}_{GL}$ versus time for three different choices of initial state: a coherent state, a two-mode squeezed state and a two-mode squeezed thermal state, whose general covariance matrix (in quadrature basis) has the form

$$\sigma_0 = \begin{pmatrix} (\cosh r\,(n_G + n_L + 1) + n_L - n_G)\mathbb{1}_2 & \sinh r\,(n_G + n_L + 1)\,\sigma_z \\ \sinh r\,(n_G + n_L + 1)\,\sigma_z & (\cosh r\,(n_G + n_L + 1) + n_G - n_L)\mathbb{1}_2 \end{pmatrix} \tag{3.23}$$

where $\sigma_z = \left(\begin{smallmatrix} 1 & 0 \\ 0 & -1 \end{smallmatrix}\right)$, $r$ is the squeezing parameter and $n_L(n_G)$ is the mean number of photons in mode $L(G)$. Note that changing the initial states does not even affect the numerical asymptotic value except for the BP where a little discrepancy between different initial states arises. We checked that this discrepancy disappears if Von Neumann entropy is used instead of Rényi-2 entropy.

## 3.5 Physical mechanisms behind generation of correlations

Generation of QCs during the *transient* dynamics can be understood noticing that the coupling Hamiltonian acts on the modes like a beam splitter. When acting on $|\alpha_L\rangle \otimes |\alpha_G\rangle$, this term alone cannot correlate the modes, only mixing their amplitudes [63]. The same holds for the loss term. The gain process, on the other hand, turns a coherent state into a *mixture*

$$|\alpha\rangle\langle\alpha| \to \int d^2\alpha' P(\alpha')\,|\alpha'\rangle\langle\alpha'|$$

with $P(\alpha') \geq 0$ (coherence reduced) [64]. The combined action of gain and beam splitter on $|\alpha_L\rangle\langle\alpha_L| \otimes |\alpha_G\rangle\langle\alpha_G|$ turns it into

$$\int d^2\alpha'_G P(\alpha'_G)\,|\tilde{\alpha}'_L\rangle\langle\tilde{\alpha}'_L| \otimes |\tilde{\alpha}'_G\rangle\langle\tilde{\alpha}'_G|$$

where both $\tilde{\alpha}'_{L(G)}$ depend on both $\alpha'_{L(G)}$. Although not entangled, such a state is generally discordant because coherent states form a *non*-orthogonal basis [65]. We observe that an analogous effect is obtained if the gain is replaced by a local thermal bath. Indeed, the ability of some local non-unitary channels to favor creation of discord was demonstrated in [54]. For instance, local gain or loss can create QCs starting from a state featuring only classical correlations (a process which is not possible for entanglement) [66–69], which was experimentally confirmed in Ref. [70].

| $\mathcal{PT}$ line | UP | EP | BP |
|---|---|---|---|
| $S$ | $\log\left(\frac{4\gamma^2 g^2}{g^2-\gamma^2}\,t^2\right)$ | $\log\left(\frac{4g^4}{3}t^4\right)$ | $2\Omega\,t+\log\left(\frac{\gamma^3(\gamma+\Omega)}{\Omega^4}\right)$ |
| $S_L$ | $\log\left(\frac{2\gamma g^2}{g^2-\gamma^2}\,t\right)$ | $\log\left(\frac{4g^3}{3}t^3\right)$ | $2\Omega\,t+\log\left(\frac{\gamma g^2}{2\Omega^3}\right)$ |
| $S_G$ | | | $2\Omega\,t+\log\left(\frac{\gamma(\gamma+\Omega)^2}{2\Omega^3}\right)$ |

Table 3.1: Asymptotic behavior of entropies $S$ and $S_{L(G)}$ for balanced gain-loss rates.

The special nature of this dynamics mostly arises from the *long-time* behavior of correlations. To shed light on it, we first show that discord can be expressed in the form

$$\mathcal{D}_{LG}=\log\!\left(1+\frac{e^{\mathcal{I}}-1}{e^{S_G}+1}\right), \tag{3.24}$$

(with an analogous expression for $\mathcal{D}_{GL}$). This identity, which we now prove, holds true for *any* Gaussian state generated by (2.20) and subject to a local heterodyne measurement.

Despite the fact that a closed expression for bipartite Gaussian quantum discord can be obtained, this is generally lengthy and uninformative regardless of the chosen entropy measure. However, in our dynamics with an initial product of coherent states, the isotropy of the problem suggests that the measurement which maximizes discord is likely to be phase-insensitive. Indeed, it can be checked that heterodyne detection (i.e., projection onto coherent states) is the optimal measurement. In our dynamics it can also be checked that cross correlations are always smaller than local uncertainties (this is of course not true for *any* Gaussian state). These facts allow us to write quantum discord as in Eq. (3.24) according to the following lemma.

**Lemma.** *For a heterodyne measurement Gaussian discord with Rényi-2 entropy of a Gaussian state as in Eq.* (3.14) *whose cross correlations are smaller than local uncertainties (i.e.,* $|C|<\sqrt{|L|}\sqrt{|G|}$*) can be written as*

$$\mathcal{D}_{LG}=\log\left(1+\frac{e^{\mathcal{I}}-1}{e^{S_G}+1}\right),\qquad \mathcal{D}_{GL}=\log\left(1+\frac{e^{\mathcal{I}}-1}{e^{S_L}+1}\right). \tag{3.25}$$

*Proof.* A heterodyne measurement on $G$ turns the covariance matrix (CM) into

$$\sigma_{|G}=\begin{pmatrix} L & C\\ C^T & G+\sigma_M\end{pmatrix} \tag{3.26}$$

where $\sigma_M=\mathbb{1}_2$ is the CM of the measurement outcome [30]. Let

$$\tilde{L}=L-C(G+\sigma_M)^{-1}C^{\mathrm{T}} \tag{3.27}$$

be the Schur complement and let us denote $|A|\equiv\det(A)$. Using the definition of Gaussian discord with Rényi-2 entropy [61]

$$\mathcal{D}_{LG}=\frac{1}{2}\log\left(\frac{|\tilde{L}|\,|G|}{|\sigma|}\right) \tag{3.28}$$

we get

$$\mathcal{D}_{LG}\;=\;\frac{1}{2}\log\left(\frac{|G|}{|G+\sigma_M|}\frac{|G+\sigma_M|\,|\tilde{L}|}{|\sigma|}\right)=\frac{1}{2}\log\left(\frac{|G|}{|G+\sigma_M|}\frac{|\sigma_{|G}|}{|\sigma|}\right).$$

Now using the assumption $|C| < \sqrt{|L|}\sqrt{|G|}$ we can write

$$\mathcal{D}_{LG} = \frac{1}{2}\log\left(\frac{e^{2S_G}}{(e^{S_G}+1)^2}\frac{(e^S+e^{S_L})^2}{e^{2S}}\right) = \log\left(1+\frac{e^{\mathcal{I}}-1}{e^{S_G}+1}\right).$$

An analogous proof holds for $\mathcal{D}_{GL}$.

□

Using (3.25) we plot asymptotic discord in Fig. 3.5.

Together with $\mathcal{I} = S_G + S_L - S$, (3.24) allows to explain the dynamics of classical and QCs in terms of a *competition* among global and local entropies. The long-time expressions of $S$ and $S_{L(G)}$ are provided in Table 3.1. All of these *diverge* in time (either logarithmically or linearly depending on the phase). Hence, (3.24) simplifies to

$$\mathcal{D}_{LG} \approx \log\left(1 + e^{-(S-S_L)} - e^{-S_G}\right), \tag{3.29}$$

which shows that the survival of QCs depends on the difference $S - S_L$ alone. Using the expressions in Table 3.1, (3.29) yields exactly the scalings in Eqs. (3.18), (3.19) and (3.20).

In the UP, $S_G$ and $S_L$ grow at the same rate and their sum is *almost* equal to the global entropy $S$. Their difference is small (showing this requires sub-leading contributions not shown in Table 3.1) and yields a constant $\mathcal{I}$ in the long-time limit. (3.24) then entails that discord vanishes. In the BP, instead, the gain process dominates the entropy balance and the total entropy is slaved to the local one, $S \approx S_G$. This then implies $\mathcal{I} \approx S_L$. On top of that, the divergences of $S$ and $S_L$ cancel out, so that $S - S_L$ is convergent, in turn entailing a finite value of QCs via (3.29).

As mentioned previously, any two-mode Gaussian state with *finite* mean energy satisfies $\mathcal{D} \neq 0 \Leftrightarrow \mathcal{I} \neq 0$ [60]. This property can be retrieved from (3.24) when $S_G$ is *finite*. Notwithstanding, for $S_G \to \infty$, discord can vanish asymptotically even if $\mathcal{I}$ does not (e.g. in the UP and at EP, see Fig. 3.2).

## 3.6 Dynamics of correlations beyond the PT line

To complete our study, we address the rich dynamics of correlations beyond the $\mathcal{PT}$ line, i.e., for unbalanced gain and loss ($\gamma_L \neq \gamma_G$). The phase portrait in Fig. 3.6 displays five distinct dynamical regimes, obtained by applying standard stability analysis. Indeed, the Schrödinger-like equation for the mean-field $\dot{\psi} = -i\mathcal{H}\psi$ is nothing but a two dimensional linear dynamical system whose asymptotic behavior is fully characterized by the eigenvalues

$$\lambda_\pm = \frac{1}{2}(\gamma_G - \gamma_L \pm \sqrt{(\gamma_G+\gamma_L)^2 - 4g^2}) \tag{3.30}$$

of $-i\mathcal{H}$. If $\lambda_+\lambda_- < 0$ then the origin $O = (0,0)$ is a saddle point for the dynamical system. If both $\lambda_\pm$ are real numbers then $O$ is a source (sink) if both $\lambda_\pm > 0$ ($\lambda_\pm < 0$), otherwise $O$ is a repulsive (attractive) spiral if both $\mathrm{Re}\lambda_\pm > 0$ ($\mathrm{Re}\lambda_\pm < 0$). The boundaries separating regions with different behaviors are exactly the $\mathcal{PT}$ line ($\gamma_L = \gamma_G < g$), the hyperbola ($\gamma_L\gamma_G = g^2$) and the EP line ($\gamma_L + \gamma_G = 2g$), as shown in Fig. 3.6.

Accordingly, the long-time behavior of the CM is determined by the Lyapunov stability criterion: equation

$$Y\sigma_\infty + \sigma_\infty Y^{\mathrm{T}} + 4D = 0 \tag{3.31}$$

has a (finite) solution if and only if the eigenvalues of $Y$ have negative real parts. We observe that, by expressing the CM in terms of ladder operators $\hat{A}_i = (\hat{a}_L, \hat{a}_G, \hat{a}_L^\dagger, \hat{a}_G^\dagger)$

(instead of quadratures as in the main text), matrix $Y$ entering Eq. (3.4) turns into

$$\widetilde{Y} = \begin{pmatrix} -i\mathcal{H} & \mathbf{0} \\ \mathbf{0} & i\mathcal{H}^\dagger \end{pmatrix}. \tag{3.32}$$

The eigenvalues of $Y$ are thus same as those of $\widetilde{Y}$ (as a unitary transformation preserves the spectrum) and are in turn the same as those of matrix $-i\mathcal{H}$ with a double degeneracy. Therefore the CM dynamics mimics that of the Schrödinger-like equation for the mean-field: it admits a stationary value for $\mathrm{Re}\lambda_\pm < 0$ [regions III+IV in Fig. 3.6 ], otherwise it diverges.

The regions in Fig. 3.6(a) are limited by the $\mathcal{PT}$ line, the EP line $\gamma_L + \gamma_G = 2g$ and the hyperbola $\gamma_L\gamma_G = g^2$. There is a stable region (III+IV), where both distinct eigenvalues $\lambda_\pm$ of matrix $Y$ (cf. (3.4)) have negative real part (note that for $g > \gamma_G$, if $\gamma_L$ is large enough the dynamics becomes unstable). This is the usual bounded-energy region featuring non-zero stationary values of $\mathcal{I}$ and $\mathcal{D}$. Symmetric to that is a totally unstable region (I+II), where both $\mathrm{Re}\lambda_\pm > 0$. Remarkably, this *whole* region is characterized by asymptotically vanishing discord [cf. Fig. 3.6(c)]. The EP line separates two kinds of divergence (convergence) in the totally unstable (stable) region: below this line repulsive (attractive) spirals occur, and sources (sinks) above it. In conclusion, there is an unstable region (V) (saddle points) with linearly divergent $\mathcal{I}$ and stationary QCs [cf. (b) and (d)]. Eq. (3.29) can be directly applied to the unstable regions beside the $\mathcal{PT}$ line to explain the behavior of QCs. Yet another remarkable feature is that the region (I+III+IV) is characterized by asymptotic finite values of $\mathcal{I}$. In particular, in region I, $\mathcal{I}$ displays extremely long-lived oscillations [see Fig. 3.6(a)].

## 3.7 Summary

In this chapter, through a fully master equation description, we investigated the dynamical behaviors of total and quantum correlations in a typical gain-loss system exhibiting mean-field $\mathcal{PT}$-symmetric physics. Starting from a coherent state, QCs without entanglement are created and, in a large region of parameter space, approach to a non-zero value. For balanced gain and loss, and in the long-time limit, distinct $\mathcal{PT}$ symmetric phases exhibit dramatically different time scalings of both total and quantum correlations. This points to a new distinction between phases with unbroken/broken $\mathcal{PT}$ symmetry in the dynamics of entropic quantities, whose knowledge requires accounting for the full quantum nature of the field.

In terms of quantum technologies, stationary QCs beyond entanglement (occurring e.g. in the unbroken phase) are potentially appealing in that this form of correlations have found several applications in recent years, [71, 72] such as information encoding [73], remote-state preparation [74], entanglement activation [75–78], entanglement distribution [79–82], quantum metrology and sensing [83] and so on. This suggests that quantum noise could embody a resource, rather than a hindrance, to the exploitation of $\mathcal{PT}$-symmetric systems for useful applications. This is indeed one of the major points we will make in Chapter 5 (and in the whole thesis), though from a different perspective.

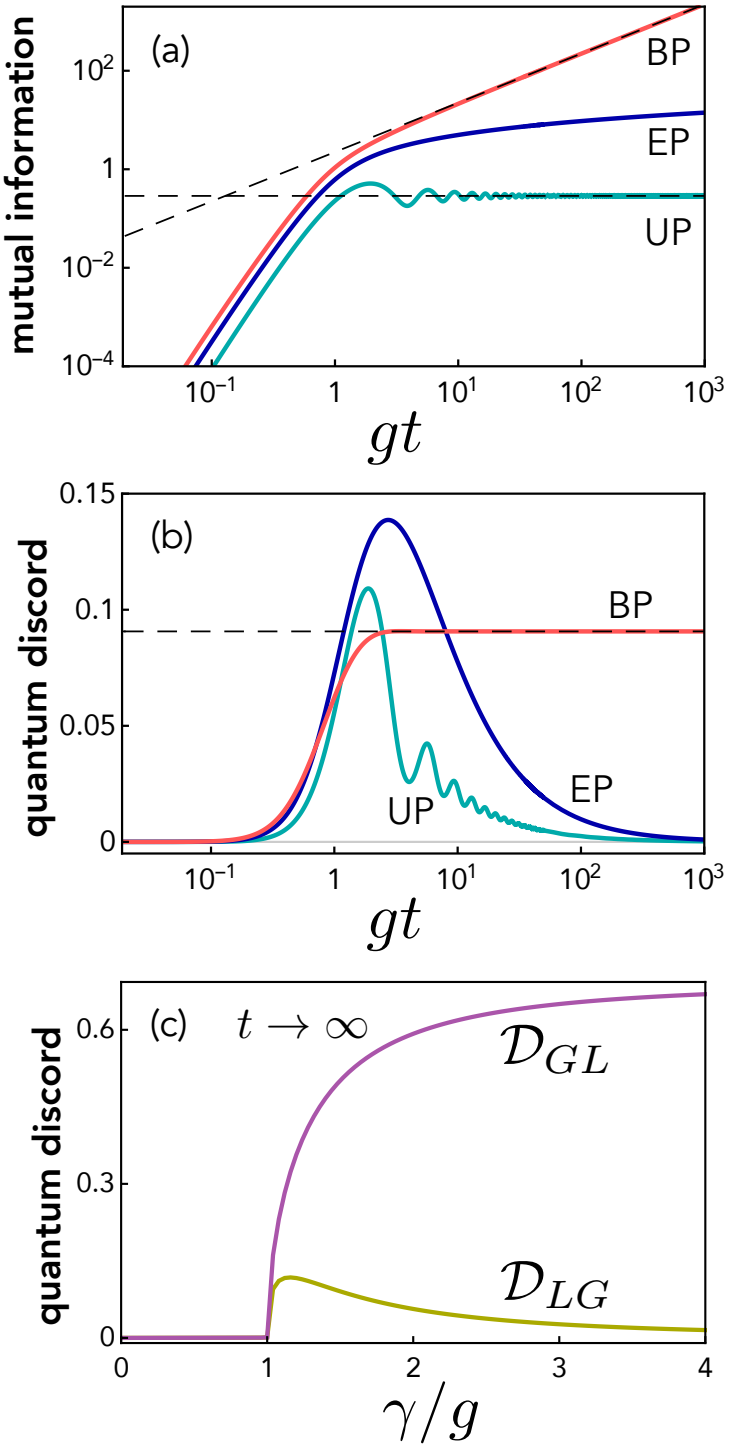


Figure 3.2: Dynamics of mutual information and quantum correlations on the $\mathcal{PT}$ line ($\gamma_L = \gamma_G = \gamma$). This includes the unbroken phase (UP) $\gamma < g$, the exceptional point (EP) $\gamma = g$ and the broken phase (BP) for $\gamma > g$. (a) and (b): Mutual information $\mathcal{I}$ (a) and discord $\mathcal{D}_{LG}$ (b) for $\gamma = g/2$ (UP, green), $\gamma = 3g/2$ (BP, red) and $\gamma = g$ (EP, blue). A qualitatively analogous behavior is exhibited by $\mathcal{D}_{GL}$. (c): Asymptotic value of discord, $\mathcal{D}_{LG}(\infty)$ (yellow) and $\mathcal{D}_{GL}(\infty)$ (purple).

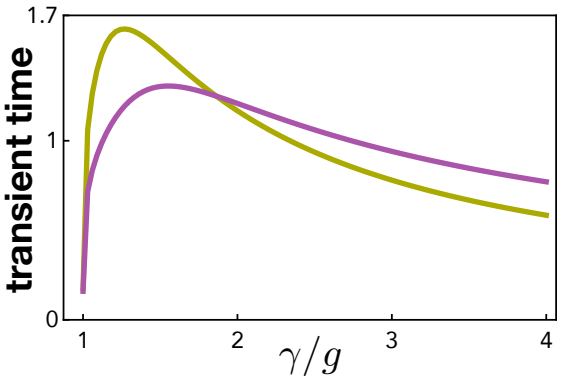


Figure 3.3: Transient time $\tau_{LG}$ (yellow) and $\tau_{GL}$ (purple) in units of $g^{-1}$ versus gain/loss rate $\gamma$ in units of $g$.

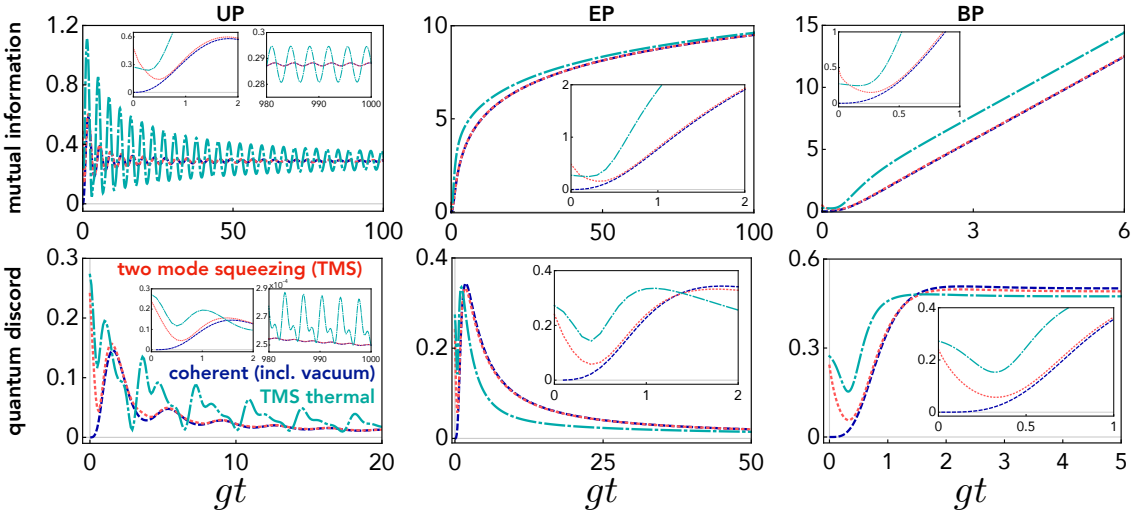


Figure 3.4: Typical time behavior on the $\mathcal{PT}$ line of mutual information (top panels) and discord $\mathcal{D}_{GL}$ (bottom) for different choices of the initial state as in (3.23): coherent (blue, $r = 0$, $n_L = n_G = 0$), two mode squeezed (red, $r = 0.5$, $n_L = n_G = 0$) and two mode squeezed thermal (green, $r = 0.5$, $n_L = 3$, $n_G = 7$) state. The three columns represent UP ($\gamma = g/2$), EP ($\gamma = g$) and BP ($\gamma = 3g/2$).

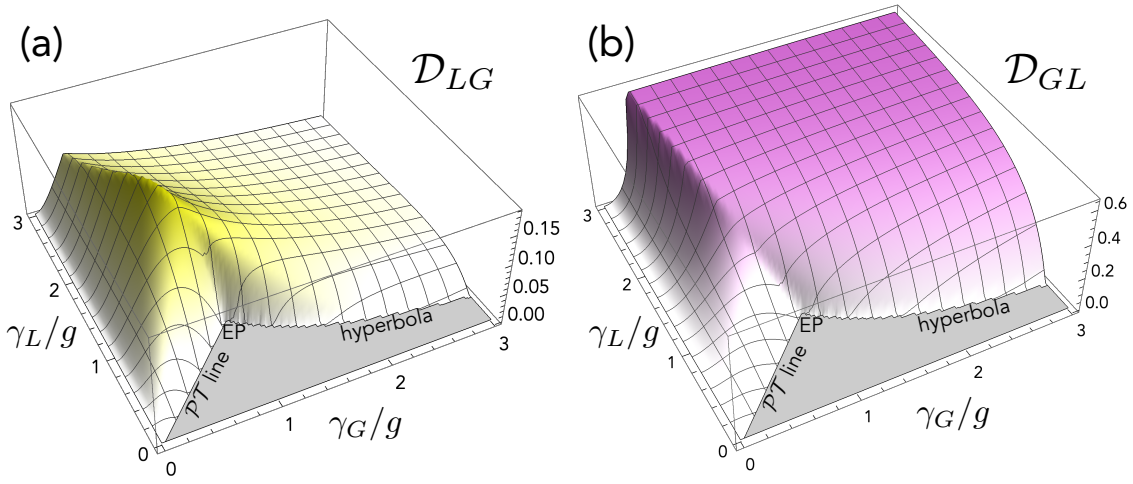


Figure 3.5: Long time QCs as measured by $\mathcal{D}_{LG}$ (a) and $\mathcal{D}_{GL}$ (b) on the plane $\gamma_G - \gamma_L$ (in units of $g$). $\mathcal{PT}$ line, EP and hyperbola are highlighted to clarify the relation with Fig. 3.6. The plots are the generalizations of Fig. 3.2(c) [i.e. the $\mathcal{PT}$ line] to the general case of unbalanced gain an loss.

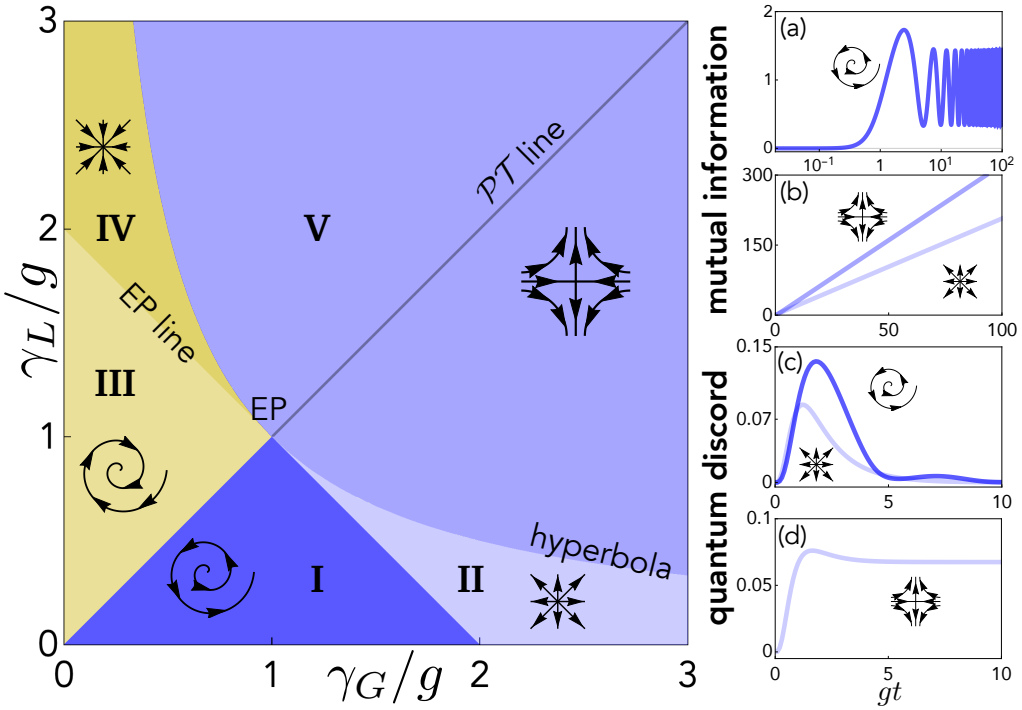


Figure 3.6: (Left): Stability diagram for the dynamics ruled by (2.20) with generally unbalanced gain and loss. (Right): Typical time evolution of the mutual information [(a), (b)] and discord [(c), (d)] corresponding to the points highlighted in the diagram.

# Chapter 4

# Cavity and waveguide QED: a brief review

In this chapter we make a brief overview about light matter interaction in cavity-QED and waveguide QED, providing the minimal tools necessary for the next chapter. We focus our attention on the so-called atom-photon dressed states and on the effective atom-atom Hamiltonian mediated by a photon.

## 4.1 Introduction

One of the many milestones in the field of quantum optics, i.e. light-matter interaction at the quantum level, has been the realization of coherent interaction between atoms (matter) and single modes of the electric field (light) [84]. This is best represented in cavity QED (quantum electrodynamics), that is a setup where an atom (or many) interacts with a protected cavity mode.

On the one hand, atoms can be modeled as *pseudo-spins*, i.e. two-level quantum systems (qubits). We label the two states as $|g\rangle$ and $|e\rangle$ as for *ground* and *excited*, respectively, with energy difference $\omega_e$. This is of course an approximation, based on the assumption that other transitions to other energy levels are negligible with respect to the $|g\rangle \leftrightarrow |e\rangle$ transition.

On the other hand, the spatial confinement of the electric field in a cavity with volume $V$ and mirrors' distance $L$ has two major consequences:

($i$) only one mode $\hat{a}$ of the field can be taken into account (the *cavity mode*)[1],

($ii$) the atom-field coupling $g$ is enhanced.

Indeed, the energy spacing among field modes is proportional to $L^{-1}$ and $g \propto V^{-1/2}$ [85].

Therefore, under dipole and rotating wave approximations [86], the cavity QED Hamiltonian describing a single atom interacting with a single cavity mode, the so called *Jaynes-Cummings model*, reads

$$H_{\mathrm{JC}} = \omega_e \sigma^\dagger \sigma + \omega_0 \hat{a}^\dagger \hat{a} + g\left(\sigma^\dagger \hat{a} + \mathrm{H.c.}\right) \tag{4.1}$$

where $\omega_0$ is the energy of mode $\hat{a}$ (recall that we set $\hbar = 1$) and $\sigma = |g\rangle\langle e|$. The last term in Eq. (4.1) describes the coherent exchange of excitation between the atom and the cavity.

The number of excitations $\hat{N} = \sigma^\dagger\sigma + \hat{a}^\dagger\hat{a}$ is a constant of motion ($[\hat{N}, H_{\mathrm{JC}}] = 0$), therefore $H_{\mathrm{JC}}$ can be block diagonalized in each subspace spanned by $\{|g, n\rangle, |e, n-1\rangle\}$,

[1] Confinement leads to quantization. Then, only the resonant mode is relevant in the atom-light interaction, the others being far detuned.

where the first (second) entry in the ket represents the atomic (photonic) state. These states are the *bare* modes of the system, that is the eigenstates of the free Hamiltonian $H_0 = H_{\rm JC} - g(\sigma^\dagger \hat{a} + \text{H.c.})$. As in any two-dimensional system, interaction modifies the energy splitting, as the eigenvalues become

$$E_{\pm,n} = n\omega_0 + \Delta \pm \sqrt{\Delta^2 + g^2 n} \tag{4.2}$$

with $\Delta = (\omega_e - \omega_0)/2$ (atom-cavity detuning). The corresponding eigenstates are a pair of *atom-photon dressed states*[2]:

$$\left|\Psi_n^+\right\rangle = \cos\tfrac{\theta}{2}\,|g,n\rangle + \sin\tfrac{\theta}{2}\,|e,n-1\rangle \tag{4.3}$$

$$\left|\Psi_n^-\right\rangle = -\sin\tfrac{\theta}{2}\,|g,n\rangle + \cos\tfrac{\theta}{2}\,|e,n-1\rangle \tag{4.4}$$

with $\theta = \arctan(g\sqrt{n}/\Delta)$ being the mixing angle.

In the absence of interaction the two levels would be resonant. In the presence of the interaction, we see from Eq. (4.2) that the energy splitting depends on the interaction strength *and* on the detuning. Two separate regimes can then be considered.

For large detuning $\Delta \gg g$, first-order processes are ineffective hence energies are slightly perturbed and so are the eigenstates. For small detuning $\Delta \ll g$ the interaction is of first order (for zero detuning the degeneracy is lifted), and eigenstates are given by substantially superposing the bare eigenstates. Furthermore, vacuum-Rabi oscillations occur, whose amplitude is higher in strong coupling regime ($\Delta \ll g$) than those occurring in weak coupling.

As an example, considering the single excitation subspace (which will be the relevant one also in the following), we can write the energies in Eq. (4.2) as

$$E_\pm = \omega_0 + \Delta \pm \sqrt{\Delta^2 + g^2} \tag{4.5}$$

and

$$|+\rangle = \cos\frac{\theta}{2}\,|g\rangle|1\rangle + \sin\frac{\theta}{2}\,|e\rangle|\text{vac}\rangle \tag{4.6}$$

$$|-\rangle = -\sin\frac{\theta}{2}\,|g\rangle|1\rangle + \cos\frac{\theta}{2}\,|e\rangle|\text{vac}\rangle \tag{4.7}$$

where $|\text{vac}\rangle$ is the ground state of the field and $|\pm\rangle = \left|\Psi_1^\pm\right\rangle$. This particular case shows how these atom-photon dressed states can be thought of as one excitation shared by the atom and the field.

## 4.2 QED in structured photonic lattices

In recent years it has been possible to realize experimentally setups that are a generalization (theoretically speaking) of the one presented in the previous section. Instead of considering an emitter coupled to the field where *all three dimensions* are localized (cavity QED), a new paradigm of light-matter interaction, that of *waveguide QED*, where only 2 dimensions are localized, has been established. In this scenario a single atom is interacting with a 1D continuum of modes.

The experimental challenge is coherently coupling one or more emitters to the field, so that the preferred decay channel is that into the waveguide instead of the surrounding free space. This can be achieved in several platforms such as cold atoms coupled to the evanescent field of a nanofiber [87] or superconducting qubits coupled to transmission lines [88, 89].

[2]The atom is no longer *naked*, as it is dressed by the photon

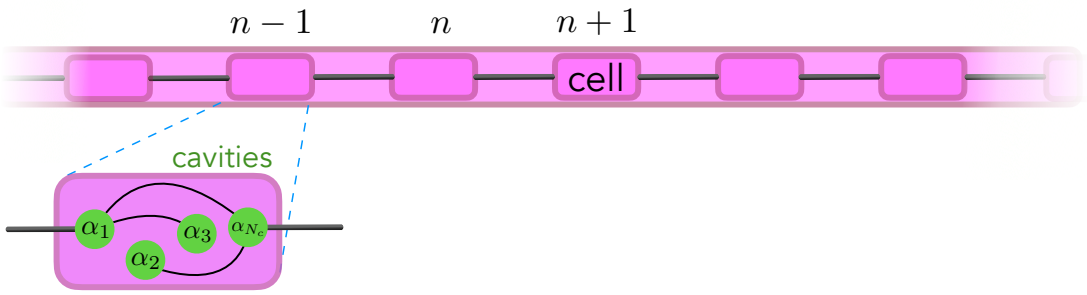


Figure 4.1: Pictorial representation of a structured photonic lattice (waveguide). The array is composed of $N \to \infty$ unit cells, with nearest neighbor couplings. Each cell contains the same couplings pattern between $N_c < \infty$ cavities (green dots).

The waveguide QED model we will consider is that of two-level systems coupled to a one-dimensional array of coupled cavities as in Refs. [90–92]. In recent years it was shown how a *structured* array can exhibit many unconventional properties [92,93]. By "structured array" we specifically mean, as in Ref. [94], one where each unit lattice cell couples to nearest-neighbor unit cells, allowing any possible couplings among cavities *within* the unit cell[3].

The full Hamiltonian of the system is then

$$H = H_e + H_f + H_{int} \tag{4.8}$$

The first term is the free emitters Hamiltonian, which for $N_e$ emitters reads

$$H_e = \omega_e \sum_{i=1}^{N_e} \sigma_i^\dagger \sigma_i \tag{4.9}$$

where $\sigma_i = |g\rangle_i\langle e|$.

The second term in Eq. (4.8) is the Hamiltonian of the field of the structured array. We will adopt the same notation as in Ref. [94] so that we consider a one-dimensional lattice made of $N$ unit cells, each of them containing $N_c$ cavities; $a_{n,\alpha}$ describes the photonic excitation in the $\alpha$th cavity within the $n$th unit cell, see Fig. 4.1. As we are considering all possible kinds of interactions inside a unit cell, writing the field Hamiltonian in real space would result in a cumbersome expression. We then consider the limit $N \to \infty$ limit and take periodic boundary conditions so as to write the free field Hamiltonian in Fourier space as

$$H_f = \sum_k \left(\tilde{a}_{k,1}^\dagger, \ldots, \tilde{a}_{k,N_c}^\dagger\right) h_f(k) \begin{pmatrix} \tilde{a}_{k,1} \\ \vdots \\ \tilde{a}_{k,N_c} \end{pmatrix} \tag{4.10}$$

where $\tilde{a}_{k,\alpha} = \frac{1}{\sqrt{N}} \sum_n e^{-ikn} a_{n,\alpha}$, $\alpha = 1, \ldots, N_c$, and

$$h_f(k) = \omega_0 \mathbb{1}_{N_c} + \begin{pmatrix} \delta_1(k) & f_{12}(k) & \ldots & f_{1N_c}(k) \\ f_{12}^*(k) & \delta_2(k) & \ldots & f_{2N_c}(k) \\ \ldots & \ldots & \ldots & \ldots \\ f_{1N_c}^*(k) & f_{2N_c}^*(k) & \ldots & \delta_{N_c}(k) \end{pmatrix} \tag{4.11}$$

is the Hamiltonian in Fourier space and $\omega_0$ is the free energy of each cavity (the free cavities' Hamiltonian is $\omega_0 \sum_{n,\alpha} a_{n,\alpha}^\dagger a_{n,\alpha}$). We can set $\omega_0 = 0$ as the energy reference so that we can discard free cavity dynamics.

[3] Everything is Hermitian up to now, we will add non-Hermiticity later on.

Diagonalizing $h_{\rm f}(k)$ one gets $D(k) = U h_{\rm f}(k) U^\dagger$ where $D(k) = {\rm diag}[E_1(k), \dots, E_{N_{\rm c}}(k)]$, $E_\alpha(k)$'s being the *bands* of the lattice.

This way the field Hamiltonian can be put in diagonal form

$$H_{\rm f} = \sum_k \Psi_k^\dagger D(k) \Psi_k \tag{4.12}$$

where

$$\Psi_k^\dagger = \left( \tilde{a}_{k,1}^\dagger, \dots, \tilde{a}_{k,N_{\rm c}}^\dagger \right) U^\dagger \,. \tag{4.13}$$

The *structure* of this photonic bath stems from the fact that, having bands, then *band gaps* may occur. Band gap closings, by tuning a system parameter, is a way for distinguishing between different topological phases [92, 95].

The final term in Eq. (4.8) describes the atom-cavity interaction under the same assumptions of Sec. 4.1. We write here the kind of interaction where a single emitter can in principle exchange excitation with multiple cavities (*giant atom*) with hopping rate $g$

$$H_{\rm int} = g \sum_{i=1}^{N_{\rm e}} \left( \sigma_i^\dagger \sum_{j=1}^{N_i} a_{n_j,\alpha_j} + {\rm H.c.} \right) \tag{4.14}$$

where $N_i$ is the number of coupling points of atom $i$: if $N_i = 1$ then it is locally coupled to one cavity, otherwise it is a giant atom [96] (usually two are considered). This interaction is of Jaynes-Cummings type, see Eq. (4.1)

### 4.2.1 Atom-photon dressed states

In Sec. 4.1, we saw how in cavity QED the eigenstates of the system are given by a superposition of atomic and photonic bare states, that is how the photon dresses the atom. In particular the lower energy dressed state in the Jaynes-Cummings model in the single-excitation subspace can be written to first order in $g$ as

$$|-\rangle = |e\rangle\,|0\rangle - \frac{g}{2\Delta}\,|g\rangle\,|1\rangle \,. \tag{4.15}$$

That is, the atomic eigenstate $|e\rangle$ is modified by the interaction acquiring a *small* photonic part. In the one-excitation sector one usually adopts a lighter notation where $|e\rangle$ is the state with the excitation being in the atomic component and the field in the vacuum, i.e. $|e\rangle\,|{\rm vac}\rangle$. The state $|n\rangle$ is instead the one where the excitation is in the $n$th cavity, i.e. $a_n^\dagger\,|g\rangle\,|{\rm vac}\rangle$.

Analogous considerations hold in waveguide QED. Without atom-interaction the bare eigenstates are $|e\rangle$ and $\{|k\rangle\}$ where the latter are field's eigenstates[4]. Indeed, when the atom-field interaction is turned on (weak coupling)[5], the bare eigenstates change as [97][6]

$$|e\rangle \;\to\; |\Psi_\mu\rangle \equiv |e\rangle + g\,|\varphi_{\rm ph}\rangle = |e\rangle + g\,\hat{G}_{\rm f}(\omega_\mu)\,|n,\alpha\rangle \,, \tag{4.16}$$

$$|k\rangle \;\to\; \left|k^+\right\rangle \equiv |k\rangle + \hat{G}^+(\omega_k) H_{\rm int}\,|k\rangle \,. \tag{4.17}$$

with energies $\omega_\mu$ and $\omega_k$, respectively.

[4] Observe that since the photonic lattice is translationally invariant, $|k\rangle$ are obtained through Bloch's theorem and are delocalized wave functions spread on the entire lattice. Moreover, even under open boundary conditions ($N < \infty$), if $N$ is sufficiently large the eigenstates are still delocalized wavefuction spread on the lattice. Therefore, the profile of free photonic eigenstates does not change substantially from periodic to open boundary condition for a sufficiently large lattice. We highlight this property here as this dramatically changes for a special class of non-Hermitian Hamiltonians [4].

[5] We consider here local coupling for simplicity.

[6] We are being sketchy on purpose here.

In these equations

$$\hat{G}(z) = \frac{1}{z - H} \tag{4.18}$$

is the Green's function [97] of Hamiltonian $H$ (same goes for the Green's function $\hat{G}_{\rm f}(z)$ corresponding to $H_{\rm f}$). Eq. (4.16) expresses the fact that, as in Eq. (4.15), the bare atomic eigenstate acquires a photonic component

$$|\varphi_{\rm ph}\rangle = \hat{G}_{\rm f}(\omega_\mu)\,|n,\alpha\rangle\ , \tag{4.19}$$

where $\omega_\mu$'s are the discrete poles of $\hat{G}(z)$, that is the energies of these new eigenstates $|\Psi_\mu\rangle$ (they are generally more than one), and $|n,\alpha\rangle$ labels the lattice site of the cavity to which the atom is coupled to.

Similarly, Eq. (4.17) expresses how the unbound modes $|k\rangle$ are modified by the interaction ($g$ is hidden into $H_{\rm int}$) and $\omega_k$ are the corresponding energies (observe that in thermodynamic limit $|k^+\rangle$'s are eigenstates of $H$ with the same energies $\omega_k$'s of the unperturbed modes $|k\rangle$'s), while

$$\hat{G}^+(\omega_k) = \lim_{\varepsilon\to 0} \hat{G}(\omega_k + i\varepsilon)\,. \tag{4.20}$$

The single photon dressed states $|\Psi_\mu\rangle$ are responsible for non-Markovian behaviors of atomic decay such as Rabi oscillations [91] and fractional decay [92,98]. Finally, they can mediate interactions in the case of many emitters coupled to the waveguide.

### 4.2.2 Dipole-dipole mediated Hamiltonian

In the case of many emitters coupled to the same photonic bath, which are not directly coupled to each other, it turns out that their common environment can mediate an interaction among them [99–102]. Indeed, one of the interests in waveguide QED is devising unconventional atom-atom interaction by properly structuring the photonic bath they are coupled to. A recent example of this has been the realization of topological interaction in a tight-binding photonic lattice with staggered coupling (SSH model) [92,93]. By placing the atomic frequency in the middle of the bandgap it is possible to implement a topologically dependent coherent interaction among atoms [92].

The dipole-dipole interaction is mediated by the previously described atom-photon dressed states [90,93,103] following this scheme: emitter $i$ induces its own dressed state $|\Psi_i\rangle$; if emitter $j$ is coupled to the $(n_j,\alpha_j)$th cavity and $\langle n_j,\alpha_j|\Psi_i\rangle \neq 0$ then emitter $j$ is coupled to emitter $i$, with coupling strength proportional to the overlap $\langle n_j,\alpha_j|\Psi_i\rangle$, and vice versa. More specifically, as we will discuss in the following chapter, the effective atomic Hamiltonian $\mathcal{H}$ has matrix elements

$$\mathcal{H}_{ij} = g\,\langle n_i,\alpha_i|\Psi_j\rangle \tag{4.21}$$

describing the hopping amplitude from emitter $j$ to emitter $i$.

In light of the discussion in the previous section, it is important to highlight the relation between $\mathcal{H}$ and the normal modes of the bare lattice. As discussed in Ref. [94], assuming for simplicity local atom-cavity coupling of the form

$$H_{\rm int} = g\sum_{i=1}^{N_{\rm e}} \left(\sigma_i^\dagger a_{n_i,\alpha_i} + \text{H.c.}\right) \tag{4.22}$$

we get

$$\begin{aligned}\mathcal{H}_{ij} &= \langle \mathrm{vac}|\, \sigma_i H_{\mathrm{int}} \frac{1}{\Delta - H_{\mathrm{f}}} H_{\mathrm{int}} \sigma_j^\dagger \,|\mathrm{vac}\rangle \\ &= \langle \mathrm{vac}|\, \sigma_i H_{\mathrm{int}} \sum_k |k\rangle\langle k| \, \frac{1}{\Delta - H_{\mathrm{f}}} \sum_k |k\rangle\langle k| \, H_{\mathrm{int}} \sigma_j^\dagger \,|\mathrm{vac}\rangle \\ &= \sum_k \frac{\langle \mathrm{vac}|\, \sigma_i H_{\mathrm{int}} \,|k\rangle \, \langle k|\, H_{\mathrm{int}} \sigma_j^\dagger \,|\mathrm{vac}\rangle}{\Delta - \omega_k} = g^2 \sum_k \frac{\langle n_i, \alpha_i|k\rangle \, \langle k|n_j, \alpha_j\rangle}{\Delta - \omega_k} \end{aligned} \tag{4.23}$$

where $|\mathrm{vac}\rangle$ is the vacuum state of the whole atom-field system, $\Delta$ is the atomic frequency (it is not very relevant for the point we want to make here) and the completeness relation has been used [cf. Eq. (1.3)] with $|k\rangle$'s being the eigenstates of $H_{\mathrm{f}}$.

Eq. (4.23) highlights the fact that the interaction among emitters $i$ and $j$ depends on the overlap of the corresponding cavities they are coupled to with the normal modes of the bare field. Of course Eqs. (4.23) and (4.21) are equivalent as going on with the calculations in Eq. (4.23) one gets

$$\mathcal{H}_{ij} = g^2 \, \langle n_i, \alpha_i| \sum_k \frac{|k\rangle\langle k|}{\Delta - \omega_k} \, |n_j, \alpha_j\rangle = g^2 \, \langle n_i, \alpha_i| \, \hat{G}_{\mathrm{f}}(\Delta) \, |n_j, \alpha_j\rangle = g \, \langle n_i, \alpha_i|\Psi_j\rangle \tag{4.24}$$

where we used Eq. (4.16) and set the atomic energy in resonance with the dressed state ($\Delta = \omega_\mu$). As discussed in the previous section, if the photonic lattice is large enough, the normal modes change only slightly in passing from periodic to open boundary conditions[7]. This is intuitive from the physical viewpoint, as the interaction between two emitters deep in the bulk cannot depend on the boundary conditions of the field[8].

Notwithstanding, regardless of how fancy and complicated the photonic lattice structure, the mediated atom-atom coupling will be either reciprocal, so that besides dissipation terms (possibly appearing if atoms couple to modes with velocity, that is if the atomic energy lies in a band), the induced emitter Hamiltonian is always Hermitian, or, if non-reciprocal, interactions will typically be long-range [104, 105].

In addition, a general result under our working hypothesis shows that the interaction strength decreases exponentially with emitter-emitter distance [94], since the photonic component is typically exponentially localized.

[7] Except for edge modes, if any.

[8] This property matters as for a certain class of non-Hermitian tight binding lattices, in passing from periodic to open boundary conditions, the bulk eigenstates' profile can change drastically, a phenomenon known as *non-Hermitian skin effect* [4]. This behavior may change the single elements in the sum in Eq. (4.23), however the coupling is obtained by summing over all possible contributions.

# Chapter 5

# Exotic QED in a non-Hermitian waveguide

In the previous chapter we always assumed that the whole system, atoms and waveguide, was closed. Indeed the Hamiltonian appearing in Eq. (4.8) is Hermitian.

The results we are going to discuss in this chapter concern instead the case where non-Hermiticity comes into the game. This is not just a philosophical question, but actually well motivated by the following facts:

(*i*) whenever one considers an array of coupled cavities it is always important to assess how the observed effects are affected by dissipation on the cavities [91],

(*ii*) it has been shown how patterned dissipation (that is, only some specific cavities are assumed to have a low $Q$ factor) and reservoir engineering can lead to non-reciprocity in specific models [4, 106],

(*iii*) a non-uniform dissipation pattern yield exceptional points in the non-Hermitian field Hamiltonian. This last point was a major motivation for the following study as the harnessing of exceptional points in quantum nanophotonics, currently of great interests [8].

## 5.1 Introduction

The dissipation of energy into an external environment is traditionally regarded as a detriment in physics as it usually spoils the presence of several phenomena, particularly quantum coherence. As we outlined in the previous chapters, a longstanding tool for describing detrimental effects are non-Hermitian (NH) Hamiltonians [28].

In recent years it was realized and experimentally confirmed that systems described by NH Hamiltonians can exhibit under suitable conditions a variety of exotic phenomena [6, 14]. Among these are: coalescence of eigenstates at exceptional points [8] (cf. Chap. 2), unconventional geometric phase [107], breakdown of bulk-boundary correspondence [108], critical behavior of quantum correlations around exceptional points [20, 55, 109], non-Hermitian skin effect [110].

As a consequence, well-established concepts as the Bloch theory of bands and even the very notion of "bulk" may require a revision in non-Hermitian physics [111]. Such NH effects are widely studied in several areas (such as mechanics, acoustics, electrical circuits, biological systems) [6] and, most importantly in view of what we are going to show here, optics and photonics [112, 113].

In this chapter, we investigate NH physics in a setup where a set of emitters (such as atoms, superconducting qubits or resonators) are coupled to a photonic lattice, implemented by an array of coupled cavities [91,99,100,102,103,114–121].

The range and strength of these second-order interactions come from the profile of atom-photon dressed states (usually arising within photonic bandgaps) which in turn depends on the lattice *structure* [122]. Experimental realizations have been demonstrated in various architectures such as circuit QED [123–125], cold atoms coupled to photonic crystal waveguides [126] and optical lattices [127,128].

Assessing the effect of photon leakage in quantum optics setups is a routine task, even through NH Hamiltonians (see e.g. Ref. [116]), the typical configuration considered is that of uniform losses.

In contrast, here we consider an engineered *pattern* of photonic losses so as to affect the photonic normal modes' profile. The basic question we address is whether and to what extent shaping the field structure through patterned leakage (besides photonic hopping rates) can affect the nature of atom-photon interactions, hence photon-mediated couplings.

In light of the discussion at the end of the previous chapter, we know this might be the case for two reasons at least: normal modes might be highly affected by the field's boundary conditions and, most importantly, in non-Hermitian Hamiltonians left eigenstates are not the bras of right eigenstates. The generalization of Eq. (4.23) to a non-Hermitian bath Hamiltonian becomes

$$\mathcal{H}_{ij} = g^2 \sum_k \frac{\langle n_i, \alpha_i | k_\mathrm{R} \rangle \langle k_\mathrm{L} | n_j, \alpha_j \rangle}{[\Delta - \omega_k] \langle k_\mathrm{L} | k_\mathrm{R} \rangle} \tag{5.1}$$

where $|k_{\mathrm{R,L}}\rangle$ are the right and left eigenstates of $H_\mathrm{f}$, i.e.

$$H_\mathrm{f} |k_\mathrm{R}\rangle = \omega_k |k_\mathrm{R}\rangle \tag{5.2}$$

$$\langle k_\mathrm{L}| H_\mathrm{f} = \omega_k \langle k_\mathrm{L}| \tag{5.3}$$

and the biorthogonal completeness relation

$$\mathbb{1} = \sum_k \frac{|k_\mathrm{R}\rangle\langle k_\mathrm{L}|}{\langle k_\mathrm{L}|k_\mathrm{R}\rangle} \tag{5.4}$$

has been used.

Considering a paradigmatic case study, we will show that photons can mediate dissipative non-reciprocal interactions between the emitters with unconventional features such as:

(*i*) loss-dependent interaction range (from purely long-range to purely nearest-neighbour),

(*ii*) formation of short- and long-range metastable atom-photon dressed states

(*iii*) insensitivity to the field boundary conditions (BCs).

## 5.2 Setup and Hamiltonian

The setup we consider [see Fig. 5.1(a)] comprises a composite 1D photonic lattice (coupled-cavity array), whose unit cell consists of a pair of cavities labeled by $a$ and $b$. Importantly, only $b$ cavities are dissipative, the associated loss rate being $\gamma$. By denoting with $a_n$ ($b_n$) the bosonic annihilation operator of cavity $a$ ($b$) in the $n$th cell, the bare Hamiltonian of the field reads (we set $\hbar = 1$)

$$H_\mathrm{f} = \sum_{n=1}^{N} \left[ t_1 a_n^\dagger b_n + \frac{t_2}{2} \left( a_n^\dagger b_{n+1} + b_n^\dagger a_{n+1} - i a_n^\dagger a_{n+1} + i b_n^\dagger b_{n+1} \right) + \text{ H.c.} \right] - i\gamma b_n^\dagger b_n \,. \tag{5.5}$$

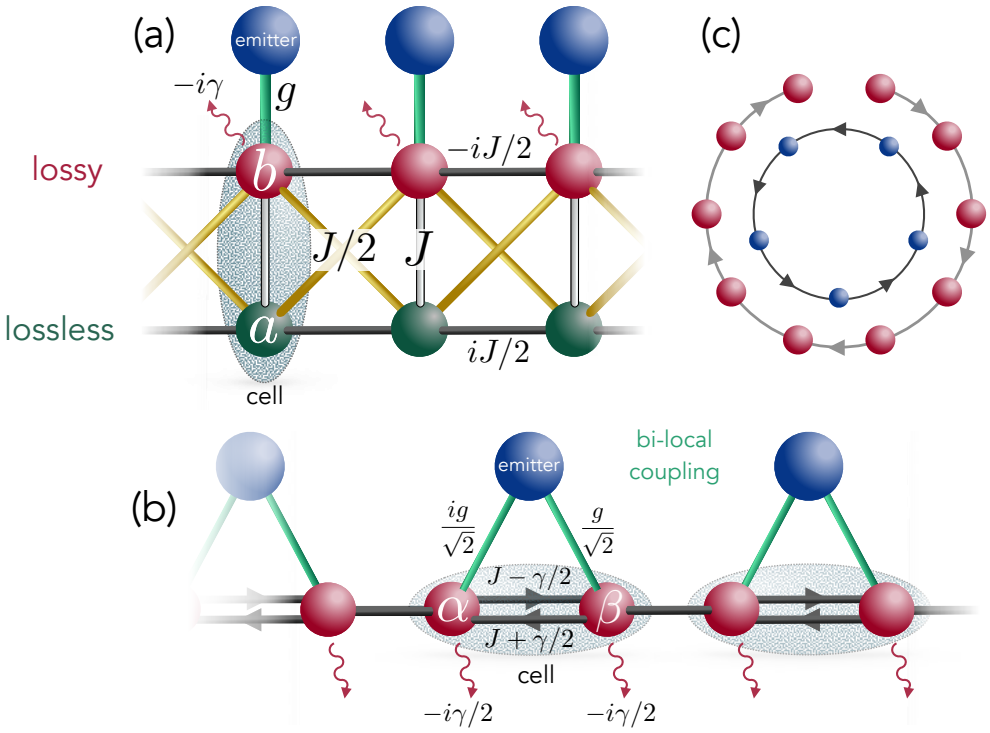


Figure 5.1: (a): Setup: photonic lattice with unit cell comprising a pair of cavities labeled $a$ (lossless) and $b$ (lossy). Each quantum emitter is locally coupled to a lossy cavity. (b): Same setup as (a) in the picture defined by the unitary (intra-cell) transformation (5.8). All cavities are now lossy with uniform loss rate $\gamma/2$ while intra-cell couplings are non-reciprocal. The bare photonic lattice is a non-Hermitian generalization of the SSH model. Each emitter now couples to the lattice at *two* different sites whose respective couplings differ by a $\pi/2$ phase. (c): Schematics of the bare field Hamiltonian $H_{\mathrm{f}}$ (odd $N$) under open BCs (open loop) and the corresponding induced effective Hamiltonian of the emitters, $H_{\mathrm{eff}}$ (closed loop) for $N_{\mathrm{e}} = N$, and $\gamma = 2J$. Both Hamiltonians feature fully non-reciprocal couplings but with opposite chirality, where $H_{\mathrm{eff}}$ in particular implements a dissipative Hatano-Nelson model. Remarkably, $H_{\mathrm{eff}}$ is translationally invariant despite the bare field (hence the total system) breaks translational invariance.

with $N$ the numbers of lattice cells. We will mostly be concerned with the case $t_1 = t_2 = J$ for which $H_\mathrm{f}$ becomes

$$H_\mathrm{f} = \frac{J}{2}\sum_{n=1}^{N}\left[a_n^\dagger b_{n+1} + b_n^\dagger a_{n+1} - i a_n^\dagger a_{n+1} + i b_n^\dagger b_{n+1} + 2a_n^\dagger b_n + \mathrm{H.c.}\right] - i\gamma\sum_{n=1}^{N} b_n^\dagger b_n\,. \quad (5.6)$$

We will consider the general case in Eq. (5.5) only when the parameters $t_{1,2}$ will be kept explicit. The first four terms in Eq. (5.6) describe the interaction between neighbouring cells, i.e. the $a$-$a$ and $b$-$b$ horizontal couplings and the $a$-$b$ diagonal couplings with strength $J/2$ [see Fig. 5.1(a)]. The fifth term and its Hermitian conjugate describe the intra-cell interaction, i.e. the vertical $a$-$b$ couplings (strength $J$), whereas the last term accounts for the local losses on $b$ cavities.

Note that for $\gamma = 0$ we would have $H_\mathrm{f}^\dagger = H_\mathrm{f}$, namely field's non-Hermiticity comes only from the local losses on $b$ cavities (the overall setup is then passive). Model (5.6) is well-known in the non-Hermitian physics literature as *Lee model* [4, 108], though usually considered with local gain on one sublattice and local losses on the other.

### 5.2.1 Energy spectrum of the bare photonic lattice

Before going on, we want to highlight spectral properties of the bare field alone. A distinctive and counterintuitive feature of certain non-Hermitian tight-binding models, more precisely those having a point gap spectrum under periodic BCs [129], is a high sensitivity of the spectrum to boundary conditions (BCs) [4]. Indeed, one can check that under periodic BCs the spectrum of (5.5) is topologically non-trivial exhibiting a line gap (for $t_2 \neq t_1$) and a point gap (for $\gamma > 0$), see Fig. 5.2.

On the contrary, the spectrum under open BCs is always trivial in terms of point-gap topology. This discrepancy implies that the appearance of EPs depends on the BCs: under periodic BCs $H_\mathrm{f}$ is always diagonalizable, while under open BCs it exhibits an EP at $\gamma = 2t_1$ (i.e. at $\gamma = 2J$ for $t_1 = t_2 = J$ as considered in the main text).

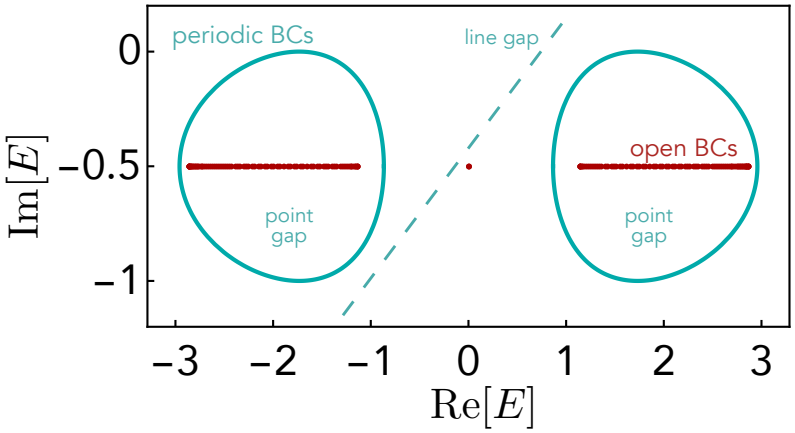


Figure 5.2: *Energy spectrum of the bare lattice.* Under periodic BCs the field energy spectrum can exhibit a line and point gap [$t_2 = 2t_1$, $\gamma = t_1$] (cyan). High sensitivuty to BCs is manifest in that the spectrum of the field under open BCs (red) is a topologically different curve in the complex $(\mathrm{Re}[E], \mathrm{Im}[E])$ plane.

### 5.2.2 Atom-photon interaction

The system we want to consider comprises $N_\mathrm{e}$ identical two-level quantum emitters ("atoms"), each locally coupled under the rotating wave approximation to a dissipative

cavity $b$ [see Fig. 5.1(a)]. The total Hamiltonian is thus

$$H = H_{\rm f} + \sum_{i=1}^{N_{\rm e}} g\,(\sigma_i^\dagger b_{n_i} + b_{n_i}^\dagger \sigma_i) \tag{5.7}$$

with $n_i$ the cavity directly coupled to the $i$th atom and where $\sigma_i = |g\rangle_i\langle e|$ is the pseudo-spin ladder operator of the $i$th atom with $|g\rangle$ and $|e\rangle$ respectively the ground and excited states. The free atoms and cavities' Hamiltonian are respectively $\omega_e \sum_i \sigma_i^\dagger \sigma_i$ and $\omega_0 \sum_n (a_n^\dagger a_n + b_n^\dagger b_n)$, but we take $\omega_0 = 0$ as energy reference and set the atoms in resonance with the cavities $\omega_e = \omega_0$.

The physical properties which we are going to focus on involve only a single excitation and are thus insensitive to the nature of ladder operators $\sigma_i$ of the emitters, which could thus be thought as cavities/oscillators themselves [130, 131]. This system may as well be implemented in an all-photonic scenario.

A key feature of the bare photonic lattice [cf. Fig. 5.1(a) and Hamiltonian $H_{\rm f}$] is that, for $\gamma \neq 0$, photons propagate preferably from right to left in a *non-reciprocal* fashion. Thus losses endow the structure with an intrinsic left-right asymmetry. It is possible to show that, in the lossless case, the complex $a - a$ couplings energetically favor left propagating photons and the $b - b$ couplings favour right propagating ones.

Indeed, under the standard Peierls substitution (see e.g. Refs. [132]), the kinetic energy associated to a hopping term is minimized by the momentum $k = \theta$, where $\theta$ is the complex phase of the hopping amplitude, which is $\theta = -\pi/2$ for the $a-a$ couplings and $\theta = \pi/2$ for the $b-b$ couplings. Turning on dissipation (i.e. for $\gamma \neq 0$) the left-right symmetry is broken because right-propagating photons (lying predominantly on $b$ sites) are more subject to dissipation than left-propagating ones. This effectively results in photons propagating leftwards with higher probability than rightwards.

### 5.2.3 Mapping to a non-Hermitian SSH lattice

Such a dissipation-induced non-reciprocity, which was shown also in other lattices (see e.g. Ref. [106, 133]), can be formally derived by performing the field transformation [4] $\{a_n, b_n\} \to \{\alpha_n, \beta_n\}$ with

$$a_n = \tfrac{1}{\sqrt{2}}(\alpha_n - i\beta_n)\,, \quad b_n = -\tfrac{i}{\sqrt{2}}(\alpha_n + i\beta_n)\,. \tag{5.8}$$

This unitary transformation, which is local in each unit cell in that it mixes cavity modes $a_n$ and $b_n$, defines a new picture where the free field Hamiltonian now reads [see Fig. 5.1(b)]

$$H_{\rm f}' = \sum_n \left[\left(J + \frac{\gamma}{2}\right)\alpha_n^\dagger \beta_n + \left(J - \frac{\gamma}{2}\right)\beta_n^\dagger \alpha_n + J\,(\alpha_{n+1}^\dagger \beta_n + \text{H.c.})\right] - i\frac{\gamma}{2}\sum_n (\alpha_n^\dagger \alpha_n + \beta_n^\dagger \beta_n). \tag{5.9}$$

This tight-binding Hamiltonian is a non-Hermitian version of the Su–Schrieffer–Heeger (SSH) model [4, 134]. In contrast to the original picture, $H_{\rm f}'$ presents uniform loss on *all* cavities with rate $\gamma/2$. Notably, intra-cell couplings are now explicitly *non-reciprocal* for non-zero $\gamma$: the hopping rate of a photon from site $\alpha_n$ to $\beta_n$ differs from that from $\beta_n$ to $\alpha_n$ (respectively $J + \frac{\gamma}{2}$ and $J - \frac{\gamma}{2}$). Inter-cell couplings $J$ are instead reciprocal.

Whenever $\gamma \neq 0$ [non-zero cavity leakage in the original picture, see Fig. 5.1(a)] the mapped lattice features an intrinsic chirality (i.e. non-reciprocity) as the rate of photon hopping depends on the direction (rightward or leftward). At the critical value $\gamma = 2J$, corresponding to an exceptional point (EP) of the bare lattice [108] (as anticipated above), the intra-cell couplings are fully non-reciprocal (all couplings $\alpha_n \to \beta_n$ vanish). Thus at this EP photons can only propagate leftwards.

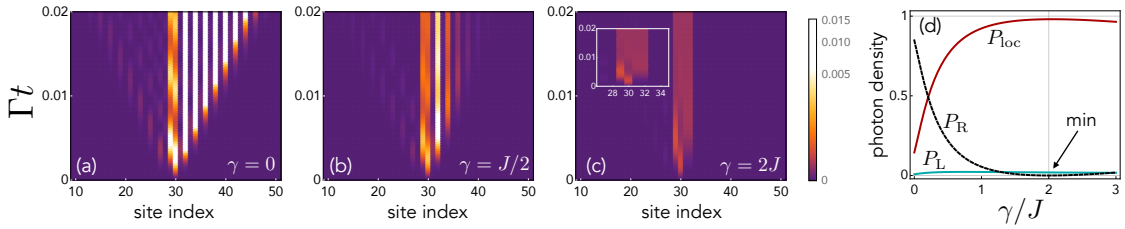


Figure 5.3: *Field dynamics during spontaneous emission.* (a)-(c): Spatial profile of photon density $|\langle\eta_n|\,|\Psi_t\rangle\,|^2$ versus time, where $|\Psi_t\rangle = e^{-iHt}\,|\Psi_0\rangle$, $|\eta_n\rangle = |g\rangle\,\eta_n^\dagger\,|\text{vac}\rangle$, $\eta = a, b$ [referring to the original picture of Fig. 5.1(a)]. In the plots, we re-indexed cavities in a way that neutral (lossy) cavities are labeled by odd (even) site indexes. We set $g = 0.1J$ and $N = 100$ with the atom coupled to the lossy cavity of cell $n = 15$ [see Fig. 5.1(a)]. Time is measured in units of $\Gamma^{-1}$ with $\Gamma = g^2/(4J)$. The atom's excited-state population $p_e = |\langle e|\langle\text{vac}|\,|\Psi_t\rangle\,|^2$ decays exponentially as $p_e(t) = e^{-\Gamma t}$. (d): Functional dependence of $P_{\text{loc}}$, $P_{\text{R}}$ and $P_{\text{L}}$ on the loss rate $\gamma/J$ (where each probability is rescaled to the sum $P_{\text{L}} + P_{\text{loc}} + P_{\text{R}}$). Here, $P_{\text{loc}}$ is the time-averaged probability to find the photon in the cell where the atom lies or the right nearest-neighbour cell (four cavities overall), while $P_{\text{L}}$ ($P_{\text{R}}$) is the probability to find it in the remaining left (right) part of the lattice. We set an average time $t_{\text{av}} \sim 20J^{-1}$ with $g$ small enough such that $t_{\text{av}} < \Gamma^{-1}$.

Consider the *total* Hamiltonian in the new picture, which using (5.8) reads [cf. Eqs. (5.7) and (5.9)]

$$H' = H'_{\text{f}} + \sum_{i=1}^{N_e} \frac{g}{\sqrt{2}} \left(\sigma_i^\dagger(\beta_{n_i} - i\alpha_{n_i}) + \text{H.c.}\right) . \tag{5.10}$$

Remarkably [see Fig. 5.1(b)] in the new picture the atom-photon interaction is no longer local as each atom is coupled to *both* cavities $\alpha$ and $\beta$ of the same cell (the atom is now *giant*, see Sec. 4.2). The corresponding (complex) couplings have the same strength but, importantly, a $\pi/2$ phase difference.

In conclusion, in the picture defined by (5.8), the system presents:

($i$) uniform losses,

($ii$) intra-cell non-reciprocal photon hopping amplitudes,

($iii$) bi-local atom-field coupling with a $\pi/2$ phase difference.

These three factors together are the key to the occurrence of the phenomena we are going to discuss.

## 5.3 Spontaneous emission of one emitter

We first consider only a single emitter ($N_{\text{e}} = 1$) and study spontaneous emission (initial joint state $|\Psi_0\rangle = |e\rangle\,|\text{vac}\rangle$ with $|\text{vac}\rangle$ the field's vacuum state) and we set $g \ll J$ (weak coupling). If $\gamma = 0$ (no loss), the bare lattice is effectively equivalent to a standard tight-binding model with uniform nearest-neighbour couplings [see Fig. 5.1(b)] yielding a single frequency band of width $2J$ with the atomic frequency at its center. Figs. 5.3(a)-(c) show the time evolution of the photon density profile across the photonic lattice for different loss rates $\gamma$, while the atom's excited-state population decays exponentially as $p_e = e^{-\Gamma t}$ with $\Gamma = g^2/(4J)$ (not shown in the figure; see caption for details).

In the Hermitian limit $\gamma = 0$ (no loss), chiral emission occurs in that the photon propagates predominantly to the right. This is a known effect [135] due to the bi-local

coupling with a $\pi/2$ phase difference in the picture of Fig. 5.1(b), which effectively suppresses the interaction of the emitter with left-going modes of the field. As the loss rate $\gamma$ is increased, the behaviour substantially changes [see Figs. 5.3(b)-(c)]. Based on the previously discussed non-reciprocity of intra-cell couplings [see Fig. 5.1(b)], one might now expect the emitted photon to propagate away mostly to the left (in contrast to the $\gamma = 0$ case). This behaviour is generally exhibited only by a tiny fraction of emitted light.

Instead, a significant part *localizes* within a very definite region of the lattice and eventually leaks out on a long time scale of the order of $\Gamma^{-1} \gg \gamma^{-1}$. This light localization dominates for $\gamma = 2J$ [see Fig. 5.1(c)], and at this value it strictly occurs in two cells only: the one directly coupled to the atom and the nearest neighbour on the right. This is illustrated in Fig. 5.3(d), where the time-averaged fraction of light localization in these two cells ($P_{\rm loc}$) is plotted versus $\gamma/J$ along with the fraction lying in the remaining left and right part of the lattice ($P_L$ and $P_R$, respectively). Observe that $P_{\rm loc}$ reaches its maximum at the EP, where $P_R = 0$ and $P_L \simeq 0$ (for $g \to 0$, $P_L \to 0$).

## 5.4 Many emitters

We consider first two quantum emitters and describe the (dissipative) dynamics of excitation transfer between them when one is initially in the excited state and the other is in the ground state. We again set $\gamma = 2J$ [see Fig. 5.1(b)], so that the photonic lattice features an intrinsic *leftward* chirality.

If the emitters lie in nearest-neighbour cells [see Fig. 5.4(a)], an excitation initially on the left atom is partially transferred to the right atom with a characteristic rate $\sim\Gamma$ with both emitters eventually decaying to the ground state (transfer is only partial because of dissipation). Remarkably, as shown in Fig. 5.4(b), the reverse process does not occur: if the excitation now sits on the right emitter, this simply decays to the ground state with the left atom remaining unexcited all the time.

Therefore, the field mediates a completely *non-reciprocal* (dissipative) interaction between the atoms. One might expect this second-order interaction to straightforwardly follow from the aforementioned intrinsic non-reciprocity of the bare lattice [recall Fig. 5.3(b) for $\gamma = 2J$]. However, note that the directionality resulting from Figs. 5.4(a) and (b) is *rightward* in opposition to that of the lattice which, as said, is leftward [cf. Fig. 5.3(b)]. In the following, we will show that the lattice unidirectionality is indeed a key ingredient for such a non-reciprocal atomic crosstalk, but – remarkably – not the only one.

Besides being non-reciprocal, the emitters' effective interaction is *exactly* limited to atoms sitting in *nearest-neighbor* cells. This can be checked [see Figs. 5.4(c) and (d)] by placing the emitters in any pair of *non*-nearest-neighbor cells, in which case, no matter what atom is initially excited, no transfer occurs. A relevant exception to this behavior yet appears when the lattice is open and atoms sit just on the two opposite edge cells. In this configuration [see Figs. 5.4(e) and (f)], counter-intuitively, the coupling is again non-zero and fully non-reciprocal. The related strength and directionality is the same (up to a sign) as if the lattice were periodic and the two edge emitters were sitting in nearest-neighbor cells [see Figs. 5.4(a) and (b)].

Analogous results to those in Fig. 5.4 are valid also for many emitters, in particular in the case $N_{\rm e} = N$ (one atom per unit cell). Fig. 5.5 is the $N$-atom analogue of Fig. 5.4(f): it shows how an excitation initially on the $N$th atom (the one on the right edge cell) is first transferred to atom 1 (sitting on the left edge), then atom 2, then 3 and etc. This behavior is of course compatible with nearest-neighbor non-reciprocal (rightward) effective couplings between the atoms where – notably – the emitters on the edges couple to one another as if the lattice were translationally invariant (ring). In fact, it can be checked that plots in Fig. 5.5 remain *identical* if the lattice is now subject to periodic BCs (no

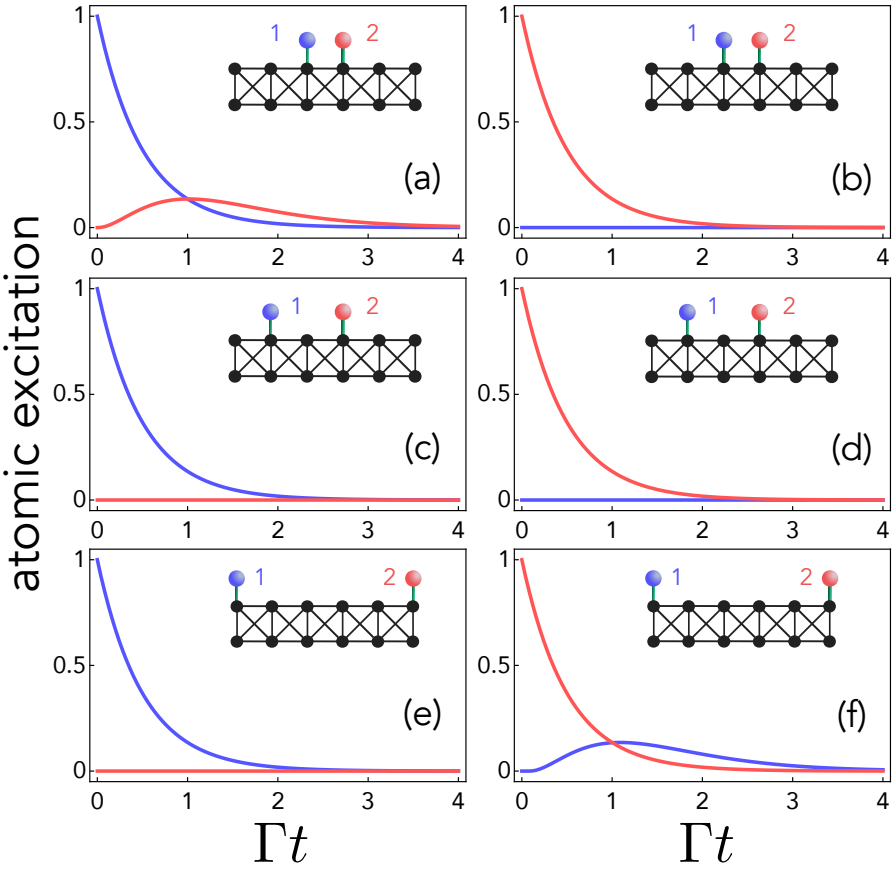


Figure 5.4: *Excitation transfer between two quantum emitters.* We consider a pair of quantum emitters ($N_e = 2$) and set $J = \gamma/2$. We plot the time behavior of the emitter 1's excited-state probability $p_1$ (blue line) and that of emitter 2, $p_2$ (red) for the initial state $|\Psi_0\rangle = |e\rangle_1 |g\rangle_2 |\text{vac}\rangle$ [panels (a), (c), (e)] and $|\Psi_0\rangle = |g\rangle_1 |e\rangle_2 |\text{vac}\rangle$ [panels (b), (d), (f)], where $p_1 = |{}_1\langle e| {}_2\langle g| \langle \text{vac}| |\Psi_t\rangle|^2$ and an analogous definition holds for $p_2$. The inset in each panel shows the cells where the emitters are coupled to: nearest-neighbour cells [panels (a) and (b)], non-nearest-neighbour cells in the bulk [panels (c) and (d)], edge cells [panels (e) and (f)]. We set $g = 0.1J$.

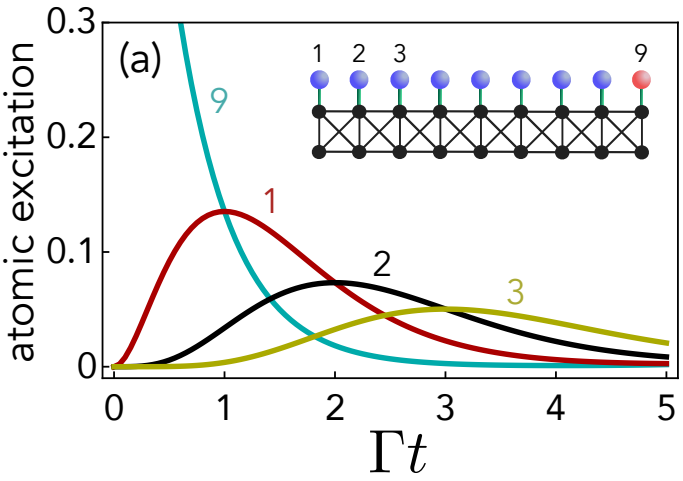


Figure 5.5: *Many-emitter excitation transfer.* We set $N_e = N = 9$ (one emitter/cell) and plot versus time the excited-state probability of atoms $n = 1$ (red line), $n = 2$ (black), $n = 3$ (yellow) and $n = 9$ (cyan) when atom $n = 9$ (sitting on the lattice right edge) is initially excited. We set $g = 0.1J$.

edges) as one would expect.

## 5.5 Effective Hamiltonian

These exotic dynamics are well-described by the effective Hamiltonian of the emitters, which for a bare lattice with periodic BCs reads

$$H_{\rm eff} = \sum_{ij} \mathcal{H}_{n_i n_j}\, \sigma_i^+ \sigma_j \tag{5.11}$$

with

$$\mathcal{H}_{m\neq n} = i\,4g^2 J\,\frac{(\gamma-2J)^{m-n-1}}{(\gamma+2J)^{m-n+1}}\,, \qquad \mathcal{H}_{mm} = -i\frac{g^2}{\gamma+2J} \tag{5.12}$$

where periodic BCs of $H_{\rm eff}$ are understood, i.e. in (5.12) any $n$ is equivalent to $n+N$, so that $H_{\rm eff}$ is *traslationally invariant*.

This non-Hermitian effective Hamiltonian can be derived analytically in the weak-coupling Markovian regime ($g \ll J$) through a straightforward non-Hermitian generalization [130] of the standard resolvent method [28, 94, 97]. For $\gamma > 0$ and $N \gg \lambda$, where we defined the interaction range $\lambda$ as

$$\lambda^{-1} = -\ln\left|\frac{\gamma-2J}{\gamma+2J}\right|\,, \tag{5.13}$$

the elements of $\mathcal{H}_{mn}$ above the main diagonal vanish (i.e. for $m < n$). Therefore, emitter-emitter couplings are non-reciprocal with rightward chirality for all $\gamma > 0$. On the other hand, the interaction range $\lambda$ is strongly dependent on $\gamma$ (see Fig. 5.6). For $\gamma = 0$ (no dissipation) $\lambda$ diverges, showing that couplings are purely long-range [see matrix plot in Fig. 5.6(b)]: all possible pairs of emitters are coupled with the same strength (in modulus) [135] [this can be checked from (5.12) for $\gamma \to 0$]. As $\gamma$ increases, the interaction range reduces until it vanishes at the lattice EP $\gamma = 2J$ – where it exhibits a critical behaviour (see cusp) – and then rises again as $\gamma > 2J$. The zero occurs because at $\gamma = 2J$ [cf. (5.12) for $\gamma \to 2J$] $\mathcal{H}_{m>n}$ is non-zero only for $m = n+1$ where it takes the value

$$\mathcal{H}_{n+1,n} = ig^2/(4J) = i\Gamma \equiv \mathcal{H}_{1N} \tag{5.14}$$

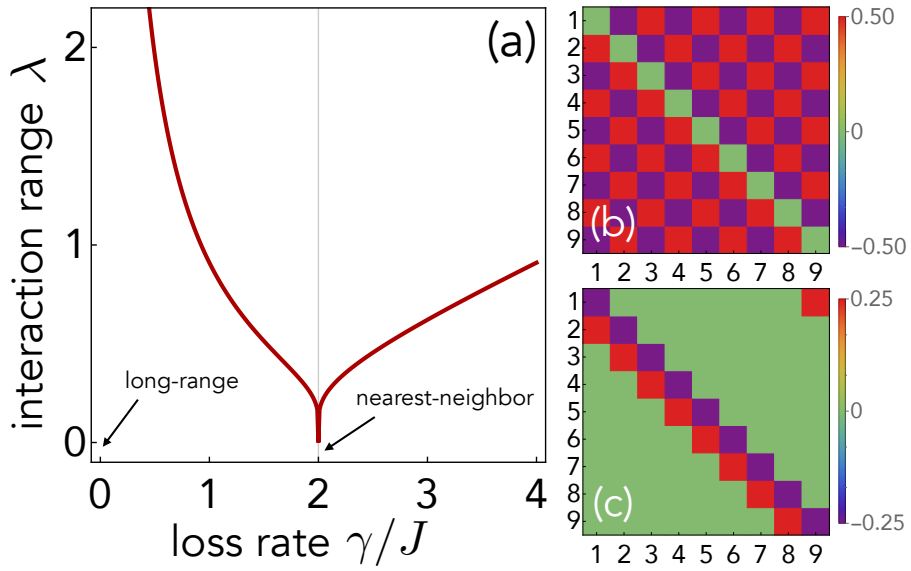


Figure 5.6: *Photon-mediated couplings between emitters.* (a): Interaction range of $H_{\text{eff}}$ (see main text) versus $\gamma$. (b) and (c): Matrix plot of $\mathcal{H}_{mn}$ [cf. (5.12)] (imaginary part) for $\gamma = 0$ (b) and for $\gamma = 2t_1$ (c) in units of $g^2$ (the real part vanishes). In panel (c), note the upper right corner witnessing that $H_{\text{eff}}$ is translationally invariant. All plots are independent of the lattice boundary conditions.

[see matrix plot in Fig. 5.6(c)]. Therefore, at this point in parameter space, besides being effectively periodic (see above), the non-reciprocal interaction between the emitters is *exactly* limited to nearest neighbors: this then is an implementation, cf. Secs 1.2.2- 4.2.2, of the *Hatano-Nelson model* [136] with fully non-reciprocal hopping rates and uniform on-site losses under periodic BCs. The results in Figs. 5.4 and 5.5 fully reflect these properties.

Even more notably and counter-intuitively, it can be demonstrated [see following subsections] that, if $N$ is odd, $H_{\text{eff}}$ is *insensitive to the BCs* of the lattice (matching the results of Fig. 5.5). In other words, even if the lattice is subject to open BCs (ring with a missing cell) $H_{\text{eff}}$ is nevertheless given by (5.11). For even $N$, the hopping rate across the missing cell is modified by just an extra minus sign [see following subsections]. Fig. 5.1(c) sketches the open lattice for $N_{\text{e}} = N$ (one atom per cell) and $\gamma = 2J$: both $H_{\text{f}}$ and $H_{\text{eff}}$ present fully-non-reciprocal couplings yet with opposite directionality and, moreover, $H_{\text{eff}}$ is periodic while $H_{\text{f}}$ is not. We therefore get in particular that photons are able to mediate translationally-invariant interactions between the atoms despite the field (hence the total system) lacking translational invariance.

The reminder of this section is dedicated to the derivation of $H_{\text{eff}}$ via the resolvent method. It is a rather technical section that can be skipped without affecting readability.

### 5.5.1 Derivation of $H_{\text{eff}}$ via the resolvent method

A counter-intuitive property of $H_{\text{eff}}$ is its insensitivity to BCs. We will therefore separately consider both periodic and open BCs and show that the resulting effective Hamiltonian, up to a phase factor is indeed the same in the two cases. It is quite expected, and indeed well-known, that in many Hermitian short-ranged tight-binding models a change in the BCs does not affect the interaction between emitters when both of these sit far away from the boundaries. However, a striking feature of the present model is that this behavior occurs even for emitters sitting next to the edges. In the most extreme case, two emitters lying on the two opposite ends of the open lattice interact as if they where sitting next to each other in a lattice subject to periodic BCs. Note, however, that this

property strictly depends on the weak-coupling approximation, which requires $g \ll J/\sqrt{N}$ (for $t_1 = t_2 = J$).

In light of the previous discussion, in weak-coupling conditions, the effective Hamiltonian $H_{\rm eff}$ of a set of emitters coupled to cavities $b_{n_i}$ and $b_{n_j}$, respectively, can be calculated as [28,92,130]

$$H_{\rm eff} = \sum_{ij} \mathcal{H}_{n_i n_j} \sigma_i^+ \sigma_j^- \tag{5.15}$$

with

$$\mathcal{H}_{nm} \simeq g^2 \langle 0| b_m \hat{G}(E) b_n^\dagger |0\rangle \tag{5.16}$$

where $E$ is the bare frequency of the emitters and

$$\hat{G}(E) := \frac{1}{E - H_{\rm f}} \tag{5.17}$$

is the resolvent operator of the bare lattice (we drop subscript 'f' to simplify the notation), cf. Sec. 4.2.2. For technical reasons, in the derivation of the $H_{\rm eff}$ we need to keep $t_1 \neq t_2$, and we will obtain the case in the main in the limit $t_1 \to t_2 = J$. We will next derive the effective Hamiltonian first when the lattice is subject to periodic boundary conditions (PBCs). Afterward, we will enforce open boundary conditions (OBCs) by introducing an infinite on-site energy (detuning) in a unit cell of the lattice under PBCs. This effectively removes the cell from the periodic lattice, thus effectively turning the geometry into OBCs. In the remainder, we will set $E = 0$ in the calculation of the resolvent (namely we set the energy zero to the emitters' frequency).

### 5.5.2 Calculation of the effective Hamiltonian under PBCs of the lattice

Due to translational invariance, the lattice Hamiltonian under PBCs can be expressed in its Fourier representation as

$$H_{\rm f}^{\rm PB} = \sum_{k=0}^{N-1} \tilde{\Phi}_{q_k}^\dagger \cdot \tilde{H}(e^{iq_k}) \cdot \tilde{\Phi}_{q_k}\,, \qquad \Phi_n := \frac{1}{\sqrt{N}} \sum_{j=0}^{N-1} \tilde{\Phi}_{q_k} e^{-iq_k x}\,, \qquad q_k := \frac{2\pi k}{N}\,. \tag{5.18}$$

where $\Phi_n := (a_n, b_n)^T$ and

$$\tilde{H}(e^{iq}) = \begin{pmatrix} -t_2 \sin q & t_1 + t_2 \cos q \\ t_1 + t_2 \cos q & t_2 \sin q - i\gamma \end{pmatrix} \tag{5.19}$$

is the single particle Hamiltonian in quasi-momentum representation. Correspondingly, the (single-particle) PBCs resolvent in the real-space representation is given by

$$G_{\rm PB}(m-n) := -\langle 0| \Phi_m \frac{1}{H^{\rm PB}} \Phi_n^\dagger |0\rangle = -\frac{1}{N} \sum_{j=0}^{N-1} \frac{e^{iq_k(m-n)}}{\tilde{H}(e^{iq_k})}\,. \tag{5.20}$$

The above expression can be calculated by resorting to the residue theorem as

$$G_{\rm PB}(n) = \frac{1}{2\pi i} \oint_\gamma dw \frac{w^n}{w^N - 1} F(w)\,, \qquad F(w) := -\frac{1}{w\tilde{H}(w)}, \qquad \text{with } e^{iq} \to w \in \mathbb{C} \tag{5.21}$$

where $0 \leq n < N$ and the path of integration $\gamma = \cup_k \gamma_k$ is the collection of small circles $\gamma_k$ centered on $e^{iq_k}$ [1] and it is crucial that none of the poles of $F(w)$ coincides with $q_k$ for $k = 0 \dots N-1$ (see Fig. 5.7). The expression for $F(w)$ is

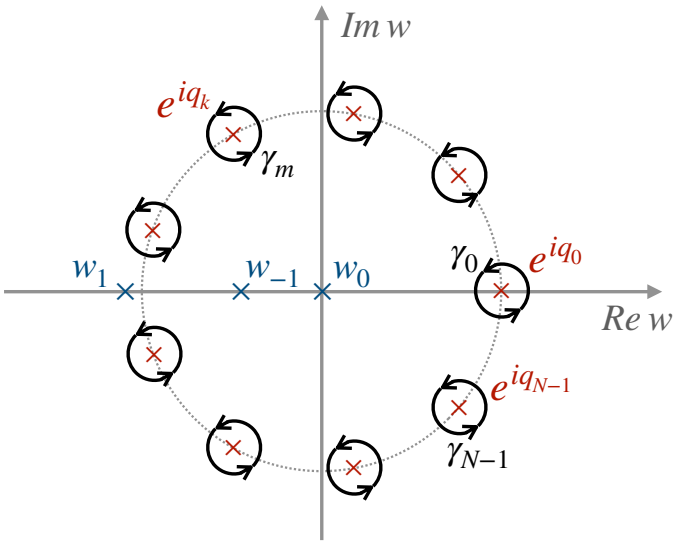


Figure 5.7: *Path of integration*- Sketch of the path of integration for the integral representation (5.21) of the resolvent $G_{\rm PB}$ under PBCs. The path $\gamma = \cup_k \gamma_k$ is the collection of small circles $\gamma_k$ centered on $e^{iq_k}$ with $q_k = \frac{2\pi k}{N}$ and $k = 0 \dots N-1$. Function $F(w)$ has three poles, $|w_{-1}| < 1$, $w_0 = 0$ and $|w_1| \geq 1$ which are distinct from all the poles $\{q_k\}_{k=0}^{N-1}$ unless $N$ is an even integer and $t_1 = t_2$. For $t_1 = t_2$ the pole $w_1 = -1$, which for even values of $N$ coincides with $e^{iq_{N/2}}$. In this case, the derivation of $G_{\rm PB}$ needs to be performed with $t_1 \neq t_2$ and $H_{\rm eff}$ is eventually calculated in the limit $t_1 \to t_2$ (see previous section).

$$F(w) = \frac{W(w)}{P(w)} \qquad W(w) := \begin{pmatrix} i\gamma w - i\frac{t_2}{2}(w^2-1) & t_1 w + \frac{t_2}{2}(w^2+1) \\ t_1 w + \frac{t_2}{2}(w^2+1) & i\frac{t_2}{2}(w^2-1) \end{pmatrix}, \tag{5.22}$$

where $P[w] := \mathrm{Det}[-w\tilde{H}(w)] = aw(w-w_1)(w-w_{-1})$ and $a = -t_2\left(t_1 + \frac{\gamma}{2}\right)$, where

$$w_0 = 0\,, \qquad w_{\pm 1} = -\frac{t_1^2 + t_2^2 \pm \sqrt{\Delta}}{t_2\,(2t_1+\gamma)} \qquad \text{with} \qquad \Delta = (t_1^2 - t_2^2)^2 + \gamma^2 t_2^2\,, \tag{5.23}$$

are the roots of $P(w)$. The roots $\{w_j\}_{j=-1}^{1}$ are the poles of $F(w)$ whose residues $G_j = \underset{w_j}{\mathrm{Res}}[F(w)]$ are given by

$$G_0 = \frac{1}{2t_1 - \gamma}\begin{pmatrix} i & 1 \\ 1 & -i \end{pmatrix}, \qquad G_{\pm 1} = \mp \frac{W(w_{\pm 1})}{w_{\pm 1}\sqrt{\Delta}}\,. \tag{5.24}$$

For $\gamma > 0$ and $t_1 > 0$, one can check that $|w_{-1}| < 1$ and $|w_1| \geq 1$, where the latter inequality is saturated only when $t_1 = t_2$, in which case

$$w_1 \simeq -1\,, \qquad w_{-1} \simeq \kappa\,, \qquad \text{where } \kappa := \frac{\gamma - 2t}{\gamma + 2t}\,. \tag{5.25}$$

[1] If $f(w)$ is analytic in $e^{iq_k}$, one can easily show that

$$\frac{1}{2\pi i}\oint_{\gamma_m} \frac{dw}{w}\frac{f(w)}{w^N-1} = \underset{e^{iq_k}}{\mathrm{Res}}\frac{1}{w}\frac{f(w)}{w^N-1} = \lim_{w\to e^{iq_k}} \frac{1}{w}\frac{w-e^{iq_k}}{w^N-1} f(w) = \lim_{u\to 1}\frac{1}{u}\frac{u-1}{u^N-1} f(ue^{iq_k})$$
$$= \lim_{u\to 1}\sum_{q=0}^{N-1} u^q f(ue^{iq_k}) = Lf(e^{iq_k})$$

One can exploit the residue theorem again to calculate the integral in (5.21) as the residue at infinity minus the sum of the residues on poles different from $e^{iq_k}$, i.e.

$$G_{\rm PB}(n) := -\operatorname*{Res}_{\infty}\left[\frac{w^n}{w^N-1}F(w)\right] - \sum_{j=-1}^{1}\operatorname*{Res}_{w_j}\left[\frac{w^n}{w^N-1}F(w)\right]. \tag{5.26}$$

For $n<N$, the residue at infinity vanishes, since

$$\operatorname*{Res}_{\infty}\left[F(w)\frac{w^n}{w^N-1}\right] = -\operatorname*{Res}_{0}\left[w^{-2}F(w^{-1})\frac{w^{-n}}{w^{-N}-1}\right] = \operatorname*{Res}_{\infty}[F(w)]\lim_{w\to 0}\frac{w^{N-n}}{1-w^N} = 0\,, \tag{5.27}$$

where we used the fact that $\operatorname*{Res}_{\infty}F(w) < \infty$, since $F(w)$ is analytic except for a finite number of isolated poles. *The PBCs resolvent in real-space representation* is then given by

$$G_{\rm PB}(n) = \sum_j \frac{w_j^n}{1-w_j^N}G_j \qquad 0\le n<N\,, \tag{5.28}$$

where $G_j$ are the residues of $F(w)$ given in (5.24).

For the case $t_1 \simeq t_2$, we define $J$ and $\delta$ such that $t_1 = J(1-\delta)$ and $t_2 = J(1+\delta)$. Notice that as $\delta\to 0$, the factor $\frac{1}{1-w_1^N}$ behaves differently with even and odd number of unit cells, with $\frac{1}{1-w_1^N}\sim -\frac{\gamma}{4NJ\delta^2}$ for $N$ even and $\frac{1}{1-w_1^N}\sim \frac{1}{2}-\frac{Nt\delta^2}{\gamma}$ for $N$ odd. Indeed, we will calculate $G_{\rm PB}(n)$ for these two cases separately.

#### 5.5.2.1 $N$ odd

As noticed, *for $N$ odd* $\frac{1}{1-w_1^N}\sim\frac{1}{2}-\frac{Nt\delta^2}{\gamma}$. By inserting (5.24), (5.23) and (5.22) into (5.28) we obtain the explicit expression of the resolvent $G_{\rm PB}$, which in the limit $\delta\to 0$ reads

$$\lim_{\delta\to 0}G_{\rm PB}(n) = \begin{cases} \frac{(-1)^{\bar n}}{2J}\begin{pmatrix} i & 0\\ 0 & 0\end{pmatrix} + \frac{\kappa^{\bar n-1}}{1-\kappa^N}\frac{2}{(\gamma+2J)^2}\begin{pmatrix} -i\frac{\gamma^2}{2J} & -\gamma\\ -\gamma & i2J\end{pmatrix} & \bar n\neq 0\,,\\ \frac{1}{2J}\begin{pmatrix} i & 0\\ 0 & 0\end{pmatrix} + \frac{1}{1-\kappa^N}\frac{2}{\gamma^2-4t^2}\begin{pmatrix} -i\frac{\gamma^2}{2J} & -\gamma\\ -\gamma & i2J\end{pmatrix} + \frac{1}{\gamma-2J}\begin{pmatrix} i & 1\\ 1 & -i\end{pmatrix} & \bar n = 0\,, \end{cases} \tag{5.29}$$

with $\bar n := n\,(\mathrm{mod}\ N)$. For $\gamma>0$, with moderately large values of $N$ ($\delta^{-1}\gg N\gg -1/\ln|\kappa|$ ), the $G_{\rm PB}(n)$ can be formulated in a way which is manifestly chiral, i.e.

$$\lim_{N\to\infty}\lim_{\delta\to 0}G_{\rm PB}(n) = \begin{cases} \frac{(-1)^n}{2J}\begin{pmatrix} i & 0\\ 0 & 0\end{pmatrix} + \frac{2\kappa^{\bar n-1}}{(\gamma+2J)^2}\begin{pmatrix} -i\frac{\gamma^2}{2J} & -\gamma\\ -\gamma & i2J\end{pmatrix} & n>0\,,\\ -\frac{1}{\gamma+2J}\begin{pmatrix} i\frac{\gamma}{2J} & 1\\ 1 & i\end{pmatrix} & n=0\\ -\frac{(-1)^n}{2J}\begin{pmatrix} i & 0\\ 0 & 0\end{pmatrix} & n<0 \end{cases} \tag{5.30}$$

where we relabelled $n=-\frac{N-1}{2}\dots\frac{N-1}{2}$ and neglected contributions smaller than $\kappa^{N/2}$.

#### 5.5.2.2 $N$ even

For $N$ even, we notice that $\frac{1}{1-w_1^N} \sim -\frac{\gamma}{4NJ\delta^2}$. Indeed, the divergence as $\delta \to 0$ is related to a technical assumption in the derivation of $G_{\rm PB}$ which prescribes that none of the poles $w_{\pm 1}$ should coincide with $e^{iq_k}$ for $m = 0 \dots N-1$. This assumption fails for even values of $N$ and $t_1 = t_2$. Indeed, $w_1 = -1$ for $t_1 = t_2$ and $e^{iq_{N/2}} = -1$ for even values of $N$. However, we can derive the resolvent $G_{\rm PB}(n)$ for $\delta \neq 0$ and show that the effective Hamiltonian has a finite and meaningful limit for $\delta \to 0$. Hence, up to the zero-th order in $\delta$

$$\lim_{\delta\to 0} G_{\rm PB}(n) = \begin{cases} \frac{(-1)^{\bar n}}{N} \begin{pmatrix} -i\frac{\gamma}{(2J\delta)^2} + i\frac{N-2\bar n}{2J} & \frac{1}{J\delta} \\ \frac{1}{J\delta} & \frac{i}{\gamma} \end{pmatrix} + \frac{\kappa^{\bar n}-1}{1-\kappa^N} \frac{2}{(\gamma+2J)^2} \begin{pmatrix} -i\frac{\gamma^2}{2J} & -\gamma \\ -\gamma & 2it \end{pmatrix} & \bar n \neq 0\,, \\ \frac{i}{2N} \begin{pmatrix} -i\frac{\gamma}{(2J\delta)^2} + i\frac{N}{2J} & \frac{1}{J\delta} \\ \frac{1}{J\delta} & \frac{i}{\gamma} \end{pmatrix} + \frac{1}{1-\kappa^N} \frac{2}{\gamma^2-4t^2} \begin{pmatrix} -i\frac{\gamma^2}{2J} & -\gamma \\ -\gamma & i2J \end{pmatrix} + \frac{1}{\gamma-2J} \begin{pmatrix} i & 1 \\ 1 & -i \end{pmatrix} & \bar n = 0\,, \end{cases} \tag{5.31}$$

Again, for $\gamma > 0$ and for sufficiently large values of $N$ ($\delta^{-2} \gg N \gg -1/\ln|\kappa|$ ) we can neglect terms of order $1/N$ and $\kappa^N/2$

$$\lim_{N\to\infty}\lim_{\delta\to 0} G_{\rm PB}(n) = \begin{cases} \frac{(-1)^n}{2J} \begin{pmatrix} i - i\frac{\gamma}{4JN\delta^2} & 0 \\ 0 & 0 \end{pmatrix} + \frac{2\kappa^{n-1}}{(\gamma+2J)^2} \begin{pmatrix} -i\frac{\gamma^2}{2J} & -\gamma \\ -\gamma & 2it \end{pmatrix} & n > 0\,, \\ -\frac{1}{2J+\gamma} \begin{pmatrix} i\frac{\gamma}{2J} & 1 \\ 1 & i \end{pmatrix} - \frac{\gamma}{8NJ^2\delta^2} \begin{pmatrix} i & 0 \\ 0 & 0 \end{pmatrix} & n = 0\,, \\ \frac{(-1)^n}{2J} \begin{pmatrix} -i\frac{\gamma}{4JN\delta^2} & 0 \\ 0 & 0 \end{pmatrix} & n < 0\,. \end{cases} \tag{5.32}$$

with a similar notation as in (5.30).

#### 5.5.2.3 Effective Hamiltonian

For $\gamma > 0$ and for sufficiently large values of $N$ ($\delta^{-2} \gg N \gg -1/\ln|\kappa|$ ) we can neglect terms of order $1/N$ and $\kappa^N/2$ in (5.29) and (5.31), and the effective Hamiltonian can be expressed *for both even and odd values of* $N$ as

$$\mathcal{H}^{\rm PB}_{mn} = g^2 G_{\rm PB}(m-n)_{bb} = ig^2 \begin{cases} 4J\frac{(\Gamma-2t)^{\overline{m-n}-1}}{(\gamma+2J)^{\overline{m-n}+1}} & \overline{m-n} \neq 0\,, \\ -\frac{1}{\gamma+2J} & \overline{m-n} = 0\,, \end{cases} \tag{5.33}$$

where $\overline{n-m} := n - m \pmod N$. This expression is the same as Eq. (5.12). The above expression, can also be cast in a form which is manifestly chiral

$$\mathcal{H}^{\rm PB}_{mn} = g^2 G_{\rm PB}(m-n)_{bb} = ig^2 \begin{cases} 4J\frac{(\gamma-2J)^{m-n-1}}{(\gamma+2J)^{m-n+1}} & m > n\,, \\ -\frac{1}{\gamma+2J} & m = n\,, \\ 0 & m < n\,, \end{cases} \tag{5.34}$$

where $-N/2 < m - n < N/2$.

### 5.5.3 Calculation of the effective Hamiltonian under OBCs of the lattice

As mentioned, an $N$-site lattice with OBCs can be realised by removing a cell from a periodic lattice with $N+1$ sites. Thus, the OBCs Hamiltonian $H_{\rm f}^{\rm OB}$ can be effectively

obtained by adding an infinite on-site energy to a single cell, say $n = 0$, to the PBCs Hamiltonian of a $N + 1$-site lattice, i.e.

$$H_{\rm f}^{\rm OB} = H_{\rm f}^{\rm PB} + H_1 \quad \text{with} \quad H_1 = \xi \hat{P} \quad \text{where} \quad \hat{P} = \sum_{\ell} \Phi_0^\dagger \Phi_0 \quad \text{and} \quad \xi \to \infty \,. \tag{5.35}$$

Correspondingly, the resolvent operator $\hat{G}_{\rm OB}(E) := (E - H_{\rm f}^{\rm OB})^{-1}$ can be obtained non-perturbatively as [97]

$$\hat{G}_{\rm OB}(E) = \hat{G}_{\rm PB}(E) - \hat{G}_{\rm PB}(E)\hat{P}\frac{1}{\hat{G}_{\rm PB}(E)}\hat{P}\hat{G}_{\rm PB}(E) \,. \tag{5.36}$$

We are interested in the case $E = 0$, in which case the real-space representation of the resolvent $G_{\rm OB}(m,n) := -\langle 0| \Phi_m \frac{1}{H^{\rm OB}} \Phi_n^\dagger |0\rangle$ takes the form

$$G_{\rm OB}(m,n) = G_{\rm PB}(m-n) - G_{\rm PB}(m) G_{\rm PB}(0)^{-1} G_{\rm PB}(-n) \,. \tag{5.37}$$

Similarly to PBCs, we will calculate the OBCs effective Hamiltonian as $g^2$ times the resolvent operator on the $b$ sublattice [cf. (5.15)], i.e. $\mathcal{H}_{\rm nm}^{\rm OB} = g^2 G_{\rm OB}(m,n)_{bb}$. For the same technical reasons discussed in the PBCs case, we need to treat even and odd values of $N$ separately.

#### 5.5.3.1 N even

Note that an even number of sites $N$ in the OB lattice corresponds to an odd number of sites $N+1$ in the corresponding PB lattice. To evaluate the expression (5.37) it is sufficient to consider the contributions of the resolvent $G_{\rm PB}(n)$ in the neighbourood of $n = 0$, where the potential barrier $H_1$ acts. For simplicity, we will assume $N$ sufficiently large and use the more convenient formulation (5.30) of $G_{\rm PB}$ with $N + 1$ sites. A straightforward calculation leads to

$$\begin{aligned} G_{\rm OB}(m,n)_{bb} &= G_{\rm PB}(m-n)_{bb} - \left[G_{\rm PB}(m) G_{\rm PB}(0)^{-1} G_{\rm PB}(-n)\right]_{bb} \\ &= \begin{cases} -G_{\rm PB}(m-n-1)_{bb} & \text{for } m > 0 \wedge n < 0 \\ G_{\rm PB}(m-n)_{bb} & \text{otherwise} \end{cases} . \end{aligned} \tag{5.38}$$

Due to the vanishing terms of expression (5.30) for $n < 0$, the only non-trivial value of the perturbation $\left[G_{\rm PB}(m) G_{\rm PB}(0)^{-1} G_{\rm PB}(-n)\right]_{bb}$ may come from the case with $m > 0$ and $n < 0$. This case corresponds to cells $m$ and $n$ lying on opposite sides of the potential barrier, with $m > n$. Remarkably, the value assumed by $G_{\rm OB}(m-n)_{bb}$ exactly coincides up to a phase factor with $G_{\rm PB}(m-n-1)_{bb}$. Notice the correspondence $m-n \leftrightarrow m-n-1$ between the OBCs and PBCs lattice. This correctly accounts for the missing elementary cell which has been effectively removed by the potential barrier $H_1$.

#### 5.5.3.2 N odd

Repeating the same calculations for odd values of $N$ and exploiting (5.32) with $N+1$ lattice sites yields a very similar result, i.e.

$$G_{\rm OB}(m,n)_{bb} = \begin{cases} G_{\rm PB}(m-n-1)_{bb} & \text{for } m > 0 \wedge n < 0 \\ G_{\rm PB}(m-n)_{bb} & \text{otherwise} \end{cases} . \tag{5.39}$$

Finally, relabelling the OBCs chain $n \to n-1$ for $n > 0$ and collecting the results for odd and even values of $N$ leads to

$$\mathcal{H}^{\rm OB}_{mn} = \begin{cases} (-1)^{N+1}\mathcal{H}^{\rm PB}_{mn} & m > 0 \wedge n < 0\,, \\ \mathcal{H}^{\rm PB}_{mn} & \text{otherwise}\,. \end{cases} \tag{5.40}$$

The above expression explicitly demostrates that, for $E = 0$, $\gamma > 0$, and $t_1 = t_2 > 0$, the effective Hamiltonian with open boundary conditions coincides up to a minus sign with the effective Hamiltonian with periodic boundary conditions.

As anticipated, a common feature of many Hermitian models with short-range interaction is the insensitivity of the bulk to boundary effects. I.e. for regions sufficiently far away from the borders, most of the dynamical features, such as propagations, interactions between subsystems, etc. are expected to be insensitive to the BCs.

This is not the case here. Remarkably, the effective Hamiltonian of this model displays a striking insensitivity to BCs also in the neighbourhood of the lattice edges. Indeed, (5.40) demonstrates that, even in the extreme case of two emitters coupled to the two opposite ends of the open lattice, these interact to one another as if they where coupled to neighbouring cells in the periodic lattice (up to a sign).

#### 5.5.3.3 OB with finite lattice

All the arguments above relied on the simplifying assumption that $N$ is sufficiently large. However, even relaxing this condition leads to an expression similar to (5.40) above. For example for $N$ even, using (5.29) with $N+1$ yields

$$\begin{aligned} G_{\rm OB}(m,n)_{bb} &= G_{\rm PB}(m-n)_{bb} - \left[G_{\rm PB}(m)G_{\rm PB}(0)^{-1}G_{\rm PB}(-n)\right]_{bb} \\ &= -\frac{1-\kappa^N}{1+\kappa^{N-1}}G_{\rm PB}(m-n-1)_{bb}\,, \end{aligned} \tag{5.41}$$

which shows that the finite-size formula converges exponentially to (5.40), i.e.

$$H^{\rm OB}_{\rm eff}(m,n) = \begin{cases} -\frac{1-\kappa^N}{1+\kappa^{N-1}}H^{\rm PB}_{\rm eff}(m-n-1) & m > 0 \wedge n < 0\,, \\ H^{\rm PB}_{\rm eff}(m-n) & \text{otherwise}\,. \end{cases} \tag{5.42}$$

## 5.6 Atom-photon dressed state

The effective Hamiltonian (5.11), as we anticipated in the previous chapter, can be understood in terms of an atom-photon dressed state $|\Psi\rangle$ mediating a 2nd-order interaction between two generic emitters $i$ and $j$. The resulting $i$-$j$ coupling is non-zero provided that $|\Psi\rangle$ has non-zero amplitude on the location of $j$, as we will show in more details in the following sections. Similar descriptions were successfully adopted for dissipationless interactions in lossless lattices with emitters inside bandgaps [92,99,101,115,118,120,137], in which case, importantly, $|\Psi\rangle$ is stationary. In our lossy gapless (for $t_1 = t_2 = J$) lattice, instead, interactions between atoms are dissipative and $|\Psi\rangle$ metastable.

To highlight the essential physics, we focus on the EP ($\gamma = 2J$) and consider first an emitter sitting in any *bulk* cell indexed by $n = \nu$. It is easier to consider the picture in Fig. 5.1(b) and introduce a light notation such that $|e\rangle|{\rm vac}\rangle \to |e\rangle$, while $|g\rangle|\eta_n\rangle \to |\eta_n\rangle$ with $\eta = \alpha, \beta$. By direct substitution one can check that, to the 2nd order in $g/J$, $H$ admits the eigenstate and associated energy

$$|\Psi\rangle = |e\rangle - i\tfrac{g}{\sqrt{2\gamma}}\left(|\beta_\nu\rangle - i\,|\alpha_{\nu+1}\rangle\right)\,,\quad \epsilon = -i\Gamma \tag{5.43}$$

(recall that $\Gamma = g^2/4J$). Observe that $|\Psi\rangle$ is normalized to the 2nd order in $g$, while $|\Psi\rangle \to |e\rangle$ and $\epsilon \to 0$ for $g \to 0$. Most remarkably, $|\Psi\rangle$ is exactly localized in only two

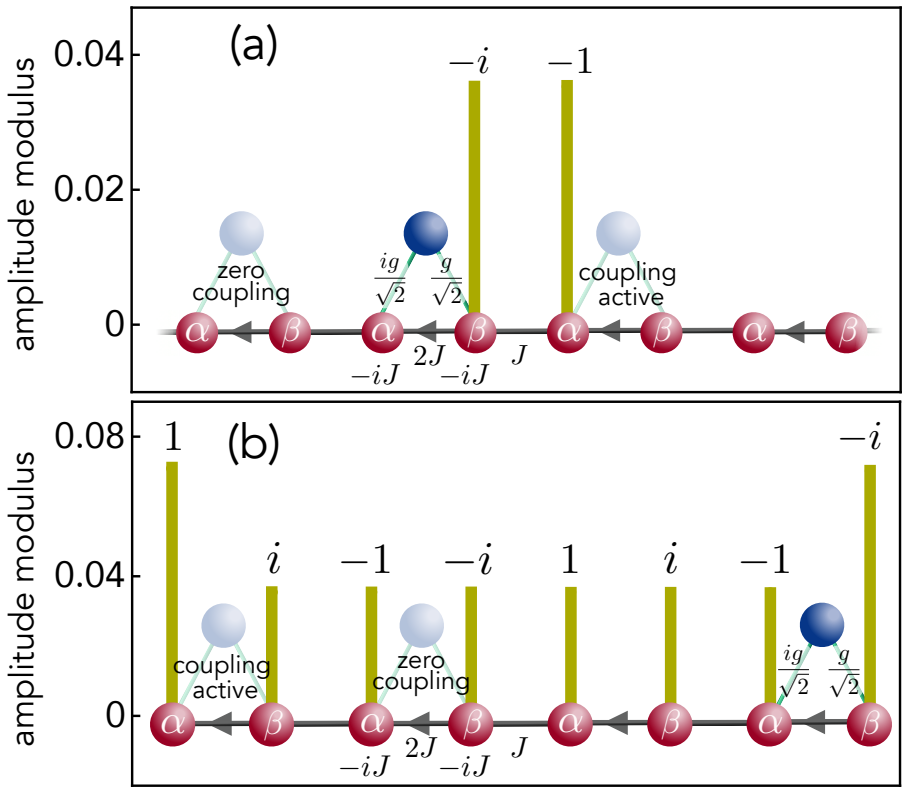


Figure 5.8: *Atom-photon dressed state mediating the atom-atom interaction.* (a): Dressed state $|\Psi\rangle$ forming when a quantum emitter ("source") is coupled to a bulk cell. Vertical bars represent the photonic wavefunction modulus. Another emitter (shaded) couples to $|\Psi\rangle$ ("coupling active"), hence to the source emitter, only provided that it sits in the right nearest-neighbor cell. If not ("zero coupling"), the two emitters do not interact. (b): Long-range dressed state arising when the source atom is coupled to the right-edge cell. Due to phase cancellation, an emitter placed in any bulk cell remains uncoupled from $|\Psi\rangle$ unless it lies on the opposite edge. We set $\gamma = 2J$ and referred to the picture in Fig. 5.1(b).

lattice cells ($\nu$ and $\nu+1$), in particular on cavities $\beta_\nu$ and $\alpha_{\nu+1}$. This strict localization is possible due to a simultaneous "decoupling" of $|\Psi\rangle$ from the lattice's right branch (sites $\beta_{\nu+1}, \alpha_{\nu+2}, ...$) and left branch (..., $\beta_{\nu-1}$, $\alpha_\nu$). The right-branch decoupling requires

$$\langle \beta_{\nu+1}|H|\Psi\rangle = 0 \tag{5.44}$$

so that $|\Psi\rangle$ has a node on $\beta_{\nu+1}$, which is guaranteed by the non-reciprocal leftward character of intra-cell hopping amplitudes. To get the left-branch decoupling, instead, we must require

$$\langle \alpha_\nu|H|\Psi\rangle = 0 \tag{5.45}$$

(so that $|\Psi\rangle$ can have a node on $\alpha_\nu$). It is easily seen [see following sections] that this condition can only occur provided that $\epsilon = -i\Gamma$ (showing the necessity of the metastable nature of the state) plus, importantly,

$$\langle \alpha_{\nu+1}|\Psi\rangle \neq 0\,. \tag{5.46}$$

The latter shows why the atom can couple to another one sitting in cell $\nu+1$: any other location will give zero coupling since $|\Psi\rangle$ vanishes everywhere outside cells $\nu$ and $\nu+1$. This explains both the non-reciprocal and nearest-neighbor nature of $H_{\rm eff}$ at the lattice EP [cf. (5.11)] for atoms in the bulk.

We now consider an open lattice with the source atom now sitting in the cell on the right edge [see Fig. 5.8(b)]. By direct substitution, $H$ can be shown to admit the eigenstate

$$|\Psi\rangle = |e\rangle - \frac{g}{\sqrt{2}\gamma}\sum_{n=1}^{N} e^{i\pi n}[(1+\delta_{n1})\,|\alpha_n\rangle - i\,(1+\delta_{nN})\,|\beta_n\rangle] \tag{5.47}$$

with associated energy $\epsilon = -i\Gamma$. This eigenstate is normalized to leading order in $g$ under the condition $g \ll \gamma/\sqrt{N}$ [in line with the Markovian regime assumed to derive (5.11)]. Contrarily to (5.43), $|\Psi\rangle$ is extended across the entire photonic lattice [see Fig. 5.8(b)]. In the bulk sites, the photonic wavefunction has flat modulus but – notably – non-uniform phase.

Remarkably, the arrangement of phases combines with the bi-local character of atom-field coupling [see Figs. 5.1(b) and 5.8(b)] so that, due to phase cancellation, another emitter placed in any bulk cell cannot couple to $|\Psi\rangle$ (hence to the source emitter). This conclusion however does not apply to the leftmost cell, where $|\langle\alpha_1|\Psi\rangle| \neq |\langle\beta_1|\Psi\rangle|$: thus emitters placed on *opposite* edges are able to interact. For odd $N$, the resulting coupling strength matches that of nearest-neighbor emitters in the case of Fig. 5.8(a).

Finally, we stress that the emergence of states (5.43) and (5.47) relies on the simultaneous occurrence of properties $(i)$-$(iii)$ at the end of Sec. 5.2, highlighting in particular the importance of the non-Hermitian nature of the above physics.

### 5.6.1 Derivation of the dressed state

Consider the emitter in a bulk cell $\nu$ in the picture of Fig. 5.1(b), the coupling thus being bi-local [condition (iii)]. A dressed state

$$|\Psi\rangle = A_e\,|e\rangle + B_\nu\,|\beta_\nu\rangle + A_{\nu+1}\,|\alpha_{\nu+1}\rangle$$

such that $H\,|\Psi\rangle = \epsilon\,|\Psi\rangle$ can appear only if: $\gamma = 2J$ (we are assuming $t_1 = t_2 = J$) [condition (ii), i.e. full non-reciprocity], avoiding amplitudes beyond $|\alpha_{\nu+1}\rangle$ to the right. Imposing $\langle\alpha_\nu|\,H\,|\Psi\rangle = 0$, where condition (iii) is crucial, and the Schrödinger equation (SE) projected on $|e\rangle$, one gets $\epsilon = -i\Gamma$ and $A_e = i\,\gamma\sqrt{2}B_\nu/g$. Projecting next the SE on $|\beta_\nu\rangle$ and $|\alpha_{\nu+1}\rangle$, exploiting condition (i) (uniform losses) and in the weak-coupling regime, yields $A_{\nu+1} = -iB_\nu$ [see Eq. (5.43)].

For open BCs of the lattice and an emitter in cell $N$ (right edge), properties (i)-(iii) yield the appearance of an eigenstate at the same energy $\epsilon = -i\Gamma$. By imposing SE, one finds

$$\begin{aligned} A_n &= (1+\delta_{n,1})\,e^{i\pi n}A_e/\gamma\sqrt{2} \\ B_n &= -ig\,(1+\delta_{n,N})\,e^{i\pi n}A_e/\gamma\sqrt{2} \end{aligned}$$

showing that amplitudes on bulk sites are half of those on sites $\alpha_1$ and $\beta_N$ and, most importantly, that there is a $\pi/2$ phase difference between nearest-neighbor sites.

### 5.6.2 Relationship of $H_{\text{eff}}$ with dressed states

The biorthogonal completeness relation corresponding to $H_{\rm f}$ (recall that in general $H_{\rm f} \neq H_{\rm f}^\dagger$) reads

$$\sum_k |\psi_k^R\rangle\langle\psi_k^L| = \mathbb{1} \tag{5.48}$$

where $\mathbb{1}$ is the identity operator and $|\psi_k^R\rangle$ ($\langle\psi_k^L|$) are right (left) eigenstates of $H_{\rm f}$. Using this, as discussed in Sec. 4.24, it is easily shown that the matrix element of the effective Hamiltonian [cf. (5.16)] can be equivalently rearranged as

$$\mathcal{H}_{\mu\nu} = \langle 0|\,\sigma_\mu V\hat{G}(0)V\sigma_\nu^\dagger\,|0\rangle = g^2\,\langle b_\mu|\,\hat{G}(0)\,|b_\nu\rangle = g\,\langle b_\mu|\Psi\rangle \tag{5.49}$$

(we changed cell indexes as $n \to \nu$ and $m \to \mu$ to comply with the notation used at the beginning of this Section). Here, $V = H - H_{\rm f}$ [cf. Eq. (5.7)] is the atom-field interaction Hamiltonian while

$$|\Psi\rangle = |e\rangle + g\,\hat{G}(0)\,|b_\nu\rangle \tag{5.50}$$

is the atom-photon dressed state seeded by an atom coupled to the $\nu$th cell. The last step in (5.49) relies on the weak-coupling assumption as in this regime $|\Psi\rangle$ [see Eq. (5.43)], is normalized to the 2nd order in $g$.

## 5.7 Summary

The results presented in this chapter introduce a new quantum optics/photonics paradigm, in which "structured" leakage on the field can devise unprecedented emission properties and second-order atom-atom dissipative interactions. Beyond engineered dissipation, a crucial ingredient for the predicted physics was shown to be the effectively non-local nature of emitter-field coupling (in a suitable picture).

Such emitters subject to such unconventional *non-local* interaction can be implemented via superconducting qubits [138], cold atoms [139] or all-photonic setups [140–144]. From this perspective, the discussed results arise from an particular combination of giant atoms physics, non-Hermitian Hamiltonians and, to some extent, chiral quantum optics [145–147], holding the promise for further developments e.g. using three-local coupling [148] and 2D non-Hermitian lattices [149].

In conclusion, we want to stress that our setup [cf. Fig. 5.1] is fully passive[2]. In our framework, this naturally follows from the decay nature of the studied phenomena, a type of non-unitary dynamics currently receiving considerable attention also in other scenarios [150]. On the other hand, the dissipative nature of our system favors an experimental verification of the predicted dynamics, e.g. in photonics (where non-Hermitian Hamiltonians are often implemented through their passive counterparts [23]).

A circuit-QED implementation appears possible as well: arrays of resonators coherently coupled to superconducting qubits – including excitation transfer mediated by atom-photon bound states – were experimentally demonstrated [93, 124, 125] and implementations of lattices like the one in Fig. 5.1(a) were realized [151]. Patterned losses can be engineered by interspersing resonators with low and high quality factors. This is feasible in state-of-the-art settings where external losses can be reduced up to four orders of magnitude compared to photon-hopping rates, while large losses can be obtained and controlled by connecting selectively lattice resonators to transmission lines [93, 124, 125].

[2] More precisely, it is passive-$\mathcal{PT}$-symmetric [cf. Sec. 1.2.4]: by balancing losses on $b$ sites with the same amount on gain on $a$ sites, the bare lattice enjoys $\mathcal{PT}$ symmetry [4, 108].

# Part II

# Mathematics of non self-adjoint operators

# Chapter 6

# Non self-adjoint operators from quantum theory

In the first part of this dissertation we discussed non-Hermitian Hamiltonians from a physical standpoint as powerful tools to describe effectively the dynamics of open systems. In this part instead we are going to follow a different approach, often considered in the literature [12, 152], that is we will assume that the *full* Hamiltonian is non-Hermitian and investigate the consequences.

## 6.1 Mathematical framework

Consider a Hilbert space $\mathcal{H}$, that is a pair $(\mathcal{V}, \langle\cdot,\cdot\rangle)$ where the first entry is a complex vector space, possibly infinite dimensional, hosting the *states* of the system, and the second entry is the inner product. We are not going to use the Dirac notation for states here as it implicitly implies that the inner product is fixed, an hypothesis we will drop in the following. Therefore the states will just be denoted by $\varphi, \psi \in \mathcal{H}$ without kets or bras.

Let $H$ be a possibly unbounded operator on $\mathcal{H}$ whose domain, which we assume to be dense in $\mathcal{H}$, is denoted by $D(H)$[1]. Let us define

$$D(H^\dagger) = \{\phi \in \mathcal{H} \,|\, \exists \psi \in \mathcal{H} \text{ s.t. } \langle H\varphi, \phi\rangle = \langle \varphi, \psi\rangle \;\; \forall \varphi \in \mathcal{H}\} \tag{6.1}$$

As $D(H)$ is assumed to be dense, we can replace $\exists$ with $\exists!$ in (6.1). Therefore it is possible to define an operator $H^\dagger$, called the *adjoint* of $H$, on $D(H^\dagger)$ defining $\psi := H^\dagger\phi$ for all $\phi \in D(H^\dagger)$.

An operator $H$ is then said to be self-adjoint if

$$\langle H\varphi, \phi\rangle = \langle \varphi, H\phi\rangle \quad \forall \varphi, \phi \in D(H) \qquad \text{and} \qquad D(H) = D(H^\dagger). \tag{6.2}$$

The first property is the *symmetry* or *Hermiticity* of $H$, usually taken as sufficient condition for self-adjointness in quantum mechanics. The second property may seem pedantic, but indeed two operators are the same if their action *and* their domains are the same. This does not represent an issue for bounded operators (which can be defined on all $\mathcal{H}$), but it may be for unbounded ones.

The importance of self adjoint operators in quantum mechanics comes from the reality of their spectrum and the orthogonality (and completeness) of eigenstates. However, as pointed out in the first part, numerous instances of non-selfajoint operators with real spectrum were found in recent years, the most known being a generalized version of the quantum harmonic oscillator $H = p^2 - (ix)^N$ for $N > 2$ (unbounded) [9] acting on $\mathcal{H} =$

[1] If $H$ is closed, i.e. its graph is closed, and $D(H) = \mathcal{H}$, then $H$ will be bounded (*closed graph theorem*).

$\mathcal{L}^2(\mathbb{R})$, or the gain-loss *Hamiltonian* $H = i\gamma\sigma_z + g\sigma_x$ (bounded) [16] acting on $\mathcal{H} = \mathbb{C}^2$. The lack of Hermiticity can be in some cases traced back to the inner product. Before dealing with this issue we want to set some notation and states some general properties regarding non self-adjoint operators.

Let $H$ be an operator defined on $D(H) \subset \mathcal{H}$ so that $H \neq H^\dagger$ and let

$$H\varphi_n = E_n\varphi_n \tag{6.3}$$

$$H^\dagger\psi_n = \tilde{E}_n\psi_n \tag{6.4}$$

be the corresponding eigenequations[2]. It holds that $\tilde{E}_n = E_n^*$ (complex conjugate) as[3]

$$\tilde{E}_n^* \langle\psi_n, \varphi_n\rangle = \langle\tilde{E}_n\psi_n, \varphi_n\rangle = \langle H^\dagger\psi_n, \varphi_n\rangle = \langle\psi_n, H\varphi_n\rangle = \langle\psi_n, E_n\varphi_n\rangle = E_n \langle\psi_n, \varphi_n\rangle, \tag{6.5}$$

unless of course $\langle\psi_n, \varphi_n\rangle = 0$. Eigenstates corresponding to different eigenvalues are not necessarily orthogonal

$$E_n \langle\varphi_m, \varphi_n\rangle = \langle\varphi_m, E_n\varphi_n\rangle = \langle\varphi_m, H\varphi_n\rangle = \langle H^\dagger\varphi_m, \varphi_n\rangle \neq E_m\langle\varphi_m, \varphi_n\rangle, \tag{6.6}$$

the same holding for $\{\psi_n\}_n$. However, the sets $\mathcal{F}_\varphi = \{\varphi_n\}_n$ and $\mathcal{F}_\psi = \{\psi_n\}_n$ are *bi-orthogonal*, that is

$$E_n \langle\psi_m, \varphi_n\rangle = \langle\psi_m, E_n\varphi_n\rangle = \langle\psi_m, H\varphi_n\rangle = \langle H^\dagger\psi_m, \varphi_n\rangle = \langle E_m^*\psi_m, \varphi_n\rangle = E_m\langle\psi_m, \varphi_n\rangle. \tag{6.7}$$

Therefore, if eigenvalues' multiplicity is 1, then $\langle\psi_m, \varphi_n\rangle = 0$. As we will discuss shortly, when the operator $H$ can be factorized in terms of pseudo-ladder operators, the sets $\mathcal{F}_\varphi$ and $\mathcal{F}_\psi$ will acquire useful properties.

### 6.1.1 "Fixing" the Hilbert space

A possible solution in the direction of making sense of non self-adjoint operator is that of *fixing* the inner product in order to restore Hermiticity [11, 153]. The basic idea is that, if $H$ is not self-adjoint in $\mathcal{H} = (\mathcal{V}, \langle\cdot,\cdot\rangle)$ it may very well be in a new Hilbert space $\mathcal{H}_2 = (\mathcal{V}, \langle\cdot,\cdot\rangle_2)$. Therefore by changing the inner product, which indeed is a change of the notion of *metric*, it is in some cases possible to restore Hermiticity, see Ref. [154] for a counterexample. We want to highlight now in more details this procedure [11].

A linear operator $\eta : \mathcal{H} \to \mathcal{H}$ is a *metric operator* if it is bijective, Hermitian ($\langle\psi, \eta\varphi\rangle = \langle\eta\psi, \varphi\rangle$, $\forall\psi, \varphi \in \mathcal{H}$) and positive definite ($\langle\varphi, \eta\varphi\rangle \geq 0$, $\forall\varphi \in \mathcal{H}$). A bounded operator $H$ on $\mathcal{H}$ is called *$\eta$-pseudo-Hermitian* if $H^\dagger = \eta H\eta^{-1}$, i.e. $\langle\psi, H\varphi\rangle = \langle\eta H\eta^{-1}\psi, \varphi\rangle$. These definitions are relevant in that if $H$ is not self-adjoint with respect to the scalar product $\langle\cdot,\cdot\rangle$ but it is $\eta$-pseudo-Hermitian for some metric operator $\eta$, then we can define a new inner product as $\langle\cdot,\cdot\rangle_\eta := \langle\cdot, \eta\,\cdot\rangle$ so that $H$ is self-adjoint in $\mathcal{H}_\eta = (\mathcal{V}, \langle\cdot,\cdot\rangle_\eta)$, indeed

$$\langle\psi, H\varphi\rangle_\eta = \langle\psi, \eta H\varphi\rangle = \langle\psi, \underbrace{\eta H\eta^{-1}}_{H^\dagger}\eta\varphi\rangle = \langle(H^\dagger)^\dagger\psi, \eta\varphi\rangle = \langle H\psi, \varphi\rangle_\eta\ . \tag{6.8}$$

These properties are relevant as a connection with $\mathcal{PT}$ symmetry can be established. Indeed it can be proved that $H$ is pseudo-Hermitian if and only if it has a complete set of common eigenvectors with an invertible antilinear operator [155]. As $\mathcal{PT}$ is a particular antilinear invertible operator and, if $[H, \mathcal{PT}] = 0$ and $\mathcal{PT}$ is unbroken, then $H$ can be made Hermitian by fixing the Hilbert space inner product.

We illustrate this procedure now in the case of the gain-loss Hamiltonian $H = i\gamma\sigma_z + g\sigma_x$ under unbroken $\mathcal{PT}$ symmetry ($\gamma < g$), as under these assumption the eigenstates of

[2] We are assuming for simplicity no degeneracies.

[3] In our notation the inner product is linear in the second argument and antilinear in the first one.

$H$ are also eigenstates of $\mathcal{PT}$. In order to construct the metric operator, a general method, in the finite dimensional case at least, is to define it as [153]

$$\eta = \sum_n P_n^{\psi} \tag{6.9}$$

where $P_n^{\psi}$ is the orthogonal projector onto the eigenspace of $\psi_n$ [cf. Eq. (6.4)]. For this specific example the eigenequations read

$$H\varphi_{\pm} = \lambda_{\pm}\varphi_{\pm} \tag{6.10}$$

$$H^{\dagger}\psi_{\pm} = \lambda_{\pm}\psi_{\pm} \tag{6.11}$$

where $\lambda_{\pm} = \pm\sqrt{g^2-\gamma^2}$ and $\varphi_{\pm}$ are given in Eq. (1.8) and

$$\psi_{\pm} = \begin{pmatrix} i\gamma - \lambda_{\pm} \\ -g \end{pmatrix}. \tag{6.12}$$

The projectors are therefore given by $P_n^{\psi} = (\psi_n \otimes \psi_n^*)/\langle \psi_n, \psi_n \rangle$ with $n = \pm$ and the metric operator is $\eta = \mathbb{1}_2 + (\gamma/g)\sigma_y$. It is then easy to check that $\langle \psi, H\varphi \rangle_{\eta} = \langle H\psi, \varphi \rangle_{\eta}$, $\forall \psi, \varphi \in \mathcal{H}$.

## 6.2 Non self-adjoint Hamiltonians and pseudo-bosons

In view of the following chapter we introduce here a particular class of non self-adjoint Hamiltonians, without changing the Hilbert space inner product. On the one hand we will discuss how such operators con be constructed through a generalization of canonical commutation rules of bosonic operators (*pseudo-bosons*). On the other hand, most importantly, we will show that many relevant non-Hermitian Hamiltonians can indeed be factorized in terms of suitable pseudo-bosonic operators, therefore highlighting how these are not just mathematical abstract tools to *construct* non self-adjoint operators, but indeed can *appear* in several contexts. The following discussion is based on [12, 156, 157].

### 6.2.1 Non self-adjoint Hamiltonians *from* pseudo-bosons

One way of diagonalizing the simple harmonic oscillator Hamiltonian $H = (p^2 + x^2)/2$, here with dimensionless operators, is by introducing the operator $c = (x + ip)/\sqrt{2}$ and its adjoint $c^{\dagger} = (x - ip)/\sqrt{2}$ so that $H = N + 1/2$, with $N = c^{\dagger}c$. The operators $c$ and $c^{\dagger}$ are called respectively lowering and raising operators as $c\varphi_n = \sqrt{n}\varphi_{n-1}$, yielding in particular $c\varphi_0 = 0$, and $c^{\dagger}\varphi_n = \sqrt{n+1}\varphi_{n+1}$, $\varphi_n$ being an eigenstate of $H$ with eigenvalue $E_n = n + 1/2$. Two key properties are that: (i) the operator $a$ has a non-zero vacuum ($\varphi_0$), (ii) $c$ and $c^{\dagger}$ satisfy the bosonic canonical commutation rule $[c, c^{\dagger}] = \mathbb{1}$. Pseudo-bosonic operators arise as a generalization of this setting in that one considers the commutation relation $[a, b] = \mathbb{1}$, with $b \neq a^{\dagger}$ in general.

Consider two operators $a$ and $b$ acting on $\mathcal{H}$ whose domain are $D(a)$ and $D(b)$, with analogous notation for their adjoints. Let $D \subset D(a) \cap D(b)$ be a dense subset of $\mathcal{H}$, stable under the action of both $a$, $b$ and their adjoints. The operators $a$ and $b$ are said to be *D-pseudo-bosonic* if $[a, b] = \mathbb{1}$, i.e. $[a, b]\phi = \phi$, $\forall \phi \in D$.

We observe that it is not required that $b = a^{\dagger}$, but other assumptions need to be made in order to make this setting a proper extension of the self-adjoint harmonic oscillator:

1. $a$ has a non-zero vacuum: $\exists \varphi_0 \in D$ so that $a\varphi_0 = 0$,

2. $b^{\dagger}$ has a non-zero vacuum: $\exists \psi_0 \in D$ so that $b^{\dagger}\psi_0 = 0$,

3. the set $\mathcal{F}_\varphi = \{\varphi_n\}_{n\geq 0}$, with $\varphi_n = \frac{1}{\sqrt{n!}}\, b^n \varphi_0$, is a basis for $\mathcal{H}$.

Some comments are in order. The definitions of $\varphi_n$'s and $\psi_n = \frac{1}{\sqrt{n!}}(a^\dagger)^n\varphi_0$ make sense because of the stability of $D$ under the action of $d$ and $b^\dagger$, and $\varphi_n, \psi_n \in D$. From the commutation relation the following lowering and raising relations hold

(*i*) $b\,\varphi_n = \sqrt{n+1}\,\varphi_{n+1}$ for $n \geq 0$,

(*ii*) $a\,\varphi_0 = 0$ and $a\,\varphi_n = \sqrt{n}\,\varphi_{n-1}$ for $n \geq 1$,

(*iii*) $a^\dagger\psi_n = \sqrt{n+1}\,\psi_{n+1}$ for $n \geq 0$,

(*iv*) $b^\dagger\psi_0 = 0$ and $b^\dagger\psi_n = \sqrt{n}\,\psi_{n-1}$ for $n \geq 1$,

(*v*) $N\varphi_n = n\varphi_n$ and $N^\dagger\psi_n = n\psi_n$, with $N = ba$ for $n \geq 0$.

It can be proved that also the set $\mathcal{F}_\psi = \{\psi_n\}_{n\geq 0}$ is a basis. Finally, by choosing the normalization of $\varphi_0$ and $\psi_0$ so that $\langle\psi_0, \varphi_0\rangle = 1$, $\mathcal{F}_\varphi$ and $\mathcal{F}_\psi$ are biorthonormal, i.e. $\langle\psi_m, \varphi_n\rangle = \delta_{mn}$. Other properties of pseudo-bosons have been discussed in the literature, as in Ref. [158]. What we want to highlight here is that this mathematical procedure allows one to explicitly *construct* non self-adjoint operators ($N \neq N^\dagger$) with real discrete positive spectrum $\{n\}_{n\geq 0}$.

### 6.2.2 Non self-adjoint Hamiltonians *factorizable with* pseudo-bosons

Here we want to show two concrete models where the non-Hermitian Hamiltonian can be written in terms of pseudo-bosonic operators [12], justifying their definition.

#### 6.2.2.1 Extended harmonic oscillator

Consider the manifestly non self-adjoint Hamiltonian of an *extended* quantum harmonic oscillator,

$$H_\nu = \frac{1}{2\nu}\left(p^2 + x^2\right) + i\sqrt{2}\,p \tag{6.13}$$

which is know to display a real spectrum for $\nu > 0$ [159]. As discussed in [12], by defining $A_\nu = a - \nu$ and $B_\nu = a^\dagger + \nu$, $a$ being the lowering operator of the Hermitian quantum harmonic oscillator, we have that $[A_\nu, B_\nu] = \mathbb{1}$ and $H_\nu = \nu^{-1}\left(B_\nu A_\nu + \gamma_\nu \mathbb{1}\right)$, with $\gamma_\nu = \nu^2 + 1/2$.

The operators $A_\nu$ and $B_\nu$ are indeed pseudo-bosonic as all the relative assumptions can be verified, indeed the biorthogonal sets $\mathcal{F}_\varphi = \{\varphi_n(x)\}_n$ and $\mathcal{F}_\psi = \{\psi_n(x)\}_n$ upon which $B_\nu$ and $A_\nu$ act as raising operators, respectively, are given by

$$\varphi_n(x) = \frac{1}{\sqrt{n!}}\, B_\nu^n \varphi_0(x) = \frac{e^{-\nu^2}}{\pi^{1/4}\sqrt{2^n n!}}\left(x - \frac{\mathrm{d}}{\mathrm{d}x} + \sqrt{2}\nu\right)^n e^{-(x-\nu\sqrt{2})^2/2}, \tag{6.14}$$

$$\psi_n(x) = \frac{1}{\sqrt{n!}}\,(A_\nu^\dagger)^n \psi_0(x) = \frac{e^{\nu^2}}{\pi^{1/4}\sqrt{2^n n!}}\left(x - \frac{\mathrm{d}}{\mathrm{d}x} - \sqrt{2}\nu\right)^n e^{-(x+\nu\sqrt{2})^2/2}. \tag{6.15}$$

These satisfy the eigenequations $H_\nu\varphi_n = E_n\varphi_n$ and $H_\nu^\dagger\psi_n = E_n\psi_n$ with $E_n = (n + \gamma_\nu)/\nu$.

#### 6.2.2.2 The Swanson model

Another widespread model in the literature of non self-adjoint operators with real spectrum is the Swanson model [160–162], whose Hamiltonian is

$$H_\theta = \frac{1}{2}\left(p^2 + x^2\right) - \frac{i}{2}\tan(2\theta)\left(p^2 - x^2\right) \tag{6.16}$$

with $-\pi/4 < \theta < \pi/4$. Introducing the operators

$$A_\theta = \cos(\theta)\, a + i\sin(\theta)\, a^\dagger, \quad B_\theta = \cos(\theta)\, a^\dagger + i\sin(\theta)\, a, \tag{6.17}$$

where $a$ is again the lowering operator for the Hermitian quantum harmonic oscillator, one can write the Hamiltonian as $H_\theta = \omega_\theta\left(B_\theta A_\theta + \frac{1}{2}\mathbb{1}\right)$, with $\omega_\theta = [\cos(2\theta)]^{-1}$. The commutation rule $[A_\theta, B_\theta] = \mathbb{1}$ holds, and if $\theta \neq 0$ then $A_\theta^\dagger \neq B_\theta$. The Swanson Hamiltonian is then factorized in terms of pseudo-bosonic operators, indeed the square integrable vacua of $A_\theta$ and $B_\theta^\dagger$ are $\varphi_0^{(\theta)} = N_\varphi \exp\left(-e^{2i\theta}x^2/2\right)$ and $\psi_0^{(\theta)} = N_\psi \exp\left(-e^{-2i\theta}x^2/2\right)$, respectively, where $N_\varphi$ and $N_\psi$ are normalization constants satisfying $N_\varphi^* N_\psi = e^{-i\theta}/\sqrt{\pi}$ so that $\langle \psi_0^{(\theta)}, \varphi_0^{(\theta)} \rangle = 1$. The eigenstates of $H_\theta$ and $H_\theta^\dagger$ built with the ladder operators $A_\theta$ and $B_\theta$ are then

$$\varphi_n^{(\theta)}(x) = \frac{1}{\sqrt{n!}}\, B_\theta^n \varphi_0^{(\theta)}(x) = \frac{N_\varphi}{\sqrt{2^n n!}} H_n(e^{i\theta}x) \exp\left(-e^{2i\theta}x^2/2\right) \tag{6.18}$$

$$\psi_n^{(\theta)}(x) = \frac{1}{\sqrt{n!}}\, (A_\theta^\dagger)^n \psi_0^{(\theta)}(x) = \frac{N_\psi}{\sqrt{2^n n!}} H_n(e^{i\theta}x) \exp\left(-e^{-2i\theta}x^2/2\right) \tag{6.19}$$

where $H_n(x)$ is the $n$th Hermite polynomial.

The two examples presented here are just some of several that can be found in the literature [12]. Also, they are one dimensional. In the next chapter we will use pseudo-bosonic operators to factorize Hamiltonians with two degrees of freedom.

# Chapter 7

# Quantization of dissipative systems

In this chapter we discuss the failure of the canonical quantization for the damped harmonic oscillator using the Bateman lagrangian. In particular, we prove that no square integrable vacuum (in the sense of pseudo-bosons) exists for the *natural* ladder operators of the system, and that the only vacua can be found as distributions, that is, not in a standard Hilbert space.

## 7.1 Introduction

The problem of quantization for dissipative systems, and the Damped Harmonic Oscillator (DHO) in particular, has a long story. There are two main approaches: (i) through a time-independent lagrangian, proposed by Bateman and studied by many authors along the years, see Refs [163–168] and references therein, based on the idea that associated to the damped oscillator there is a second amplified one, acquiring all the energy lost by the damped one; (ii) through an explicitly time-dependent lagrangian, see Refs [165,168–170] and references therein, which reproduces the equation of motion of the DHO without the need of introducing its amplified counterpart. More recently, another non standard, time-independent, lagrangian has been introduced for the DHO, where it was shown that there is no need to introduce any dual oscillator. However [171], in this case the quantization proved to be quite hard, if not entirely impossible, in the sense that the Schrödinger equation admits no exact solution, apparently.

In the following sections, we will focus on Bateman's approach, and we will show that the system quantization is indeed impossible within the realm of Hilbert spaces. More in detail, we will diagonalize the Hamiltonian for the system in terms of pseudo-bosonic operators, but we will also prove that, contrarily to what stated in some contributions in the literature, it is not possible to use these ladder operators to construct biorthogonal sets in some Hilbert space $\mathcal{H}$. This impossibility, which was somehow recognized by many authors [172,173] leaves the possibility open for working in the space of distributions.

## 7.2 A no-go result

The classical equation of motion for the DHO is

$$m\ddot{x} + \gamma\dot{x} + kx = 0, \tag{7.1}$$

where $m, \gamma$ and $k$ are the mass, friction coefficient and the spring constant, respectively. The Bateman lagrangian reads

$$L = m\dot{x}\dot{y} + \frac{\gamma}{2}(x\dot{y} - \dot{x}y) - kxy. \tag{7.2}$$

Besides Eq. (7.1), this lagiangian produces also

$$m\ddot{y} - \gamma\dot{y} + ky = 0, \tag{7.3}$$

the differential equation associated to an amplified harmonic oscillator (AHO), as the friction coefficient is now negative. In [167], this is referred to as the *time reverse* equation of the one for $x(t)$, for obvious reasons. The conjugate momenta are

$$p_x = \frac{\partial L}{\partial \dot{x}} = m\dot{y} - \frac{\gamma}{2}\,y, \qquad p_y = \frac{\partial L}{\partial \dot{y}} = m\dot{x} + \frac{\gamma}{2}\,y,$$

and the corresponding classical Hamiltonian is

$$H = p_x\dot{x} + p_y\dot{y} - L = \frac{1}{m}p_xp_y + \frac{\gamma}{2m}\,(yp_y - xp_x) + \left(k - \frac{\gamma^2}{4m}\right)xy. \tag{7.4}$$

By introducing the new variables $x_1$ and $x_2$ through

$$x = \frac{1}{\sqrt{2}}(x_1 + x_2), \qquad y = \frac{1}{\sqrt{2}}(x_1 - x_2), \tag{7.5}$$

$L$ and $H$ can be written as follows:

$$L = \frac{m}{2}(\dot{x}_1^2 - \dot{x}_2^2) + \frac{\gamma}{2}(x_2\dot{x}_1 - x_1\dot{x}_2) - \frac{k}{2}(x_1^2 - x_2^2)$$

and

$$H = \frac{1}{2m}\left(p_1 - \frac{\gamma}{2}x_2\right)^2 - \frac{1}{2m}\left(p_2 - \frac{\gamma}{2}x_1\right)^2 + \frac{k}{2}(x_1^2 - x_2^2),$$

where $p_1 = \dfrac{\partial L}{\partial \dot{x}_1} = m\dot{x}_1 + \dfrac{\gamma}{2}x_2$ and $p_2 = \dfrac{\partial L}{\partial \dot{x}_2} = m\dot{x}_2 - \dfrac{\gamma}{2}x_1$. By putting $\omega^2 = \dfrac{k}{m} - \dfrac{\gamma^2}{4m^2}$ we can rewrite $H$ as follows:

$$H = \left(\frac{1}{2m}p_1^2 + \frac{1}{2}m\omega^2x_1^2\right) - \left(\frac{1}{2m}p_2^2 + \frac{1}{2}m\omega^2x_2^2\right) - \frac{\gamma}{2m}(p_1x_2 + p_2x_1). \tag{7.6}$$

In this section we will mostly consider $\omega^2 > 0$. The case $\omega^2 \leq 0$ will be briefly discussed later.

Following [174], we impose canonical quantization rules between $x_j$ and $p_k$ as: $[x_j, p_k] = i\delta_{j,k}\mathbb{1}$, working in unit $\hbar = 1$. This is equivalent to the choice in [167]. Ladder operators can now be easily introduced:

$$a_k = \sqrt{\frac{m\omega}{2}}\,x_k + i\sqrt{\frac{1}{2m\omega}}\,p_k, \tag{7.7}$$

$k = 1, 2$. These are bosonic operators since they satisfy the canonical commutation rules: $[a_j, a_k^\dagger] = \delta_{j,k}\mathbb{1}$.

Let us observe that, as these operators are unbounded, these commutators should be properly defined. For instance, both $[a_j, a_k^\dagger]$ and $[x_j, p_k]$ are well defined on Schwartz test functions: $[a_j, a_k^\dagger]\varphi(x) = \varphi(x)$, for all $\varphi(x) \in \mathcal{S}(\mathbb{R})$.

In terms of these operators the quantum version of the Hamiltonian $H$ in Eq. (7.6) can be written as

$$H = H_0 + H_I \tag{7.8}$$

with

$$H_0 = \omega\left(a_1^\dagger a_1 - a_2^\dagger a_2\right), \qquad H_I = \frac{i\gamma}{2m}\left(a_1 a_2 - a_1^\dagger a_2^\dagger\right) \tag{7.9}$$

In [165,167] this Hamiltonian is diagonalized by using the $QU(2)$ algebra. Despite $H$ being (at least formally) self-adjoint, its eigenvalues appear to be complex. This is quite curious, and in [167] the authors claim that this is because $H_I$ is only formally Hermitian "*because the normalization integral for the eigenstates...is infinite, a result that follows from the fact that the eigenvalues are imaginary*". This does not sound like a deep explanation in that is quite tautological. For this reason, we propose a different approach to the analysis of $H$, based on the generalized Bogoliubov transformation considered in [174]. While this transformation turns out to be useful to diagonalize $H$ making no reference to $QU(2)$ algebra (which will be replaced in the following by formal pseudo-bosonic ladder operators [12]), the conclusions deduced in [174] needs substantial revision.

Following [174], we introduce the operators

$$A_1 = \frac{1}{\sqrt{2}}(a_1 - a_2^\dagger), \quad A_2 = \frac{1}{\sqrt{2}}(-a_1^\dagger + a_2), \tag{7.10}$$

as well as

$$B_1 = \frac{1}{\sqrt{2}}(a_1^\dagger + a_2), \quad B_2 = \frac{1}{\sqrt{2}}(a_1 + a_2^\dagger). \tag{7.11}$$

These operators satisfy the commutation relations

$$[A_j, B_k] = \delta_{j,k}\mathbb{1}, \tag{7.12}$$

with $B_j \neq A_j^\dagger$, $j = 1, 2$. Moreover, $A_1 = -A_2^\dagger$ and $B_1 = B_2^\dagger$. The fact that $B_j \neq A_j^\dagger$ follows from the fact that the one in Eqs. (7.10) and (7.11) is not a Bogoliubov transformation, but only a generalized version of it [175].

In [12] operators of this kind are analyzed in detail, producing several mathematical results (mainly on unbounded operators and biorthogonal sets of vectors), and were shown, as in the previous chapter, to appear often in concrete models [3,153,176]. As discussed in the previous chapter, the main idea is that, for operators like these, we can extend the usual ladder construction used for bosons, paying some price (like, quite often, the validity of the basis property).

In terms of these operators $H$ can now be written as follows:

$$H = H_0 + H_I \tag{7.13}$$

where

$$H_0 = \omega\left(B_1 A_1 - B_2 A_2\right), \qquad H_I = \frac{i\gamma}{2m}\left(B_1 A_1 + B_2 A_2 + \mathbb{1}\right), \tag{7.14}$$

depending only on the pseudo-bosonic number operators $N_j = B_j A_j$ [12]. This is exactly the same Hamiltonian found in [174], and it is equivalent to that given in [165,167]. In Ref. [174], the authors introduce the vacuum for the annihilation operators $A_1$ and $A_2$ as the action of an unbounded operator on the vacuum of $a_1$ and $a_2$, and construct new vectors out of this vacuum, claiming they form a Fock basis with unit norm. The next theorem, which is the main result of this chapter, shows that this is not the case and suggests a possible way out to solve this issue.

**Theorem.** *There is no non-zero function $\varphi_{00}(x_1, x_2)$ satisfying*

$$A_1\varphi_{00}(x_1, x_2) = A_2\varphi_{00}(x_1, x_2) = 0.$$

*Also, there is no non-zero function $\psi_{00}(x_1, x_2)$ satisfying*

$$B_1^\dagger\psi_{00}(x_1, x_2) = B_2^\dagger\psi_{00}(x_1, x_2) = 0.$$

*Proof.* Let us assume that a non-zero function $\varphi_{00}(x_1, x_2)$ satisfying $A_1\varphi_{00}(x_1, x_2) = A_2\varphi_{00}(x_1, x_2) = 0$ does exist. Hence we should have also $(A_1 - A_2)\varphi_{00}(x_1, x_2) = 0$ and $(A_1 + A_2)\varphi_{00}(x_1, x_2) = 0$, so that

$$(x_1 - x_2)\varphi_{00}(x_1, x_2) = 0, \qquad (\partial_1 + \partial_2)\varphi_{00}(x_1, x_2) = 0.$$

It is clear that there is no non-zero solution of the first equation. The only solution is a distribution: $\varphi_{00}(x_1, x_2) = \alpha\delta(x_1 - x_2)$, $\alpha \in \mathbb{C}$.

The proof for $\psi_{00}(x_1, x_2)$ is completely similar: computing $(B_1^\dagger + B_2^\dagger)\psi_{00}(x_1, x_2) = 0$ and $(B_1^\dagger - B_2^\dagger)\psi_{00}(x_1, x_2) = 0$ we easily get

$$(x_1 + x_2)\psi_{00}(x_1, x_2) = 0, \qquad (\partial_1 - \partial_2)\psi_{00}(x_1, x_2) = 0,$$

for which exists only the weak solution $\psi_{00}(x_1, x_2) = \beta\delta(x_1 + x_2)$, $\beta \in \mathbb{C}$.

□

Notice that, compared to other works on the same subject, e.g. Refs. [172, 173], we are not assuming here that $\varphi_{00}(x_1, x_2)$ and $\psi_{00}(x_1, x_2)$ belong to any specific Hilbert space. Therefore, this result does not depend on the metric we can introduce in $\mathcal{L}^2(\mathbb{R}^2)$ to take care of possible divergences in the norms of the eigenfunctions of $H$: stated differently, replacing

$$\langle f, g\rangle = \int_{\mathbb{R}^2} \overline{f(x_1, x_2)}\, g(x_1, x_2)\, dx_1\, dx_2 \tag{7.15}$$

with some

$$\langle f, g\rangle_w = \int_{\mathbb{R}^2} \overline{f(x_1, x_2)}\, g(x_1, x_2)\, w(x_1, x_2)\, dx_1\, dx_2, \tag{7.16}$$

for any choice of weight function $w(x_1, x_2)$, will not do the job.

### 7.2.1 The overdamped case $\omega^2 < 0$

The previous results have been obtained under the constraint $\omega^2 > 0$ which allowed to define the bosonic operators (7.7). In the $\omega^2 < 0$ case, that for simplicity we assume corresponding to $\omega = \tau e^{i\pi/2}$, $\tau \in \mathbb{R}_+$, easy computations show that the commutators satisfy $[a_j, a_k^\dagger] = i\delta_{j,k}\mathbb{1}$, and hence they are not bosonic operators.

This issue is solved introducing the following operators[1]

$$a_k = e^{i\pi/4}\sqrt{\frac{m\tau}{2}}x_k + ie^{-i\pi/4}\sqrt{\frac{1}{2m\tau}}p_k, \quad b_k = e^{i\pi/4}\sqrt{\frac{m\tau}{2}}x_k - ie^{-i\pi/4}\sqrt{\frac{1}{2m\tau}}p_k, \tag{7.17}$$

$k = 1, 2$. Of course, $a_k^\dagger \neq b_k$, $k = 1, 2$, yet these operators satisfy the commutation rules $[a_j, b_k] = \delta_{j,k}\mathbb{1}$, which means that $a_k, b_k$, $k = 1, 2$, define two pairs of formal pseudo-bosonic operators [12].

Using now $b_k$ in place of $a_k^\dagger$ in Eqs. (7.10) and (7.11), we define the operators

$$A_1 = \frac{1}{\sqrt{2}}(a_1 - b_2), \quad A_2 = \frac{1}{\sqrt{2}}(-b_1 + a_2), \tag{7.18}$$

$$B_1 = \frac{1}{\sqrt{2}}(b_1 + a_2), \quad B_2 = \frac{1}{\sqrt{2}}(a_1 + b_2), \tag{7.19}$$

which again satisfy $[A_j, B_k] = \delta_{j,k}\mathbb{1}$. With this construction the Hamiltonian has the same form and properties of (7.13), and the results given in the Theorem still hold.

[1] The principal square root of $\omega$ has been chosen.

In conclusion, we observe that the case $\omega^2 = 0$ is not really interesting, in the present context, since in this case the use of bosonic or pseudo-bosonic operators is quite unlikely, being $H$ (7.6) no longer quadratic in $x_j$. It is also possible to check that nothing really changes if we consider a quantized non commutative version of the Hamiltonian in Eq. (7.6), i.e. if we assume that $[x_1, x_2] = i\theta$ and $[p_1, p_2] = i\nu$, other than having $[x_j, p_j] \neq 0$. Using the same ideas as in [177] and adopting a Bopp shift, a similar no-go result can be recovered.

## 7.3 Summary

In this chapter, based on [178], we have seen that the idea of working in an Hilbert space of square integrable functions when dealing with the Bateman lagrangian for the DHO does not work. As already mention, another approach could be that of an explicitly time-dependent Hamiltonian of the kind proposed by Caldirola and by Kanai independently [166,179,180]. This method restores square-integrability of the eigenstates, which can be exactly computed [169], but again yields curiously imaginary eigenvalues for the formally self-adjoint Caldirola-Kanai Hamiltonian $H_{CK}$, which are explained considering the domain of the operator $xp_x + p_x x$. Moreover, as discussed for instance in [181], the role of $H_{CK}$ is not fully accepted in the context of the DHO: indeed, one of the main conclusions in [181] is that $H_{CK}$ *does not describe ...a damped harmonic oscillator of mass* $m_0$ *...but a particle of mass* $m(t) = m_0 e^{\alpha t}$ *subject to a force* $F(t) = m_0 e^{\alpha t} x$*.....* This is just a small evidence that the quantization of dissipative systems is generally non trivial, and not a completely understood topic.

The main result of this chapter suggests that the possible way out to overcome the mathematical issues arising in the quantization of the DHO is to reconsider the system in a distributional setting [182,183]. Of course, one needs to define the proper ladder operators used to write the Hamiltoanian, control the notion of biorthogonality of the eigenstates, and check whether this approach has some concrete usefulness for the analysis of the DHO.

# Chapter 8

# Tridiagonality and non self-adjoint Hamiltonians

In this chapter we study the properties of a particular class of non self-adjoint operators with tridiagonal representation using biorthogonal sets of vectors. We will make no attempt to make the Hamiltonian Hermitian in some sense and take non self-adjointess as a starting assumptions. We will show how to compute eigenstates through recurrence relation, how to factorize such Hamiltonians and perform the same analysis on their supersymmetric partners. Some examples are then discussed, and a connection with bi-squeezed states is analyzed.

## 8.1 Introduction

Recently the topic of tridiagonal Hamiltonians, and their factorization, in connection with Supersymmetric quantum mechanics (SUSY QM) and with an eye to orthogonal polynomials, has received some attention [184] . It was shown how a class of self-adjoint (infinite) tridiagonal matrices can be factorized as product of two operators, and how these operators are useful to deduce results on their SUSY partners. In this analysis three-terms recurrence relations appear in connection with orthogonal polynomials. These polynomials are constructed both for $H = X^\dagger X$, and for its SUSY partner $H_{\rm susy} = XX^\dagger$.

Here we extend the analysis in the context of tridiagonal matrices which are not necessarily self-adjoint. That is, we do not assume that the diagonal elements are real, and that the non zero off-diagonal entries are related by any symmetry. The rationale behind this choice is that, as we will discuss in Section 8.3, this can be relevant in connection with $\mathcal{PT}$ symmetric quantum mechanics and its relatives [12, 16, 153], where the Hamiltonian of a given system is not required to be self-adjoint, but still satisfies some special requirement. For instance, the Hamiltonian could be $\mathcal{PT}$ symmetric. This extended version of quantum mechanics, as discussed in the first part of this dissertation, has been proved to be quite relevant in the analysis of gain-loss systems [185] from a physical point of view, and also from a mathematical one because of the many (and sometimes unexpected) issues and pitfalls coming up going from self-adjoint to non self-adjoint Hamiltonians. In particular, the role of biorthogonal sets of vectors [12], unbounded metric operators [186, 187] and pseudo-spectra [188] have been widely studied in this perspective.

In the next section we introduce the mathematical formalism for the analysis of our tridiagonal Hamiltonians. We then discuss their factorization, and use the operators introduced in this procedure to define the SUSY partner of the original Hamiltonian. As our Hamiltonian $H$ will not be self-adjoint in general, we will also discuss the role of $H^\dagger$ and of its SUSY partner. Hence we deal with four related Hamiltonians. We will discuss the consequences of the diagonalization of $H$, showing how three-terms relations can be

deduced also in this more general settings. Section 8.3 is devoted to examples, which are treated in many details. In Section 8.4 we consider an extended setting and its connection to bi-squeezed states of the type originally introduced in [189].

## 8.2 The functional settings

Let $\mathcal{F}_\varphi = \{\varphi_n\}_{n\geq 0}$ and $\mathcal{F}_\psi = \{\psi_n\}_{n\geq 0}$ be two biorthogonal sets of vectors in a Hilbert space $\mathcal{H}$, which we assume to be infinite-dimensional, except when stated, and separable. Otherwise, if $dim(\mathcal{H}) < \infty$, the treatment simplifies significantly, from the mathematical point of view, mainly because all the operators necessary for us are bounded. In what follows $\mathcal{F}_\varphi$ and $\mathcal{F}_\psi$ will be required to be either $\mathcal{D}$-quasi bases or, much stronger requirement, Riesz bases. We recall that [12] $\mathcal{F}_\varphi$ and $\mathcal{F}_\psi$ are $\mathcal{D}$-quasi bases, where $\mathcal{D}$ is some dense subspace of $\mathcal{H}$, and if, for all $f, g \in \mathcal{D}$,

$$\langle f, g\rangle = \sum_{n=0}^{\infty} \langle f, \varphi_n\rangle \langle \psi_n, g\rangle = \sum_{n=0}^{\infty} \langle f, \psi_n\rangle \langle \varphi_n, g\rangle . \tag{8.1}$$

We will assume that $\varphi_n$ and $\psi_n$ belongs to $\mathcal{D}$. We also recall that, by definition, $\mathcal{F}_\varphi$ and $\mathcal{F}_\psi$ are (biorthogonal) Riesz bases if an orthonormal basis $\mathcal{F}_e = \{e_n\}_{n\geq 0}$ exists, together with a bounded operator $T$ with bounded inverse, such that $\varphi_n = Te_n$ and $\psi_n = (T^{-1})^\dagger e_n$. In the following we will always assume that $\mathcal{D}$ is stable under the action of $T$, $T^\dagger$ and their inverse. We also assume that $e_n \in \mathcal{D}$ for all $n$, so that $\varphi_n, \psi_n \in \mathcal{D}$ automatically. We refer to Refs. [12,190] for examples when these assumptions are satisfied. We observe that if $\mathcal{F}_\varphi$ and $\mathcal{F}_\psi$ are (biorthogonal) Riesz bases, they are $\mathcal{D}$-quasi bases. The opposite implication is false: $\mathcal{D}$-quasi bases are, in general, not Riesz bases. Also, they are often not even bases [12].

Let now $H$ be an operator, not necessarily bounded or self-adjoint, such that $D(H) \supseteq \mathcal{D}$, so that $H$ is densely defined. In what follows it will be useful to assume also that $D(H^\dagger) \supseteq \mathcal{D}$.

**Definition 1.** *$H$ is called $(\varphi, \psi)$-tridiagonal if three sequences of complex numbers exist, $\{b_n\}$, $\{a_n\}$ and $\{b'_n\}$, such that*

$$\langle \psi_n, H\varphi_m\rangle = b_n\delta_{n,m+1} + a_n\delta_{n,m} + b'_n\delta_{n,m-1}, \tag{8.2}$$

*for all $n, m \geq 0$. Furthermore, $H$ is called e-tridiagonal if $H$ is $(e, e)$-tridiagonal.*

This definition is a generalization of the one in [184] in two ways: first, $H$ is not required to be self-adjoint. For this reason no relation is assumed, in general, between $\{b_n\}$ and $\{b'_n\}$, and $a_n$ can be complex. Second, we are replacing a single basis with two biorthogonal sets, $\mathcal{F}_\varphi$ and $\mathcal{F}_\psi$, none of which is even necessarily a basis. However, as often explicitly checked in concrete examples involving $\mathcal{D}$-quasi bases [12], both $\mathcal{F}_\varphi$ and $\mathcal{F}_\psi$ are assumed to be complete in $\mathcal{H}$: the only vector $f \in \mathcal{H}$ which is orthogonal to all the $\varphi_n$'s, or to all the $\psi_n$'s, is $f = 0$.

**Lemma 2.** *$H$ is $(\varphi, \psi)$-tridiagonal if and only if $H^\dagger$ is $(\psi, \varphi)$-tridiagonal. Moreover, if $\mathcal{D}$ is stable under the action of $H$ and if $\mathcal{F}_\varphi$ and $\mathcal{F}_\psi$ are Riesz bases, then $H$ is $(\varphi, \psi)$-tridiagonal if and only if $H_0 := T^{-1}HT$ is e-tridiagonal.*

The proof is easy and will not be given here. We stress that $D(H_0) \supseteq \mathcal{D}$ and that $\mathcal{D}$ is stable also under the action of $H_0$.

Using Eq. (8.2) we get that

$$H\varphi_m = b'_{m-1}\varphi_{m-1} + a_m\varphi_m + b_{m+1}\varphi_{m+1}. \tag{8.3}$$

Indeed, as $\mathcal{F}_\psi$ and $\mathcal{F}_\varphi$ are biorthogonal, we can rewrite Eq. (8.2) as

$$\big\langle \psi_n, \big(H\varphi_m - b'_n\varphi_{m-1} + a_n\varphi_m + b_n\varphi_{m+1}\big)\big\rangle = 0,$$

which must be satisfied for all $n$. Since the set $\mathcal{F}_\psi$ is complete, Eq. (8.3) follows. Observe that $b'_{-1} = 0$ here and in the following. Similarly, recalling that $\psi_n \in D(H^\dagger)$ and that $\langle \psi_n, H\varphi_m\rangle = \langle H^\dagger\psi_n, \varphi_m\rangle$, from Eq. (8.2) and from the completeness of $\mathcal{F}_\varphi$ we find that[1]

$$H^\dagger\psi_m = \overline{b'_m}\,\psi_{m+1} + \overline{a_m}\,\psi_m + \overline{b_m}\,\psi_{m-1}. \tag{8.4}$$

This formula shows that $\overline{b_0} = b_0 = 0$. Also, Eqs. (8.3) and (8.4) show that $\varphi_m$ is not an eigenstate of $H$, and that $\psi_m$ is not an eigenstate of $H^\dagger$, except if $b_m = b'_m = 0$ for all $m$. Clearly, when this happens, $H$ is diagonal, rather than tridiagonal. Under the assumptions of Lemma 2, Eqs. (8.3) and (8.4) produce, for $H_0$, the following equations:

$$H_0 e_m = b'_{m-1}e_{m-1} + a_m e_m + b_{m+1}e_{m+1}, \quad H_0^\dagger e_m = \overline{b'_m}\,e_{m+1} + \overline{a_m}\,e_m + \overline{b_m}\,e_{m-1}. \tag{8.5}$$

**Lemma 3.** *Let $\mathcal{D}$ be stable under the action of $H$ and let $\mathcal{F}_\varphi$ and $\mathcal{F}_\psi$ be Riesz bases. If $H_0 = H_0^\dagger$, then $a_n \in \mathbb{R}$ and $b_m = \overline{b'_{m-1}}$ for all $m \geq 0$. Vice versa, if $a_m \in \mathbb{R}$ and $b_m = \overline{b'_{m-1}}$, then $\langle f, H_0 g\rangle = \langle H_0 f, g\rangle$, for all $f, g \in \mathcal{E}$, where $\mathcal{E}$ is the linear span of the $e_n$'s.*

The proof is a simple consequence of formula (8.5). In particular, $b_m = \overline{b'_{m-1}}$ is automatically satisfied for $m = 0$, since, as we have already noticed, $b_0 = b'_{-1} = 0$. Observe that $\mathcal{E}$ is dense in $\mathcal{H}$, since $\mathcal{F}_e$ is an orthonormal set of vectors in the dense set $\mathcal{D}$. Hence $\mathcal{F}_e$ is an orthonormal basis for $\mathcal{H}$. Notice that this Lemma shows that $H_0$ can be non self-adjoint too. This is often not the case in $\mathcal{PT}$ quantum mechanics [16], or for pseudo-hermitian operators [153], where non self-adjoint Hamiltonians are shown to be similar to self-adjoint ones, and the similarity is implemented exactly as above, in $H_0 := T^{-1}HT$. This is not in general the case here.

### 8.2.1 Factorization

Following [184], we now discuss when and how $H$ can be factorized, and we use this factorization to introduce the supersymmetric versions of $H$ and $H^\dagger$.

We first introduce an operator $X$ on $\mathcal{L}_\varphi = \text{l.s.}\{\varphi_n\}$, the linear span of the $\varphi_n$'s, which is dense in $\mathcal{H}$ as $\mathcal{F}_\varphi$ is complete in $\mathcal{H}$ [12]. We define $X$ by his action as

$$X\varphi_n = c_n\varphi_n + d_n\varphi_{n-1} \tag{8.6}$$

This is not a lowering operator for $\mathcal{F}_\varphi$, if $c_n \neq 0$. Completeness of $\mathcal{F}_\varphi$, and its biorthogonality with $\mathcal{F}_\psi$, allows us to deduce that $X^\dagger\psi_n = \overline{c_n}\,\psi_n + \overline{d_{n+1}}\,\psi_{n+1}$, which is a raising operator for $\mathcal{F}_\psi$ only if $c_n = 0$ for all $n$. Analogously, we can introduce an operator $Y$ on the linear span of the $\psi_n$'s, $\mathcal{L}_\psi = \text{l.s.}\{\psi_n\}$, as in Eq. (8.6):

$$Y\psi_n = c'_n\psi_n + d'_n\psi_{n-1}, \tag{8.7}$$

whose adjoint acts on $\varphi_n$ as follows: $Y^\dagger\varphi_n = \overline{c'_n}\,\varphi_n + \overline{d'_{n+1}}\,\varphi_{n+1}$. Again, $Y$ and $Y^\dagger$ are not ladder operators, except if $c'_n = 0$. Also, we require that $d_0 = d'_0 = 0$, in order to avoid the appearance of $\varphi_{-1}$ or $\psi_{-1}$ in the two formulas above. We can write $H\varphi_n = Y^\dagger X\varphi_n$ if the following relations hold:

$$a_n = c_n\,\overline{c'_n} + d_n\,\overline{d'_n}, \qquad b'_{n-1} = d_n\,\overline{c'_{n-1}}, \qquad b_{n+1} = c_n\,\overline{d'_{n+1}}. \tag{8.8}$$

[1] $\overline{z}$ denotes the complex conjugate of $z$.

Under the same conditions we also deduce the equality $H^\dagger\psi_n = X^\dagger Y\psi_n$, which shows that also $H^\dagger$ can be factorized in terms of the same operators.

The operators $X$ and $Y^\dagger$ satisfy the following commutation relation

$$[X,Y^\dagger]\varphi_n = \left(d_{n+1}\overline{d'_{n+1}} - d_n\overline{d'_n}\right)\varphi_n + d_n\left(\overline{c'_n} - \overline{c'_{n-1}}\right)\varphi_{n-1} + (c_{n+1}-c_n)\,\overline{d'_{n+1}}\varphi_{n+1}. \quad (8.9)$$

Notice that, in particular, if $X$ and $Y$ are ladder operators (i.e. $c_n = c'_n = 0$), then this formula simplifies to $[X,Y^\dagger]\varphi_n = \left(d_{n+1}\overline{d'_{n+1}} - d_n\overline{d'_n}\right)\varphi_n$, becoming the standard pseudo-bosonic commutation relation [12, 172, 177, 191], if $d_n = d'_n = \sqrt{n}$: $[X,Y^\dagger]\varphi_n = \varphi_n$, for all $n$.

Observe that, when $c_n = 0$, even if $d_n \neq \sqrt{n}$, it is always possible to define new vectors, $\hat\varphi_n$, satisfying $X\hat\varphi_n = \sqrt{n}\hat\varphi_{n-1}$. It is indeed sufficient to put $\hat\varphi_n = \frac{\sqrt{n!}}{d_n!}\varphi_n$, $n \geq 0$, where $d_0! = 1$ and $d_n! = d_1 d_2 \cdots d_n$, $n \geq 1$. Analogously, if $c'_n = 0$ and $d'_n \neq \sqrt{n}$, it is again possible to define the new vectors $\hat\psi_n = \frac{\sqrt{n!}}{d'_n!}\psi_n$, satisfying $Y\hat\psi_n = \sqrt{n}\hat\psi_{n-1}$. This change of normalization of the vectors has consequences in Eq. (8.8), and in the computation of

$$\left\langle \hat\varphi_n, \hat\psi_m \right\rangle = \frac{n!}{d_n!\,d'_n!}\delta_{n,m}.$$

In general, these two families are still biortogonal, but no longer biorthonormal.

We also want to observe that, even if $X$ and $Y^\dagger$ are in general not pseudo-bosonic operators, we can still consider linear combinations of them, $C := \alpha X + \beta Y^\dagger$, $D := \gamma X + \delta Y^\dagger$, and look for conditions to make them pseudo-bosonic. In particular, if $\alpha\delta \neq \beta\gamma$, we have

$$[C,D]\varphi_n = (\alpha\delta-\beta\gamma)\Big((d_{n+1}\overline{d'_{n+1}} - d_n\overline{d'_n})\varphi_n + (d_n\overline{c'_n} - d_n\overline{c'_{n-1}})\varphi_{n-1} + (c_{n+1}\overline{d'_{n+1}} - c_n\overline{d'_{n+1}})\varphi_{n+1}\Big),$$

which reduces to $[C,D]\varphi_n = \varphi_n$ by fixing $c_n = c_0$, $c'_n = c'_0$, $\forall n > 0$ and $d_n\overline{d'_n} = \frac{n}{\alpha\delta-\beta\gamma}$, $\forall n \geq 0$. Therefore, we also have $[D^\dagger, C^\dagger]\psi_n = \psi_n, \quad \forall n \geq 0$. We observe that $H = Y^\dagger X$ can be written in terms of the operators $C, D$ as

$$H = -\frac{1}{(\alpha\delta-\beta\gamma)^2}\left(\delta\gamma C^2 + \alpha\beta D^2 - (\alpha\delta+\beta\gamma)CD + \alpha\delta\mathbb{1}\right).$$

Having factorized $H$ and $H^\dagger$, we want to consider now their SUSY partners $H_{\rm susy} = XY^\dagger$ and $H^\dagger_{\rm susy} = YX^\dagger$. Using Eq. (8.6) and $Y^\dagger\varphi_n = \overline{c'_n}\,\varphi_n + \overline{d'_{n+1}}\,\varphi_{n+1}$ we deduce that

$$H_{\rm susy}\varphi_n = B'_{n-1}\varphi_{n-1} + A_n\varphi_n + B_{n+1}\varphi_{n+1}, \quad (8.10)$$

where

$$A_n = c_n\,\overline{c'_n} + d_{n+1}\,\overline{d'_{n+1}}, \qquad B'_{n-1} = d_n\,\overline{c'_n}, \qquad B_{n+1} = c_{n+1}\,\overline{d'_{n+1}}. \quad (8.11)$$

Eq. (8.10) implies that $H_{\rm susy}$ is $(\varphi,\psi)$-tridiagonal:

$$\langle\psi_n, H_{\rm susy}\varphi_m\rangle = B_n\delta_{n,m+1} + A_n\delta_{n,m} + B'_n\delta_{n,m-1},$$

which coincides with Eq. (8.2), with $(a_n, b_n, b'_n)$ replaced by $(A_n, B_n, B'_n)$. Hence, Lemma 2 implies that $H^\dagger_{\rm susy}$ is $(\psi,\varphi)$-tridiagonal, and we can easily check that

$$H^\dagger_{\rm susy}\psi_n = \overline{B_n}\psi_{n-1} + \overline{A_n}\psi_n + \overline{B'_n}\psi_{n+1}, \quad (8.12)$$

which coincides with Eq. (8.4) with the above replacement.

### 8.2.2 Diagonalization of the Hamiltonians and consequences

If $H$ is $(\varphi,\psi)$-tridiagonal, then $\mathcal{F}_\varphi$ is not a set of eigenstates of $H$. However, we can use its vectors to look for these eigenstates, at least if $\mathcal{F}_\varphi$ is a basis for $\mathcal{H}$, as we will assume here. This implies that its biorthogonal set $\mathcal{F}_\psi$ is a basis as well [192].

Let $\Phi_n$ be an eigenstate of $H$, with eigenvalue $E_n$:

$$H\Phi_n = E_n\Phi_n. \tag{8.13}$$

Observe that, in general, $E_n$ is also unknown. Expand $\Phi_n$ in terms of $\mathcal{F}_\varphi$ and using its biorthogonality with $\mathcal{F}_\psi$ we have

$$\Phi_n = \sum_k c_k^{(n)}\,\varphi_k, \qquad c_k^{(n)} = \langle\psi_k,\Phi_n\rangle\,. \tag{8.14}$$

Assuming now that $H\sum_k c_k^{(n)}\,\varphi_k = \sum_k c_k^{(n)}\,H\varphi_k$, which is true, for instance, if $H$ is bounded or under some closability condition on $H$, and using Eq. (8.3) and the biorthogonalities of $\mathcal{F}_\psi$ and $\mathcal{F}_\varphi$, we deduce the following relation between the coefficients:

$$c_l^{(n)}E_n = c_{l-1}^{(n)}b_l + c_l^{(n)}a_l + c_{l+1}^{(n)}b'_l, \tag{8.15}$$

where $c_{-1}^{(n)} = 0$. Analogously, we can look for eigenstates of $H^\dagger$ using $\mathcal{F}_\psi$: let $\eta_n$ be the eigenstate of $H^\dagger$ corresponding to the eigenvalue $\overline{E}_n$:

$$H^\dagger\eta_n = \overline{E}_n\eta_n.$$

We expand $\eta_n$ in terms of $\mathcal{F}_\psi$:

$$\eta_n = \sum_k d_k^{(n)}\,\psi_k, \qquad d_k^{(n)} = \langle\varphi_k,\eta_n\rangle\,. \tag{8.16}$$

Now, if $H^\dagger\sum_k d_k^{(n)}\,\psi_k = \sum_k d_k^{(n)}\,H^\dagger\psi_k$, we deduce the following relation, quite similar to that in Eq. (8.15):

$$\overline{d_l^{(n)}}E_n = \overline{d_{l-1}^{(n)}}b'_{l-1} + \overline{d_l^{(n)}}a_l + \overline{d_{l+1}^{(n)}}b_{l+1}, \tag{8.17}$$

where, obviously, we have set $d_{-1}^{(n)} = 0$. Comparing this formula with Eq. (8.15) we see that, if $b_l = b'_{l-1}$, once $c_l^{(n)}$ is computed, then $d_l^{(n)}$ can be easily deduced by taking $d_l^{(n)} = \overline{c_l^{(n)}}$.

The coefficients $c_l^{(n)}$ and $d_l^{(n)}$ satisfy some summation formulas which are deduced in the following Proposition.

**Proposition 4.** *The coefficients $c_l^{(n)}$ and $d_l^{(n)}$ satisfy the equation*

$$\sum_k \overline{c_k^{(n)}}\,d_k^{(m)} = \langle\Phi_n,\eta_m\rangle = \delta_{n,m}, \tag{8.18}$$

*where the last equality holds if each eigenvalue of $H$ has multiplicity one and if the normalizations of $\Phi_n$ and $\eta_n$ are chosen in such a way that $\langle\Phi_n,\eta_n\rangle = 1$.*

*Also, if $\mathcal{F}_\Phi = \{\Phi_n\}$ and $\mathcal{F}_\eta = \{\eta_n\}$ are $\mathcal{D}$-quasi bases, then*

$$\sum_n \overline{c_k^{(n)}}\,d_l^{(n)} = \delta_{k,l}, \tag{8.19}$$

*Proof.* First of all, using the resolution of the identity in $\mathcal{D}$ given by Eq. (8.1) we have

$$\sum_k \overline{c_k^{(n)}}\, d_k^{(m)} = \sum_k \langle \Phi_n, \psi_k\rangle \langle \varphi_k, \eta_m\rangle = \langle \Phi_n, \eta_m\rangle\,.$$

The fact that $\langle \Phi_n, \eta_m\rangle = 0$ if $n \neq m$, at least if the multiplicity of $E_n$ is one, is well known.

Eq. (8.19) can be proved as follows:

$$\sum_n \overline{c_k^{(n)}}\, d_l^{(n)} = \sum_n \langle \varphi_l, \eta_n\rangle \langle \Phi_n, \psi_k\rangle = \langle \varphi_l, \psi_k\rangle = \delta_{k,l},$$

where we have used the hypothesis that $\mathcal{F}_\Phi = \{\Phi_n\}$ and $\mathcal{F}_\eta = \{\eta_n\}$ are $\mathcal{D}$-quasi bases and that $\varphi_l, \psi_k \in \mathcal{D}$. The last equality follows from the biorthogonality of $\mathcal{F}_\varphi$ and $\mathcal{F}_\psi$.

□

Let us define the following quantities

$$p_l^{(n)} = \frac{c_l^{(n)}}{c_0^{(n)}}, \qquad\qquad q_l^{(n)} = \frac{d_l^{(n)}}{d_0^{(n)}}, \tag{8.20}$$

and observe that

$$p_{-1}^{(n)} = q_{-1}^{(n)} = 0, \qquad p_0^{(n)} = q_0^{(n)} = 1, \qquad \forall n \geq 0. \tag{8.21}$$

Eqs. (8.15) and (8.17) can be rewritten as the following recurrence equations:

$$p_{l+1}^{(n)} = \frac{1}{b_l'}\left(p_l^{(n)}(E_n - a_l) - p_{l-1}^{(n)} b_l\right) \tag{8.22}$$

and

$$\overline{q_{l+1}^{(n)}} = \frac{1}{b_{l+1}}\left(\overline{q_l^{(n)}}(E_n - a_l) - \overline{q_{l-1}^{(n)}} b_{l-1}'\right) \tag{8.23}$$

which produce, in principle, the sequences $\{p_l^{(n)}\}$ and $\{q_l^{(n)}\}$, and $\{c_l^{(n)}\}$ and $\{d_l^{(n)}\}$ from Eq. (8.20) as a consequence, using Eq. (8.21). Yet, $E_n$ must be known in order to compute explicitly these coefficients. This is what happens in some situations, as the examples in the next section show.

We conclude this section adapting these results, and formulas Eqs. (8.22) and (8.23) in particular, to the SUSY partners of $H$ and $H^\dagger$. We recall that they are both tridiagonal. In particular, $H_{\rm susy}$ is $(\varphi,\psi)$-tridiagonal, and $H_{\rm susy}^\dagger$ is $(\psi,\varphi)$-tridiagonal. Also, we have already noticed that one can go from $(H, H^\dagger)$ to $(H_{\rm susy}, H_{\rm susy}^\dagger)$ simply replacing $(a_n, b_n, b_n')$ with $(A_n, B_n, B_n')$. Therefore, starting with the following eigenvalue equations,

$$H_{\rm susy}\tilde\Phi_n = \mathcal{E}_n\tilde\Phi_n, \qquad\qquad H_{\rm susy}^\dagger\,\tilde\eta_n = \overline{\mathcal{E}}_n\,\tilde\eta_n, \tag{8.24}$$

and expanding $\tilde\Phi_n$ and $\tilde\eta_n$ as follows,

$$\tilde\Phi_n = \sum_k \tilde c_k^{(n)}\,\varphi_k, \quad \tilde\eta_n = \sum_k \tilde d_k^{(n)}\,\psi_k, \qquad \tilde c_k^{(n)} = \left\langle \psi_k, \tilde\Phi_n\right\rangle, \quad \tilde d_k^{(n)} = \langle \varphi_k, \tilde\eta_n\rangle\,,$$

the following counterparts of Eqs. (8.22) and (8.23) can be found:

$$P_{l+1}^{(n)} = \frac{1}{B_l'}\left(P_l^{(n)}(\mathcal{E}_n - A_l) - P_{l-1}^{(n)} B_l\right) \tag{8.25}$$

and

$$\overline{Q_{l+1}^{(n)}} = \frac{1}{B_{l+1}}\left(\overline{Q_l^{(n)}}(\mathcal{E}_n - A_l) - \overline{Q_{l-1}^{(n)}} B_{l-1}'\right). \tag{8.26}$$

Here we introduced the *normalized* coefficients

$$P_l^{(n)} = \frac{\tilde{c}_l^{(n)}}{\tilde{c}_0^{(n)}}, \qquad Q_l^{(n)} = \frac{\tilde{d}_l^{(n)}}{\tilde{d}_0^{(n)}}, \tag{8.27}$$

which obey, in particular,

$$P_{-1}^{(n)} = Q_{-1}^{(n)} = 0, \qquad P_0^{(n)} = Q_0^{(n)} = 1, \qquad \forall n \geq 0. \tag{8.28}$$

Observe that, $\tilde{c}_k^{(n)}$ and $\tilde{d}_k^{(n)}$ satisfy the analogous statement to Proposition 4. In particular, for instance, if $\mathcal{F}_{\tilde{\Phi}} = \{\tilde{\Phi}_n\}$ and $\mathcal{F}_{\tilde{\eta}} = \{\tilde{\eta}_n\}$ are $\mathcal{D}$-quasi bases, then $\sum_n \overline{\tilde{c}_k^{(n)}}\, \tilde{d}_l^{(n)} = \delta_{k,l}$.

## 8.3 Examples

This section is devoted to the analysis of some examples of the general framework previously introduced. In particular, in Section 8.3.1 we propose a rather general method to produce general non self-adjoint tridiagonal matrices. In Section 8.3.2 we analyse in all details a shifted harmonic oscillator, with particular attention to the three terms relations previously introduced.

### 8.3.1 A shifted quantum well

Let $H_0 = p^2 + V(x)$, where $p$ is the momentum operator and $V(x)$ is the potential which is zero for $x \in [0, \pi]$, and infinite outside this region. $H_0$ is therefore the self-adjoint Hamiltonian of a particle of mass $m = \frac{1}{2}$ in an infinitely deep square-well potential. It is well known that

$$H_0\, e_n(x) = E_n e_n(x), \qquad E_n = (n+1)^2, \qquad e_n(x) = \sqrt{\frac{2}{\pi}}\, \sin((n+1)x), \tag{8.29}$$

where $x \in [0, \pi]$ and $n \geq 0$. In [193] it is shown how $H_0$, as well as the Hamiltonians of many other physical systems, can be factorized.

Let us introduce the number operator $\hat{N}$ defined on the vectors $e_n(x)$, which all together form an orthonormal basis for $\mathcal{H} = \mathcal{L}^2(0, \pi)$: $\hat{N} e_n = n e_n$, $n \geq 0$. Of course $\hat{N}$ is not bounded nor invertible. However, $\hat{N} + \mathbb{1}$ is invertible, and $(\hat{N} + \mathbb{1})^{-1}$ is bounded. Following [193] we define the operators:

$$\hat{M}_+ = \cos(x)(\hat{N} + \mathbb{1}) + \sin(x)\frac{d}{dx}, \quad \hat{M}_- = \left(\cos(x)(\hat{N} + \mathbb{1}) - \sin(x)\frac{d}{dx}\right)(\hat{N} + \mathbb{1})^{-1}\hat{N}.$$

They are ladder operators since they satisfy

$$\hat{M}_+ e_n = (n+1) e_{n+1}, \qquad \hat{M}_- e_n = n e_{n-1},$$

where we put $e_{-1} = 0$. Hence it is possible to see that $H_0 e_n = \hat{M}_- \hat{M}_+ e_n$: Furthermore, we can also check that

$$\hat{M}_+^\dagger e_n = \hat{M}_- e_n, \qquad \hat{M}_-^\dagger e_n = \hat{M}_+ e_n, \qquad [\hat{M}_-, \hat{M}_+] e_n = (2\hat{N} + \mathbb{1}) e_n$$

for all $n$. Now, let us consider the following shifted version of the ladder operators $\hat{M}_\pm$: $B = \hat{M}_+ + \alpha\mathbb{1}$, $A = \hat{M}_- + \beta\mathbb{1}$, $\alpha, \beta \in \mathbb{C}$, and the related *shifted Hamiltonian* $h = BA$. It is easy to check that $h$ is $(e, e)$-tridiagonal:

$$h e_n = \alpha n e_{n-1} + (n^2 + \alpha\beta) e_n + \beta(n+1) e_{n+1}, \tag{8.30}$$

which coincides with Eq. (8.3) by taking $b'_{n-1} = \alpha n$, $b_{n+1} = \beta(n+1)$ and $\alpha_n = n^2 + \alpha\beta$. Since $Ae_n = \beta e_n + n e_{n-1}$ and $B = \alpha e_n + (n+1)e_{n+1}$, the coefficients in Eqs. (8.6) and (8.7) are $c_n = \beta$, $c'_n = \overline{\alpha}$, $d_n = d'_n = n$ and the identities in Eq. (8.11) are satisfied.

As for the other Hamiltonians connected to $h$, it is easy to check that for $h^\dagger$, which is clearly $(e,e)$-tridiagonal in view of Lemma 2, matches with $h$ but with $\alpha$ replaced by $\overline{\beta}$ and vice versa. As for their SUSY partners, we have, for instance

$$h_{\text{susy}} = AB = [A,B] + h = h + (2\hat{N} + \mathbb{1}),$$

since $[A,B] = [\hat{M}_- + \beta\mathbb{1}, \hat{M}_+ + \alpha\mathbb{1}] = [\hat{M}_-, \hat{M}_+] = (2\hat{N} + \mathbb{1})$. It follows that

$$h_{\text{susy}} e_n = \alpha n e_{n-1} + ((n+1)^2 + \alpha\beta)e_n + \beta(n+1)e_{n+1},$$

which shows that $A_n = a_{n+1}$, $B_n = b_n$ and $B'_n = b'_n$.

We conclude this example observing that the same approach can be extended to all systems whose self-adjoint Hamiltonian can be factorized in terms of ladder operators, as those included in [193]. Once we have an $\tilde{H}_0 = \tilde{H}_0^\dagger = Q^\dagger Q$, with eigenstates $f_n$ and eigenvalues $\mathcal{E}_n$, $\tilde{H}_0 f_n = \mathcal{E}_n f_n$, shifting $Q$ and $Q^\dagger$ with two different complex quantities, $Q \to Q + \beta\mathbb{1}$ and $Q^\dagger \to Q^\dagger + \alpha\mathbb{1}$, with $\alpha$ possibly different from $\overline{\beta}$, the non self-adjoint operator $\tilde{h} = (Q^\dagger + \alpha\mathbb{1})(Q + \beta\mathbb{1})$ is $(f,f)$-tridiagonal, with obvious notation. What is not easy, or possible, in general, is to make use of the recurrence relation (8.22) to deduce the eigenstates of $\tilde{h}$, since its eigenvalues are not known a priori. In the next example and in Section 8.4 we will discuss an example where the spectrum is known, and the recurrence relations can be efficiently used to deduce the eigenvectors.

### 8.3.2 The shifted harmonic oscillator

This model has been discussed by several authors, in slightly different forms, mainly in the context of pseudo-hermitian (or $\mathcal{PT}$) quantum mechanics [16,153]

Consider a lowering operator $c$ on $\mathcal{H}$ satisfying the canonical commutation relation $[c, c^\dagger] = \mathbb{1}$. This equality must be understood on a suitable dense subspace of $\mathcal{H}$, since $c$ and $c^\dagger$ are unbounded. For instance, if $c = \frac{1}{\sqrt{2}}\left(x + \frac{d}{dx}\right)$, the Hilbert space is $\mathcal{H} = \mathcal{L}^2(\mathbb{R})$ and the dense set can be identified with $\mathcal{S}(\mathbb{R})$, the set of rapidly decreasing test functions. If we introduce the vacuum of $c$, that is a (normalized) vector $e_0 \in \mathcal{H}$ satisfying $ce_0 = 0$, we can act on it with powers of $c^\dagger$: $e_n = \frac{(c^\dagger)^n}{\sqrt{n!}} e_0$. The resulting vectors, $\{e_n\}$, form an orthonormal basis of $\mathcal{H}$, which is all made by functions of $\mathcal{S}(\mathbb{R})$ if $c$ is represented as above. These vectors are eigenstates of $H_0 = c^\dagger c$: $H_0 e_n = n e_n$, $n \geq 0$.

We now define $a = c + \alpha\mathbb{1}$ and $b = c^\dagger + \beta\mathbb{1}$, for some $\alpha, \beta \in \mathbb{C}$, with $\alpha \neq \overline{\beta}$. These operators are $\mathcal{D}$-pseudo bosonic [12,194,195], where, using coordinate representation for $c$ and $c^\dagger$, $\mathcal{D}$ can be identified with $\mathcal{S}(\mathbb{R})$. In particular, $[a,b]f = f$ for all $f \in \mathcal{D}$. If we now call $H = ba = H_0 + (\alpha c^\dagger + \beta c) + \alpha\beta\mathbb{1}$, we find that

$$He_n = (n + \alpha\beta)e_n + \alpha\sqrt{n+1}\,e_{n+1} + \beta\sqrt{n}\,e_{n-1}, \tag{8.31}$$

so that $\langle e_n, He_m\rangle = (n+\alpha\beta)\delta_{n,m} + \alpha\sqrt{n}\delta_{n,m+1} + \beta\sqrt{n+1}\delta_{n,m-1}$. We see that $H$ is $e$-tridiagonal, likewise $H^\dagger$. Incidentally, we also observe that $H^\dagger$ coincides with $H$, but with $(\alpha,\beta)$ replaced by $(\overline{\beta},\overline{\alpha})$.

Since $ce_n = \sqrt{n}\,e_{n-1}$ and $c^\dagger e_n = \sqrt{n+1}\,e_{n+1}$, we see that $ae_n = (c + \alpha\mathbb{1})e_n = \alpha e_n + \sqrt{n}\,e_{n-1}$, while $be_n = (c^\dagger + \beta\mathbb{1})e_n = \beta e_n + \sqrt{n+1}\,e_{n+1}$, so that $X = a$ and $Y^\dagger = b$ only if the following identifications hold:

$$c_n = \alpha, \quad c'_n = \overline{\beta}, \quad d_n = d'_n = \sqrt{n}. \tag{8.32}$$

Hence, since Eq. (8.31) implies that $b_n = \alpha\sqrt{n}$, $a_n = n+\alpha\beta$ and $b'_n = \beta\sqrt{n+1}$, the equalities in Eq. (8.8) are satisfied. It is clear that, in the present example, the commutation relation in Eq. (8.9) simplifies: $[X, Y^\dagger]e_n = [a, b]e_n = e_n$, for all $n \geq 0$.

As for $H_{\rm susy} = ab$, we see that

$$H_{\rm susy}e_n = ([a, b] + H)e_n = (H + \mathbb{1})e_n = (n + 1 + \alpha\beta)e_n + \alpha\sqrt{n+1}e_{n+1} + \beta\sqrt{n}e_{n-1},$$

which coincides with Eq. (8.31) except that $n + \alpha\beta$ is now replaced by $n + 1 + \alpha\beta$. We observe that $A_n = a_{n+1}$, $B_n = b_n$ and $B'_n = b'_n$, and that

$$H^\dagger_{\rm susy}e_n = (n + 1 + \overline{\alpha}\overline{\beta})e_n + \overline{\alpha}\sqrt{n}e_{n-1} + \overline{\beta}\sqrt{n+1}e_{n+1}.$$

It is now worth discussing the role of Eqs. (8.22) and (8.23) in this example. This is particularly simple here since we know that the eigenvalues of $H$ and $H^\dagger$ are just $E_n = n$, for all $n \geq 0$.

Let us first take $n = 0$, and look for the ground state of $H = ba$: $H\Phi_0 = 0$. Such an eigenstate can be easily found, simply by looking at the vacuum of $a$. Of course, $a\Phi_0 = 0$ if and only if $c\Phi_0 = -\alpha\Phi_0$. This means that $\Phi_0$ is (proportional to) a standard coherent state [196–198], with parameter $-\alpha$:

$$\Phi_0 = N_\Phi e^{-\alpha c^\dagger + \overline{\alpha}c}e_0 = N_\Phi e^{-\frac{|\alpha|^2}{2}} \sum_{k=0}^{\infty} \frac{(-\alpha)^k}{\sqrt{k!}}\, e_k, \tag{8.33}$$

where $N_\Phi$ is a normalization factor usually taken equal to one for standard coherent states [196].

In a similar way we could find the ground state of $H^\dagger$. However, the easier way to find $\eta_0$ is just to recall the above cited symmetry between $H$ and $H^\dagger$. Hence $\eta_0$ is, a part the normalization, nothing but $\Phi_0$ with $\alpha$ replaced by $\overline{\beta}$:

$$\eta_0 = N_\eta e^{-\overline{\beta}c^\dagger + \beta c}e_0 = N_\eta e^{-\frac{|\beta|^2}{2}} \sum_{k=0}^{\infty} \frac{(-\overline{\beta})^k}{\sqrt{k!}}\, e_k. \tag{8.34}$$

A connection between $N_\Phi$ and $N_\eta$ can be found by requiring that $\langle\Phi_0, \eta_0\rangle = 1$: $N_\Phi N_\eta = e^{\frac{1}{2}(|\alpha|^2+|\beta|^2+\alpha\beta)}$.

We want to show now that the same expansions as in Eqs. (8.33) and (8.34) can be obtained by means of Eqs. (8.22) and (8.23). We first specialize Eq. (8.22) to $n = 0$ and to our particular value of the coefficients:

$$p^{(0)}_{l+1} = \frac{-1}{\beta\sqrt{l+1}}\left(p^{(0)}_l(l + \alpha\beta) + p^{(0)}_{l-1}\alpha\sqrt{l}\right),$$

with, as usual, $p^{(0)}_{-1} = 0$ and $p^{(0)}_0 = 1$. It is simple now to find the general solution of this recurrence relation: $p^{(0)}_k = \frac{(-\alpha)^k}{\sqrt{k!}}$, so that $c^{(0)}_k = \frac{(-\alpha)^k}{\sqrt{k!}}\, c^{(0)}_0$, for all $k \geq 0$. Therefore, Eq. (8.14) produces

$$\Phi_0 = \sum_k c^{(0)}_k\, e_k = c^{(0)}_0 \sum_k \frac{(-\alpha)^k}{\sqrt{k!}}\, e_k,$$

which coincides with Eq. (8.33), upon identifying $c^{(0)}_0$ with $N_\Phi e^{-\frac{|\alpha|^2}{2}}$.

Using now (8.23), in the same way we recover $\eta_0$ in (8.34). This is because we find $q^{(0)}_k = \frac{(-\overline{\beta})^k}{\sqrt{k!}}$.

Observe that, in this simple example, we can also make use of the factorization $H = Y^\dagger X$ to get the same results. Indeed, the ground state $\Phi_0$ can be obtained as the vacuum of $X, X\Phi_0 = 0$ (and similarly $\eta_0$ as the ground state of $Y$). Expanding $\Phi_0$ as

$$\Phi_0 = \sum_{k\geq 0} c_k^{(0)} \varphi_k, \quad c_k^{(0)} = \langle \psi_k, \Phi_0 \rangle \,,$$

and using the biorthogonality conditions between $\mathcal{F}_\varphi$ and $\mathcal{F}_\psi$ we have

$$0 = \langle \psi_k, X\Phi_0 \rangle = c_k c_k^{(0)} + d_{k+1} c_{k+1}^{(0)} = \alpha c_k^{(0)} + \sqrt{k+1}\, c_{k+1}^{(0)},$$

and as before the solution is $c_k^{(0)} = \frac{(-\alpha)^k}{\sqrt{k!}} c_0^{(0)}$, yielding $p_k^{(0)} = \frac{(-\alpha)^k}{\sqrt{k!}}$.

We now generalize these results to the higher levels, $n > 0$, and show that the eigenstates of $H$ can be completely determined again by using Eq. (8.22). First, for the sake of clarity, we discuss the case $n = 1$ and then we extend the results.

The eigenstates of $H$ are given by [12]

$$\Phi_n = \frac{1}{\sqrt{n!}} b^n \Phi_0 \tag{8.35}$$

where $\Phi_0$ is as in Eq. (8.33). It is easy to verify that

$$b^n e_k = \sum_{i=0}^{n} \left[ \binom{n}{i} \beta^{n-i} p_k(i) \right] e_{k+i} \tag{8.36}$$

where $p_k(i) = \sqrt{k+1}\sqrt{k+2}\ldots\sqrt{k+i}$ if $i \geq 1$ and 0 if $i = 0$. Therefore

$$\Phi_n = \frac{1}{\sqrt{n!}} N_\Phi e^{-\frac{|\alpha|^2}{2}} \sum_{k=0}^{\infty} \frac{(-\alpha)^k}{\sqrt{k!}} \sum_{i=0}^{n} \left[ \binom{n}{i} \beta^{n-i} p_k(i) \right] e_{k+i}, \tag{8.37}$$

The first "excited" state will be

$$\Phi_1 = N_\Phi e^{-\frac{|\alpha|^2}{2}} \sum_{k=0}^{\infty} \frac{(-\alpha)^k}{\sqrt{k!}} \left[ k + (-\alpha)\beta \right] e_k, \tag{8.38}$$

This result can also be recovered by starting from the recurrence relation (8.22), which looks now as follows:

$$p_{l+1}^{(1)} = \frac{1}{\beta\sqrt{l+1}} \left( p_l^{(1)} (1 - (l + \alpha\beta)) - p_{l-1}^{(1)} \alpha \sqrt{l} \right) \tag{8.39}$$

with $p_{-1}^{(1)} = 0$ and $p_0^{(1)} = 1$. It is easy to show that

$$c_l^{(1)} = \frac{c_0^{(1)}}{\beta} \sum_{l=0}^{\infty} \frac{(-\alpha)^l}{\sqrt{l!}} \left[ l + (-\alpha)\beta \right] \tag{8.40}$$

which allows to retrieve Eq. (8.38) provided that $c_0^{(1)} = \beta N_\Phi e^{-\frac{|\alpha|^2}{2}}$.

For arbitrary $n > 1$ it is possible to write $\Phi_n$ as

$$\Phi_n = \frac{1}{\sqrt{n!}} N_\Phi e^{-\frac{|\alpha|^2}{2}} \sum_{k=0}^{\infty} \frac{(-\alpha)^k}{\sqrt{k!}} \sum_{j=0}^{n} \left[ \binom{n}{j} [(-\alpha)\beta]^{n-j} j! \binom{k}{j} \right] e_k \tag{8.41}$$

and show that the recurrence relation yields the same result provided that

$$c_0^{(n)} = \frac{\beta^n}{\sqrt{n!}} N_\Phi e^{-\frac{|\alpha|^2}{2}} \tag{8.42}$$

Using the symmetry between $H$ and $H^\dagger$ it is easy to check that the "excited" states of $H^\dagger$ are given by [12]

$$\eta_n = \frac{1}{\sqrt{n!}}(a^\dagger)^n \eta_0 = \frac{1}{\sqrt{n!}} N_\eta e^{-\frac{|\beta|^2}{2}} \sum_{k=0}^{\infty} \frac{(-\overline{\beta})^k}{\sqrt{k!}} \sum_{j=0}^{n} \left[ \binom{n}{j} [(-\overline{\beta})\overline{\alpha}]^{n-j} j! \binom{k}{j} \right] e_k \tag{8.43}$$

and this is the same result one gets starting from the recurrence relation (8.23), apart for a normalization factor.

A similar analysis can be repeated also for the SUSY partners of $H$ and $H^\dagger$. Of course, since in the present situation $H_{\rm susy} = H + \mathbb{1}$ and $H^\dagger_{\rm susy} = H^\dagger + \mathbb{1}$, the eigenstates in Eq. (8.24) coincide with those without the tilde: $\tilde{\Phi}_n = \Phi_n$ and $\tilde{\eta}_n = \eta_n$, while the eigenvalues obey the relation $\mathcal{E}_n = E_n + 1 = n + 1$. If we now adopt Eqs. (8.25) and (8.26), with $\mathcal{E}_0 = 1$, we recover again the correct eigenstates, apart for the normalization, which must be chosen with care.

To conclude, we observe that this example can be generalized by introducing a sort of *double translation*. More in detail, we could consider, as starting points, two $\mathcal{D}$-pseudo bosonic operators $a$ and $b$, $[a, b]f = f$ for all $f \in \mathcal{D}$, and the related (already) non self-adjoint Hamiltonian $H = ba$: $H \neq H^\dagger$. Its eigenvalues are $E_n = n$, $n \geq 0$, while its eigenvectors are those in Eq. (8.35). $H^\dagger$ has the same eigenvalues of $H$, while its eigenstates are those in Eq. (8.43). If we now introduce two complex parameters $\gamma$ and $\delta$, and two new operators $A = a + \gamma\mathbb{1}$ and $B = b + \delta\mathbb{1}$, it is clear that $[A, B]f = f$ for all $f \in \mathcal{D}$. Moreover, in general, $A \neq B^\dagger$. It is straightforward to check that $\hat{H} = BA$ is $(\Phi, \eta)$-tridiagonal, and therefore, see Lemma 2, $\hat{H}^\dagger$ is $(\eta, \Phi)$-tridiagonal. The previous discussion can be essentially repeated, with minor changes, for $\hat{H}$, $\hat{H}^\dagger$, and for their SUSY partners. In particular, if the operators $a$ and $b$ are related to two bosonic operators $c$ and $c^\dagger$ as above, $a = c + \alpha\mathbb{1}$ and $b = c^\dagger + \beta\mathbb{1}$, it is clear that $A = c$ and $B = c^\dagger$ if $\alpha = -\gamma$ and $\beta = -\delta$. In this case, $H_0 = \hat{H} = \hat{H}^\dagger$. When these equalities (or one of them) are not satisfied, the same results as in this section hold true with $(\alpha, \beta)$ replaced by $(\alpha + \gamma, \beta + \delta)$.

## 8.4 Extended settings

In this section we consider a slightly different form of the Hamiltonian which is not tridiagonal, but whose matrix elements in two biorthogonal bases can still be written as a sum of three contributions. All the hypothesis of completeness, closability and domain invariance assumed in the previous sections are maintained, if not otherwise specified.

**Definition 5.** *$H$ is called $(\varphi, \psi)_h$-tridiagonal, with $h > 0$, if three sequences of complex numbers exist, $\{b_n\}$, $\{a_n\}$ and $\{b'_n\}$, such that*

$$\langle \psi_n, H\varphi_m \rangle = b_n \delta_{n,m+h} + a_n \delta_{n,m} + b'_n \delta_{n,m-h}, \tag{8.44}$$

*for all $n, m \geq 0$. Furthermore, $H$ is called $e_h$-tridiagonal if $H$ is $(e, e)_h$-tridiagonal.*

In the previous section we analyzed the case $h = 1$, so here we consider $h > 1$. Using Eq. (8.44) and completeness of $\mathcal{F}_\varphi$ and $\mathcal{F}_\psi$, we deduce the natural extensions of Eqs. (8.3) and (8.4):

$$H\varphi_m = b'_{m-h}\varphi_{m-h} + a_m\varphi_m + b_{m+h}\varphi_{m+h}, \tag{8.45}$$

$$H^\dagger\psi_m = \overline{b'_m}\,\psi_{m+h} + \overline{a_m}\,\psi_m + \overline{b_m}\,\psi_{m-h}, \tag{8.46}$$

with the conditions that $b_j = 0$ for $j < h$ and $b'_j = 0$ for $j < 0$. It is straightforward to factorize $H$ and $H^\dagger$ by introducing the operator $X_h$ on $\mathcal{L}_\varphi$ and $Y_h$ on $\mathcal{L}_\psi$, defined as

$$X_h\varphi_n = c_n\varphi_n + d_n\varphi_{n-h}, \quad Y_h\psi_n = c'_n\psi_n + d'_n\psi_{n-h}, \quad \forall n \geq 0, \tag{8.47}$$

with $d_j = d'_j = 0, j < h$. It is immediate to check that $H\varphi_n = Y_h^\dagger X_h\varphi_n$ and $H^\dagger\psi_n = X_h^\dagger Y_h\psi_n$ by putting

$$a_n = c_n\,\overline{c'_n} + d_n\,\overline{d'_n}, \qquad b'_{n-h} = d_n\,\overline{c'_{n-h}}, \qquad b_{n+h} = c_n\,\overline{d'_{n+h}}, \tag{8.48}$$

and that in general

$$[X_h, Y_h^\dagger]\varphi_n = \left(d_{n+h}\overline{d'_{n+h}} - d_n\overline{d'_n}\right)\varphi_n + d_n\left(\overline{c'_n} - \overline{c'_{n-h}}\right)\varphi_{n-h} + \overline{d'_{n+h}}\,(c_{n+h} - c_n)\,\varphi_{n+h}. \tag{8.49}$$

In order to derive a suitable recurrence formula for the determination of the eigenstates of $H$ and $H^\dagger$, we adopt the same strategy used in Section 8.2.2. In particular, if $\Phi_n, \eta_n$ are eigenstates of $H$ and $H^\dagger$, respectively, and we expand $\Phi_n$ and $\eta_n$ as in Eqs. (8.14) and (8.16), we obtain the following recurrence formulas:

$$c_l^{(n)}E_n = c_{l-h}^{(n)}b_l + c_l^{(n)}a_l + c_{l+h}^{(n)}b'_l, \tag{8.50}$$

$$\overline{d_l^{(n)}}E_n = \overline{d_{l-h}^{(n)}}b'_{l-h} + \overline{d_l^{(n)}}a_l + \overline{d_{l+h}^{(n)}}b_{l+h}, \tag{8.51}$$

with $c_j^{(n)}, d_j^{(n)} = 0$, $j < h, j \neq 0$, and the related

$$p_{l+h}^{(n)} = \frac{1}{b'_l}\left(p_l^{(n)}(E_n - a_l) - p_{l-h}^{(n)}b_l\right), \tag{8.52}$$

$$\overline{q_{l+h}^{(n)}} = \frac{1}{b_{l+h}}\left(\overline{q_l^{(n)}}(E_n - a_l) - \overline{q_{l-h}^{(n)}}b'_{l-h}\right), \tag{8.53}$$

where the coefficients $p_j^{(n)}, q_j^{(n)}$ are defined as in (8.20) with $p_j^{(n)} = q_j^{(n)} = 0, \quad j < h$ with the exceptions $p_0^{(n)} = q_0^{(n)} = 1$.

### 8.4.1 A squeezed Hamiltonian

Despite the general $(\varphi, \psi)_h$-tridiagonal settings seems to be a straightforward extension of the $(\varphi, \psi)$-tridiagonal case, some relevant Hamiltonians can be related to them, giving rise to states having interesting features. In the following we consider an Hamiltonian from which a (bi)-squeezed state can be obtained by applying our recurrence procedure [189].

Suppose that there exist two pseudo-bosonic operators $a, b$ satisfying the commutation rules $[a, b] = \mathbb{1}$ in $\mathcal{D}$, dense subspace of $\mathcal{H}$. As usual, we suppose that $\mathcal{D}$ is stable under the action of $a$, $b$, and their adjoints. Following [12] we have

$$a\varphi_n = \sqrt{n}\varphi_{n-1}, \qquad b\varphi_n = \sqrt{n+1}\varphi_{n+1}, \tag{8.54}$$

$$b^\dagger\psi_n = \sqrt{n}\psi_{n-1}, \qquad a^\dagger\psi_n = \sqrt{n+1}\psi_{n+1}. \tag{8.55}$$

We then introduce the *squeezing-like operators*, labeled by the complex variable $z = re^{i\theta}, \quad r > 0$:

$$\mathcal{S}(z)f = \sum_{k\geq 0}\frac{1}{k!}\left(\frac{z}{2}b^2 - \frac{\overline{z}}{2}a^2\right)^k f, \quad \mathcal{T}(z)f = \sum_{k\geq 0}\frac{1}{k!}\left(\frac{z}{2}(a^\dagger)^2 - \frac{\overline{z}}{2}(b^\dagger)^2\right)^k f, \tag{8.56}$$

for all $f \in \mathcal{D}$, which under our assumptions converge strongly in $\mathcal{D}$ to $e^{\frac{1}{2}zb^2-\frac{1}{2}\bar{z}a^2}$ and to $e^{\frac{1}{2}z(a^\dagger)^2-\frac{1}{2}\bar{z}(b^\dagger)^2}$ respectively, cf. Ref. [189]. We can now introduce the operators $A = \mathcal{S}(z)a\mathcal{T}^\dagger(z), B = \mathcal{T}(z)b\mathcal{S}^\dagger(z)$ which reduce to

$$A = \cosh(r)a + e^{i\theta}\sinh(r)b, \quad B = \cosh(r)b + e^{-i\theta}\sinh(r)a, \tag{8.57}$$

see [189]. They appear to be $\mathcal{D}$-pseudo bosonic operators as they satisfy $[A, B] = \mathbb{1}$ in $\mathcal{D}$.

We now define the Hamiltonian

$$H = BA = \mu(z)ba + \lambda(z)a^2 + \lambda(\bar{z})b^2 + \sinh(r)^2\mathbb{1}, \tag{8.58}$$

where $\mu(z) = \cosh(2r), \lambda(z) = e^{-i\theta}\cosh(r)\sinh(r)$. Observe that $H$ is $(\varphi, \psi)_2$-tridiagonal, because, using the raising and lowering conditions in Eqs. (8.54) and (8.55), we have

$$\langle\psi_n, H\varphi_m\rangle = b_n\delta_{n,m+2} + a_n\delta_{n,m} + b'_n\delta_{n,m-2}, \tag{8.59}$$

with

$$a_n = n\mu(z) + \sinh(r)^2, \quad b_n = \lambda(\bar{z})\sqrt{n(n-1)}, \quad b'_n = \lambda(z)\sqrt{(n+1)(n+2)}, \tag{8.60}$$

for all $n \geq 0$.

The eigenvalues of $H$ are clearly $E_n = n$. Hence, the ground state $\Phi_0$ of $H$ satisfies $H\Phi_0 = 0$. To find the expressions for $\Phi_0$ we expand it as

$$\Phi_0 = \sum_{k\geq 0} c_k^{(0)}\varphi_k, \quad c_k^{(0)} = \langle\psi_k, \Phi_0\rangle,$$

and we can find the coefficients $c_k^{(0)}$ by means of Eqs. (8.50) and (8.52). In particular, we have

$$p_{k+2}^{(0)} = \frac{1}{b'_k}\left(-a_k p_k^{(0)} - b_k p_{k-2}^{(0)}\right), \tag{8.61}$$

with the initial conditions $p_{-2}^{(0)} = p_{-1}^{(0)} = p_1^{(0)} = 0$ and $p_0^{(0)} = 1$. This recurrence formula admits the solution

$$p_{2k}^{(0)} = \left(\frac{-e^{i\theta}\tanh(r)}{2}\right)^k \frac{\sqrt{(2k)!}}{k!}, \quad p_{2k+1}^{(0)} = 0, \quad \forall k \geq 0, \tag{8.62}$$

so that we have

$$\Phi_0 = c_0^{(0)} \sum_{k\geq 0}\left(\frac{-e^{i\theta}\tanh(r)}{2}\right)^k \frac{\sqrt{(2k)!}}{k!}\phi_{2k}.$$

Looking for the ground state $\eta_0$ of $H^\dagger$ we obtain similarly

$$\eta_0 = d_0^{(0)} \sum_{k\geq 0}\left(\frac{-e^{i\theta}\tanh(r)}{2}\right)^k \frac{\sqrt{(2k)!}}{k!}\psi_{2k}.$$

We notice that $\Phi_0$ and $\eta_0$ are (proportional) to the bi-squeezed states in [189]. In particular, choosing normalization so that $c_0^{(0)} = d_0^{(0)} = e^{-\frac{1}{2}\log(\cosh(r))}$, we get $\langle\eta_0, \Phi_0\rangle = 1$.

Of course, we can also use the factorization $H = Y^\dagger X$ to recover the same results, and recovering $\Phi_0$ as the vacuum of $X$ ($X\Phi_0 = 0$). In this case the condition (8.48) with (8.60) is satisfied by choosing

$$c_n = c'_n = \sqrt{n+1}\sinh(r), \quad d_n = d'_n = e^{-i\theta}\sqrt{n}\cosh(r),$$

and to retrieve $\Phi_0$ we require that

$$\langle \psi_k, X\Phi_0 \rangle = c_k c_k^{(0)} + d_{k+2} c_{k+2}^{(0)} = 0, \quad \forall k \geq 0.$$

This implies that the coefficients $p_k^{(0)}$ satisfy the recurrence formula

$$p_{k+2}^{(0)} = -e^{i\theta} \tanh(r) \sqrt{\frac{k+1}{k+2}} p_k^{(0)},$$

which again is satisfied by (8.62). The advantage of using the factorization $H = Y^\dagger X$ relies in the fact that we can recover a two terms recurrence formula, instead of using the recurrence formula (8.61), where three terms are involved.

Once we have retrieved the ground states of $H$ and $H^\dagger$, we can easily find the ground states of their SUSY partners. In fact, as we have

$$H_{\text{susy}} = AB = \mu(z)ba + \lambda(z)a^2 + \lambda(\overline{z})b^2 + \cosh(r)^2 \mathbb{1} = H + \mathbb{1},$$

the ground states $\tilde{\Phi}_0, \tilde{\eta}_0$ of $H_{\text{susy}}$ and $H_{\text{susy}}^\dagger$ coincide with $\Phi_0, \eta_0$, respectively, but with eigenvalues 1.

## 8.5 Summary

In this chapter we have considered non self-adjoint tridiagonal Hamiltonians and their SUSY partners, and discussed the possibility to factorize them using operators which may be pseudo-bosonic. Three-terms recurrence relations have been deduced and have been used in the construction of the eigenstates of the Hamiltonians involved in our analysis. Within the framework proposed here we have considered a shifted harmonic oscillator, and a shifted infinitely deep square well. Furthermore, we have extended our results to $(\varphi, \psi)_h$-tridiagonal matrices, and we have shown how this extension, if $h = 2$, is connected with squeezed and bi-squeezed states.

# Conclusion

This dissertation summarizes part of the research activities carried out during my PhD. The first part deals with non-Hermiticity in concrete physical systems. The results presented show how at the exceptional point of an open system unconventional behaviors can occur, from the critical behavior of quantum correlations in a bipartite system to exotic atomic interaction mediated by a non-Hermitian photonic lattice. These results, especially the latter, point to a shift of paradigm in quantum optics as non-Hermiticity becomes a necessary ingredient to achieve otherwise impossible behaviors. In the second part we dealt with non self-adjoint operators inspired by quantum mechanics and investigated their mathematical framework. In particular we addressed the problem of quantizing a dissipative system, showing that a possible way out is to go beyond the Hilbert space description, and introduced a new class of tridiagonal non-Hermitian operators and their supersymmetric partners.

# Bibliography


[1] Claude Cohen-Tannoudji, Bernard Diu, and Franck Laloë. *Quantum Mechanics, Volume 1: Basic Concepts, Tools, and Applications*. John Wiley & Sons, 2019.

[2] Carl M. Bender, Dorje C. Brody, and Hugh F. Jones. Must a Hamiltonian be Hermitian? *American Journal of Physics*, 71(11):1095–1102, October 2003.

[3] Carl M. Bender. Making sense of non-Hermitian Hamiltonians. *Rep. Prog. Phys.*, 70(6):947–1018, May 2007.

[4] Emil J. Bergholtz, Jan Carl Budich, and Flore K. Kunst. Exceptional topology of non-hermitian systems. *Rev. Mod. Phys.*, 93:015005, Feb 2021.

[5] Kohei Kawabata, Ken Shiozaki, Masahito Ueda, and Masatoshi Sato. Symmetry and topology in non-hermitian physics. *Phys. Rev. X*, 9:041015, Oct 2019.

[6] Yuto Ashida, Zongping Gong, and Masahito Ueda. Non-hermitian physics. *Advances in Physics*, 69(3):249–435, 2020.

[7] W. D. Heiss. The physics of exceptional points. *J. Phys. A: Math. Theor.*, 45(44):444016, October 2012.

[8] Mohammad-Ali Miri and Andrea Alù. Exceptional points in optics and photonics. *Science*, 363(6422), 2019.

[9] Carl M. Bender and Stefan Boettcher. Real Spectra in Non-Hermitian Hamiltonians Having $\mathcal{PT}$ Symmetry. *Phys. Rev. Lett.*, 80(24):5243–5246, June 1998.

[10] Dorje C Brody. Biorthogonal quantum mechanics. *Journal of Physics A: Mathematical and Theoretical*, 47(3):035305, 2013.

[11] Ali Mostafazadeh. Conceptual aspects of-symmetry and pseudo-hermiticity: a status report. *Physica Scripta*, 82(3):038110, 2010.

[12] Fabio Bagarello, Jean-Pierre Gazeau, Franciszek Hugon Szafraniec, and Miloslav Znojil. *Non-selfadjoint operators in quantum physics: Mathematical aspects*. John Wiley & Sons, 2015.

[13] Ilario Giordanelli and Gian Michele Graf. The real spectrum of the imaginary cubic oscillator: an expository proof. *arXiv preprint arXiv:1310.7767*, 2013.

[14] Ramy El-Ganainy, Konstantinos G. Makris, Mercedeh Khajavikhan, Ziad H. Musslimani, Stefan Rotter, and Demetrios N. Christodoulides. Non-Hermitian physics and PT symmetry. *Nat. Phys.*, 14(1):11–19, January 2018.

[15] Christian E. Rüter, Konstantinos G. Makris, Ramy El-Ganainy, Demetrios N. Christodoulides, Mordechai Segev, and Detlef Kip. Observation of parity–time symmetry in optics. *Nat. Phys.*, 6(3):192–195, March 2010.

[16] Carl M Bender. *PT symmetry: In quantum and classical physics*. World Scientific, 2019.

[17] Tosio Kato. *Perturbation theory for linear operators*, volume 132. Springer Science & Business Media, 2013.

[18] Nimrod Moiseyev and Shmuel Friedland. Association of resonance states with the incomplete spectrum of finite complex-scaled hamiltonian matrices. *Phys. Rev. A*, 22:618–624, Aug 1980.

[19] Jan Wiersig. Review of exceptional point-based sensors. *Photon. Res.*, 8(9):1457–1467, Sep 2020.

[20] Federico Roccati, Salvatore Lorenzo, G Massimo Palma, Gabriel T Landi, Matteo Brunelli, and Francesco Ciccarello. Quantum correlations in $\mathcal{PT}$-symmetric systems. *Quantum Science and Technology*, 6(2):025005, 2021.

[21] Savannah Garmon, Mariagiovanna Gianfreda, and Naomichi Hatano. Bound states, scattering states, and resonant states in $\mathcal{PT}$-symmetric open quantum systems. *Phys. Rev. A*, 92:022125, Aug 2015.

[22] Archak Purkayastha, Manas Kulkarni, and Yogesh N. Joglekar. Emergent $\mathcal{PT}$ symmetry in a double-quantum-dot circuit qed setup. *Phys. Rev. Research*, 2:043075, Oct 2020.

[23] Marco Ornigotti and Alexander Szameit. Quasi $\mathcal{PT}$-symmetry in passive photonic lattices. *Journal of Optics*, 16(6):065501, may 2014.

[24] Yogesh N Joglekar and Andrew K Harter. Passive parity-time-symmetry-breaking transitions without exceptional points in dissipative photonic systems. *Photonics Research*, 6(8):A51–A57, 2018.

[25] Heinz-Peter Breuer and Francesco Petruccione. *The Theory of Open Quantum Systems*. Oxford University Press, January 2007.

[26] Brian C. Hall. *Quantum Theory for Mathematicians*. Graduate Texts in Mathematics. Springer-Verlag, New York, 2013.

[27] LD Landau. The damping problem in wave mechanics. *Z. Phys*, 45(63):430–441, 1927.

[28] C. Cohen-Tannoudji, J. Dupont-Roc, G. Grynberg, and P. Thickstun. *Atom-photon interactions: basic processes and applications*. Wiley Online Library, 1992, 2004.

[29] Fabrizio Minganti, Adam Miranowicz, Ravindra W. Chhajlany, and Franco Nori. Quantum exceptional points of non-hermitian hamiltonians and liouvillians: The effects of quantum jumps. *Phys. Rev. A*, 100:062131, Dec 2019.

[30] Stefano Olivares. Quantum optics in the phase space. *The European Physical Journal Special Topics*, 203(1):3–24, 2012.

[31] Crispin Gardiner and Peter Zoller. *Quantum Noise: A Handbook of Markovian and Non-Markovian Quantum Stochastic Methods with Applications to Quantum Optics*. Springer Series in Synergetics. Springer-Verlag, Berlin Heidelberg, 3 edition, 2004.

[32] Bo Peng, Sahin Kaya Ozdemir, Fuchuan Lei, Faraz Monifi, Mariagiovanna Gianfreda, Gui Lu Long, Shanhui Fan, Franco Nori, Carl M. Bender, and Lan Yang. Parity–time-symmetric whispering-gallery microcavities. *Nat. Phys.*, 10(5):394–398, May 2014.

[33] Dennis Dast, Daniel Haag, Holger Cartarius, and Günter Wunner. Quantum master equation with balanced gain and loss. *Phys. Rev. A*, 90(5):052120, November 2014.

[34] Stefano Longhi. Quantum statistical signature of pt symmetry breaking. *Opt. Lett.*, 45(6):1591–1594, Mar 2020.

[35] Kosmas V Kepesidis, Thomas J Milburn, Julian Huber, Konstantinos G Makris, Stefan Rotter, and Peter Rabl. $\mathcal{PT}$-symmetry breaking in the steady state of microscopic gain–loss systems. *New Journal of Physics*, 18(9):095003, sep 2016.

[36] Hoi-Kwan Lau and Aashish A. Clerk. Fundamental limits and non-reciprocal approaches in non-Hermitian quantum sensing. *Nature Communications*, 9(1):4320, October 2018.

[37] Mengzhen Zhang, William Sweeney, Chia Wei Hsu, Lan Yang, A. D. Stone, and Liang Jiang. Quantum noise theory of exceptional point amplifying sensors. *Phys. Rev. Lett.*, 123:180501, Oct 2019.

[38] Yu-Xin Wang and A. A. Clerk. Non-Hermitian dynamics without dissipation in quantum systems. *Phys. Rev. A*, 99(6):063834, June 2019.

[39] Henning Schomerus. Quantum Noise and Self-Sustained Radiation of $\mathcal{PT}$-Symmetric Systems. *Phys. Rev. Lett.*, 104(23):233601, June 2010.

[40] Gwangsu Yoo, H.-S. Sim, and Henning Schomerus. Quantum noise and mode nonorthogonality in non-Hermitian $\mathcal{PT}$-symmetric optical resonators. *Phys. Rev. A*, 84(6):063833, December 2011.

[41] G. S. Agarwal and Kenan Qu. Spontaneous generation of photons in transmission of quantum fields in $PT$-symmetric optical systems. *Phys. Rev. A*, 85(3):031802, March 2012.

[42] Saeid Vashahri-Ghamsari, Bing He, and Min Xiao. Continuous-variable entanglement generation using a hybrid $\mathcal{PT}$-symmetric system. *Phys. Rev. A*, 96(3):033806, September 2017.

[43] S. Longhi. Quantum interference and exceptional points. *Opt. Lett.*, 43(21):5371–5374, November 2018.

[44] Saeid Vashahri-Ghamsari, Bing He, and Min Xiao. Effects of gain saturation on the quantum properties of light in a non-Hermitian gain-loss coupler. *Phys. Rev. A*, 99(2):023819, February 2019.

[45] Jan Peřina, Antonín Lukš, Joanna K. Kalaga, Wiesław Leoński, and Adam Miranowicz. Nonclassical light at exceptional points of a quantum $\mathcal{PT}$-symmetric two-mode system. *Phys. Rev. A*, 100:053820, Nov 2019.

[46] F Klauck, Lucas Teuber, Marco Ornigotti, Matthias Heinrich, Stefan Scheel, and Alexander Szameit. Observation of pt-symmetric quantum interference. *Nature Photonics*, pages 1–5, 2019.

[47] Javid Naikoo, Kishore Thapliyal, Subhashish Banerjee, and Anirban Pathak. Quantum zeno effect and nonclassicality in a $\mathcal{PT}$-symmetric system of coupled cavities. *Phys. Rev. A*, 99:023820, Feb 2019.

[48] Ávila B Jaramillo, C Ventura-Velázquez, Yogesh N Joglekar, BM Rodríguez-Lara, et al. Pt-symmetry from lindblad dynamics in a linearized optomechanical system. *Scientific Reports (Nature Publisher Group)*, 10(1), 2020.

[49] Michael A. Nielsen and Isaac L. Chuang. *Quantum Computation and Quantum Information: 10th Anniversary Edition.* Cambridge University Press, Cambridge ; New York, anniversary edizione edition, 2010.

[50] Samuel L. Braunstein and Peter van Loock. Quantum information with continuous variables. *Rev. Mod. Phys.*, 77(2):513–577, June 2005.

[51] A. McDonald, T. Pereg-Barnea, and A. A. Clerk. Phase-dependent chiral transport and effective non-hermitian dynamics in a bosonic kitaev-majorana chain. *Phys. Rev. X*, 8:041031, Nov 2018.

[52] Harold Ollivier and Wojciech H. Zurek. Quantum Discord: A Measure of the Quantumness of Correlations. *Phys. Rev. Lett.*, 88(1):017901, December 2001.

[53] L. Henderson and V. Vedral. Classical, quantum and total correlations. *J. Phys. A: Math. Gen.*, 34(35):6899–6905, August 2001.

[54] Kavan Modi, Aharon Brodutch, Hugo Cable, Tomasz Paterek, and Vlatko Vedral. The classical-quantum boundary for correlations: Discord and related measures. *Rev. Mod. Phys.*, 84(4):1655–1707, November 2012.

[55] Wanxia Cao, Xingda Lu, Xin Meng, Jian Sun, Heng Shen, and Yanhong Xiao. Reservoir-mediated quantum correlations in non-hermitian optical system. *Phys. Rev. Lett.*, 124:030401, Jan 2020.

[56] A. Ferraro, S. Olivares, and M. G. A. Paris. *Gaussian states in quantum information.* Bibliopolis, 2005.

[57] T. M. Cover and Joy A. Thomas. *Elements of Information Theory.* Wiley-Interscience, Hoboken, N.J, 2 edizione edition, 2006.

[58] Stefano Pirandola, Gaetana Spedalieri, Samuel L. Braunstein, Nicolas J. Cerf, and Seth Lloyd. Optimality of Gaussian Discord. *Phys. Rev. Lett.*, 113(14):140405, October 2014.

[59] Paolo Giorda and Matteo G. A. Paris. Gaussian Quantum Discord. *Phys. Rev. Lett.*, 105(2):020503, July 2010.

[60] Gerardo Adesso and Animesh Datta. Quantum versus Classical Correlations in Gaussian States. *Phys. Rev. Lett.*, 105(3):030501, July 2010.

[61] Gerardo Adesso, Sammy Ragy, and Antony R. Lee. Continuous Variable Quantum Information: Gaussian States and Beyond. *Open Syst. Inf. Dyn.*, 21(01n02):1440001, March 2014.

[62] Gerardo Adesso, Davide Girolami, and Alessio Serafini. Measuring gaussian quantum information and correlations using the rényi entropy of order 2. *Phys. Rev. Lett.*, 109:190502, Nov 2012.

[63] M. S. Kim, W. Son, V. Bužek, and P. L. Knight. Entanglement by a beam splitter: Nonclassicality as a prerequisite for entanglement. *Phys. Rev. A*, 65(3):032323, February 2002.

[64] S. Scheel and A. Szameit. $\mathcal{PT}$-symmetric photonic quantum systems with gain and loss do not exist. *Euro Phys. Lett.*, 122(3):34001, May 2018.

[65] N. Korolkova and G. Leuchs. Quantum correlations in separable multi-mode states and in classically entangled light. *Rep. Prog. Phys.*, 82(5):056001, March 2019.

[66] Francesco Ciccarello and Vittorio Giovannetti. Creating quantum correlations through local nonunitary memoryless channels. *Phys. Rev. A*, 85(1):010102, January 2012.

[67] Xueyuan Hu, Heng Fan, D. L. Zhou, and Wu-Ming Liu. Necessary and sufficient conditions for local creation of quantum correlation. *Phys. Rev. A*, 85(3):032102, March 2012.

[68] Alexander Streltsov, Hermann Kampermann, and Dagmar Bruß. Behavior of Quantum Correlations under Local Noise. *Phys. Rev. Lett.*, 107(17):170502, October 2011.

[69] Francesco Ciccarello and Vittorio Giovannetti. Local-channel-induced rise of quantum correlations in continuous-variable systems. *Phys. Rev. A*, 85(2):022108, February 2012.

[70] Lars S. Madsen, Adriano Berni, Mikael Lassen, and Ulrik L. Andersen. Experimental Investigation of the Evolution of Gaussian Quantum Discord in an Open System. *Phys. Rev. Lett.*, 109(3):030402, July 2012.

[71] Gerardo Adesso, Thomas R. Bromley, and Marco Cianciaruso. Measures and applications of quantum correlations. *J. Phys. A: Math. Theor.*, 49(47):473001, November 2016.

[72] Alexander Streltsov. *Quantum Correlations Beyond Entanglement: and Their Role in Quantum Information Theory.* SpringerBriefs in Physics. Springer International Publishing, 2015.

[73] Mile Gu, Helen M. Chrzanowski, Syed M. Assad, Thomas Symul, Kavan Modi, Timothy C. Ralph, Vlatko Vedral, and Ping Koy Lam. Observing the operational significance of discord consumption. *Nat. Phys.*, 8(9):671–675, September 2012.

[74] Borivoje Dakic, Yannick Ole Lipp, Xiaosong Ma, Martin Ringbauer, Sebastian Kropatschek, Stefanie Barz, Tomasz Paterek, Vlatko Vedral, Anton Zeilinger, Caslav Brukner, and Philip Walther. Quantum discord as resource for remote state preparation. *Nat. Phys.*, 8(9):666–670, September 2012.

[75] Marco Piani, Sevag Gharibian, Gerardo Adesso, John Calsamiglia, Paweł Horodecki, and Andreas Winter. All Nonclassical Correlations Can Be Activated into Distillable Entanglement. *Phys. Rev. Lett.*, 106(22):220403, June 2011.

[76] Gerardo Adesso, Vincenzo D'Ambrosio, Eleonora Nagali, Marco Piani, and Fabio Sciarrino. Experimental Entanglement Activation from Discord in a Programmable Quantum Measurement. *Phys. Rev. Lett.*, 112(14):140501, April 2014.

[77] Alexander Streltsov, Hermann Kampermann, and Dagmar Bruß. Linking Quantum Discord to Entanglement in a Measurement. *Phys. Rev. Lett.*, 106(16):160401, April 2011.

[78] Callum Croal, Christian Peuntinger, Vanessa Chille, Christoph Marquardt, Gerd Leuchs, Natalia Korolkova, and Ladislav Mista. Entangling the Whole by Beam Splitting a Part. *Phys. Rev. Lett.*, 115(19):190501, November 2015.

[79] T. K. Chuan, J. Maillard, K. Modi, T. Paterek, M. Paternostro, and M. Piani. Quantum Discord Bounds the Amount of Distributed Entanglement. *Phys. Rev. Lett.*, 109(7):070501, August 2012.

[80] Christian Peuntinger, Vanessa Chille, Ladislav Mišta, Natalia Korolkova, Michael Förtsch, Jan Korger, Christoph Marquardt, and Gerd Leuchs. Distributing Entanglement with Separable States. *Phys. Rev. Lett.*, 111(23):230506, December 2013.

[81] Christina E. Vollmer, Daniela Schulze, Tobias Eberle, Vitus Händchen, Jaromír Fiurášek, and Roman Schnabel. Experimental Entanglement Distribution by Separable States. *Phys. Rev. Lett.*, 111(23):230505, December 2013.

[82] A. Fedrizzi, M. Zuppardo, G. G. Gillett, M. A. Broome, M. P. Almeida, M. Paternostro, A. G. White, and T. Paterek. Experimental Distribution of Entanglement with Separable Carriers. *Phys. Rev. Lett.*, 111(23):230504, December 2013.

[83] Davide Girolami, Alexandre M. Souza, Vittorio Giovannetti, Tommaso Tufarelli, Jefferson G. Filgueiras, Roberto S. Sarthour, Diogo O. Soares-Pinto, Ivan S. Oliveira, and Gerardo Adesso. Quantum Discord Determines the Interferometric Power of Quantum States. *Phys. Rev. Lett.*, 112(21):210401, May 2014.

[84] Lauren Peters. *Exploring the quantum world*, volume 5. Oxford Univ. Press, Oxford, UK, 2012.

[85] Giuseppe Calajó. *Atom-photon Interactions in slow-light waveguide QED*. PhD thesis, Wien, 2019.

[86] Christopher Gerry, Peter Knight, and Peter L Knight. *Introductory quantum optics*. Cambridge university press, 2005.

[87] S. T. Dawkins, R. Mitsch, D. Reitz, E. Vetsch, and A. Rauschenbeutel. Dispersive optical interface based on nanofiber-trapped atoms. *Phys. Rev. Lett.*, 107:243601, Dec 2011.

[88] Arjan F. van Loo, Arkady Fedorov, Kevin Lalumière, Barry C. Sanders, Alexandre Blais, and Andreas Wallraff. Photon-mediated interactions between distant artificial atoms. *Science*, 342(6165):1494–1496, 2013.

[89] Marco Scigliuzzo, Giuseppe Calajò, Francesco Ciccarello, Daniel Perez Lozano, Andreas Bengtsson, Pasquale Scarlino, Andreas Wallraff, Darrick Chang, Per Delsing, and Simone Gasparinetti. Extensible quantum simulation architecture based on atom-photon bound states in an array of high-impedance resonators. *arXiv preprint arXiv:2107.06852*, 2021.

[90] Francesco Ciccarello. Resonant atom-field interaction in large-size coupled-cavity arrays. *Phys. Rev. A*, 83:043802, Apr 2011.

[91] F. Lombardo, F. Ciccarello, and G. M. Palma. Photon localization versus population trapping in a coupled-cavity array. *Phys. Rev. A*, 89:053826, May 2014.

[92] M. Bello, G. Platero, J. I. Cirac, and A. González-Tudela. Unconventional quantum optics in topological waveguide QED. *Science Advances*, 5(7):eaaw0297, jul 2019.

[93] Eunjong Kim, Xueyue Zhang, Vinicius S. Ferreira, Jash Banker, Joseph K. Iverson, Alp Sipahigil, Miguel Bello, Alejandro González-Tudela, Mohammad Mirhosseini, and Oskar Painter. Quantum electrodynamics in a topological waveguide. *Phys. Rev. X*, 11:011015, Jan 2021.

[94] Eduardo Sánchez-Burillo, Diego Porras, and Alejandro González-Tudela. Limits of photon-mediated interactions in one-dimensional photonic baths. *Phys. Rev. A*, 102:013709, Jul 2020.

[95] János K Asbóth, László Oroszlány, and András Pályi. A short course on topological insulators. *Lecture notes in physics*, 919:997–1000, 2016.

[96] Anton Frisk Kockum. Quantum optics with giant atoms—the first five years. In *International Symposium on Mathematics, Quantum Theory, and Cryptography*, pages 125–146. Springer, Singapore, 2021.

[97] Eleftherios N. Economou. *Green's Functions in Quantum Physics*, volume 7 of *Springer Series in Solid-State Sciences*. Springer Berlin Heidelberg, Berlin, Heidelberg, 2006.

[98] Savannah Garmon, Gonzalo Ordonez, and Naomichi Hatano. Anomalous-order exceptional point and non-markovian purcell effect at threshold in one-dimensional continuum systems. *Phys. Rev. Research*, 3:033029, Jul 2021.

[99] A. González-Tudela and J. I. Cirac. Quantum emitters in two-dimensional structured reservoirs in the nonperturbative regime. *Phys. Rev. Lett.*, 119:143602, Oct 2017.

[100] A. González-Tudela and J. I. Cirac. Non-Markovian Quantum Optics with Three-Dimensional State-Dependent Optical Lattices. *Quantum*, 2:97, oct 2018.

[101] A. González-Tudela, C. L. Hung, D. E. Chang, J. I. Cirac, and H. J. Kimble. Subwavelength vacuum lattices and atom-atom interactions in two-dimensional photonic crystals. *Nature Photonics*, 9(5):320–325, may 2015.

[102] Alejandro González-Tudela and Fernando Galve. Anisotropic Quantum Emitter Interactions in Two-Dimensional Photonic-Crystal Baths. *ACS Photonics*, 2019.

[103] Tao Shi, Ying-Hai Wu, A. González-Tudela, and J. I. Cirac. Bound states in boson impurity models. *Phys. Rev. X*, 6:021027, May 2016.

[104] K Stannigel, P Rabl, and P Zoller. Driven-dissipative preparation of entangled states in cascaded quantum-optical networks. *New Journal of Physics*, 14(6):063014, jun 2012.

[105] Tomás Ramos, Hannes Pichler, Andrew J. Daley, and Peter Zoller. Quantum spin dimers from chiral dissipation in cold-atom chains. *Phys. Rev. Lett.*, 113:237203, Dec 2014.

[106] A. Metelmann and A. A. Clerk. Nonreciprocal photon transmission and amplification via reservoir engineering. *Phys. Rev. X*, 5:021025, Jun 2015.

[107] C. Dembowski, B. Dietz, H.-D. Gräf, H. L. Harney, A. Heine, W. D. Heiss, and A. Richter. Encircling an exceptional point. *Phys. Rev. E*, 69:056216, May 2004.

[108] Tony E. Lee. Anomalous edge state in a non-hermitian lattice. *Phys. Rev. Lett.*, 116:133903, Apr 2016.

[109] Julian Huber, Peter Kirton, Stefan Rotter, and Peter Rabl. Emergence of pt-symmetry breaking in open quantum systems. *SciPost Phys*, 9:052, 2020.

[110] Shunyu Yao and Zhong Wang. Edge states and topological invariants of non-hermitian systems. *Phys. Rev. Lett.*, 121:086803, Aug 2018.

[111] Kazuki Yokomizo and Shuichi Murakami. Non-bloch band theory of non-hermitian systems. *Phys. Rev. Lett.*, 123:066404, Aug 2019.

[112] Liang Feng, Ramy El-Ganainy, and Li Ge. Non-Hermitian photonics based on parity–time symmetry. *Nat. Photonics*, 11(12):752, December 2017.

[113] Stefano Longhi. Parity-time symmetry meets photonics: A new twist in non-Hermitian optics. *Euro Phys. Lett.*, 120(6):64001, December 2017.

[114] Ephraim Shahmoon and Gershon Kurizki. Nonradiative interaction and entanglement between distant atoms. *Phys. Rev. A*, 87:033831, Mar 2013.

[115] J. S. Douglas, H. Habibian, C. L. Hung, A. V. Gorshkov, H. J. Kimble, and D. E. Chang. Quantum many-body models with cold atoms coupled to photonic crystals. *Nature Photonics*, 9(5):326–331, may 2015.

[116] Giuseppe Calajó, Francesco Ciccarello, Darrick Chang, and Peter Rabl. Atom-field dressed states in slow-light waveguide qed. *Phys. Rev. A*, 93:033833, Mar 2016.

[117] A. González-Tudela and J. I. Cirac. Markovian and non-markovian dynamics of quantum emitters coupled to two-dimensional structured reservoirs. *Phys. Rev. A*, 96:043811, Oct 2017.

[118] A. González-Tudela and J. I. Cirac. Exotic quantum dynamics and purely long-range coherent interactions in dirac conelike baths. *Phys. Rev. A*, 97:043831, Apr 2018.

[119] E. Sánchez-Burillo, L. Martín-Moreno, J. J. García-Ripoll, and D. Zueco. Single photons by quenching the vacuum. *Phys. Rev. Lett.*, 123:013601, Jul 2019.

[120] Luca Leonforte, Angelo Carollo, and Francesco Ciccarello. Vacancy-like dressed states in topological waveguide qed. *Phys. Rev. Lett.*, 126:063601, Feb 2021.

[121] Daniele De Bernardis, Ze-Pei Cian, Iacopo Carusotto, Mohammad Hafezi, and Peter Rabl. Light-matter interactions in synthetic magnetic fields: Landau-photon polaritons. *Phys. Rev. Lett.*, 126:103603, Mar 2021.

[122] P. Lambropoulos, Georgios M. Nikolopoulos, Torben R. Nielsen, and Søren Bay. Fundamental quantum optics in structured reservoirs. *Reports on Progress in Physics*, 63(4):455–503, apr 2000.

[123] Yanbing Liu and Andrew A. Houck. Quantum electrodynamics near a photonic bandgap. *Nature Physics*, 13(1):48–52, jan 2017.

[124] Neereja M. Sundaresan, Rex Lundgren, Guanyu Zhu, Alexey V. Gorshkov, and Andrew A. Houck. Interacting qubit-photon bound states with superconducting circuits. *Phys. Rev. X*, 9:011021, Feb 2019.

[125] Marco Scigliuzzo, Giuseppe Calajò, Francesco Ciccarello, Daniel Perez Lozano, Andreas Bengtsson, Pasquale Scarlino, Andreas Wallraff, Per Delsing, and Simone Gasparinetti. Probing nonlinear photon scattering with artificial atoms coupled to a slow-light waveguide. *Bulletin of the American Physical Society*, 2021.

[126] Jonathan D. Hood, Akihisa Goban, Ana Asenjo-Garcia, Mingwu Lu, Su-Peng Yu, E. Chang, and H. J. Kimble. Atom–atom interactions around the band edge of a photonic crystal waveguide. *Proceedings of the National Academy of Sciences*, 113(38):10507–10512, 2016.

[127] Ludwig Krinner, Michael Stewart, Arturo Pazmiño, Joonhyuk Kwon, and Dominik Schneble. Spontaneous emission of matter waves from a tunable open quantum system. *Nature*, 559(7715):589–592, jul 2018.

[128] Michael Stewart, Joonhyuk Kwon, Alfonso Lanuza, and Dominik Schneble. Dynamics of matter-wave quantum emitters in a structured vacuum. *Phys. Rev. Research*, 2:043307, Dec 2020.

[129] Nobuyuki Okuma, Kohei Kawabata, Ken Shiozaki, and Masatoshi Sato. Topological origin of non-hermitian skin effects. *Phys. Rev. Lett.*, 124:086801, Feb 2020.

[130] Stefano Longhi. Spectral singularities in a non-hermitian friedrichs-fano-anderson model. *Phys. Rev. B*, 80:165125, Oct 2009.

[131] Andrea Crespi, Francesco V. Pepe, Paolo Facchi, Fabio Sciarrino, Paolo Mataloni, Hiromichi Nakazato, Saverio Pascazio, and Roberto Osellame. Experimental investigation of quantum decay at short, intermediate, and long times via integrated photonics. *Phys. Rev. Lett.*, 122:130401, Apr 2019.

[132] Richard Phillips Feynman, Robert Benjamin Leighton, and Matthew Sands. *The Feynman lectures on physics; New millennium ed.* Basic Books, New York, NY, 2010. Originally published 1963-1965.

[133] Stefano Longhi, Davide Gatti, and Giuseppe Della Valle. Robust light transport in non-hermitian photonic lattices. *Scientific reports*, 5(1):1–12, 2015.

[134] W. P. Su, J. R. Schrieffer, and A. J. Heeger. Solitons in polyacetylene. *Phys. Rev. Lett.*, 42:1698, Jun 1979.

[135] Tomás Ramos, Benoît Vermersch, Philipp Hauke, Hannes Pichler, and Peter Zoller. Non-markovian dynamics in chiral quantum networks with spins and photons. *Phys. Rev. A*, 93:062104, Jun 2016.

[136] Naomichi Hatano and David R. Nelson. Localization transitions in non-hermitian quantum mechanics. *Phys. Rev. Lett.*, 77:570–573, Jul 1996.

[137] Eduardo Sánchez-Burillo, Chao Wan, David Zueco, and Alejandro González-Tudela. Chiral quantum optics in photonic sawtooth lattices. *Phys. Rev. Research*, 2:023003, Apr 2020.

[138] Martin V Gustafsson, Thomas Aref, Anton Frisk Kockum, Maria K Ekström, Göran Johansson, and Per Delsing. Propagating phonons coupled to an artificial atom. *Science*, 346(6206):207–211, 2014.

[139] A. González-Tudela, C. Sánchez Muñoz, and J. I. Cirac. Engineering and harnessing giant atoms in high-dimensional baths: A proposal for implementation with cold atoms. *Phys. Rev. Lett.*, 122:203603, May 2019.

[140] Stefano Longhi. Photonic simulation of giant atom decay. *Optics Letters*, 45(11):3017–3020, 2020.

[141] Anton Frisk Kockum, Göran Johansson, and Franco Nori. Decoherence-free interaction between giant atoms in waveguide quantum electrodynamics. *Phys. Rev. Lett.*, 120:140404, Apr 2018.

[142] Bharath Kannan, Max J Ruckriegel, Daniel L Campbell, Anton Frisk Kockum, Jochen Braumüller, David K Kim, Morten Kjaergaard, Philip Krantz, Alexander Melville, Bethany M Niedzielski, et al. Waveguide quantum electrodynamics with superconducting artificial giant atoms. *Nature*, 583(7818):775–779, 2020.

[143] Angelo Carollo, Dario Cilluffo, and Francesco Ciccarello. Mechanism of decoherence-free coupling between giant atoms. *Phys. Rev. Research*, 2:043184, Nov 2020.

[144] Xin Wang, Tao Liu, Anton Frisk Kockum, Hong-Rong Li, and Franco Nori. Tunable chiral bound states with giant atoms. *Phys. Rev. Lett.*, 126:043602, Jan 2021.

[145] R. Blatt and P. Zoller. Quantum jumps in atomic systems. *European Journal of Physics*, 9(4):250–256, 1988.

[146] Peter Lodahl, Sahand Mahmoodian, Søren Stobbe, Arno Rauschenbeutel, Philipp Schneeweiss, Jürgen Volz, Hannes Pichler, and Peter Zoller. Chiral quantum optics. *Nature*, 541(7638):473–480, 2017.

[147] Dario Cilluffo, Angelo Carollo, Salvatore Lorenzo, Jonathan A. Gross, G. Massimo Palma, and Francesco Ciccarello. Collisional picture of quantum optics with giant emitters. *Phys. Rev. Research*, 2:043070, Oct 2020.

[148] Lingzhen Guo, Anton Frisk Kockum, Florian Marquardt, and Göran Johansson. Oscillating bound states for a giant atom. *Phys. Rev. Research*, 2:043014, Oct 2020.

[149] Mark Kremer, Tobias Biesenthal, Lukas J Maczewsky, Matthias Heinrich, Ronny Thomale, and Alexander Szameit. Demonstration of a two-dimensional $\mathcal{PT}$-symmetric crystal. *Nature communications*, 10(1):1–7, 2019.

[150] Alexandra S Sheremet, Mihail I Petrov, Ivan V Iorsh, Alexander V Poshakinskiy, and Alexander N Poddubny. Waveguide quantum electrodynamics: collective radiance and photon-photon correlations. *arXiv preprint arXiv:2103.06824*, 2021.

[151] Hadiseh Alaeian, Chung Wai Sandbo Chang, Mehran Vahdani Moghaddam, Christopher M. Wilson, Enrique Solano, and Enrique Rico. Creating lattice gauge potentials in circuit qed: The bosonic creutz ladder. *Phys. Rev. A*, 99:053834, May 2019.

[152] Ali Mostafazadeh. Non-hermitian hamiltonians with a real spectrum and their physical applications. *Pramana*, 73(2):269–277, 2009.

[153] Ali Mostafazadeh. Pseudo-hermitian representation of quantum mechanics. *Int. J. Geom. Methods Mod. Phys.*, 07(07):1191–1306, November 2010.

[154] Fabio Bagarello and Naomichi Hatano. A chain of solvable non-hermitian hamiltonians constructed by a series of metric operators. *Annals of Physics*, 430:168511, 2021.

[155] Ali Mostafazadeh. Pseudo-Hermiticity versus PT-symmetry III: Equivalence of pseudo-Hermiticity and the presence of antilinear symmetries. *Journal of Mathematical Physics*, 43(8):3944–3951, July 2002.

[156] Fabio Bagarello. Construction of pseudobosons systems. *Journal of mathematical physics*, 51(5):053508, 2010.

[157] Fabio Bagarello. Pseudo-bosons, so far. *Reports on Mathematical Physics*, 68(2):175–210, 2011.

[158] Fabio Bagarello. A concise review of pseudobosons, pseudofermions, and their relatives. *Theoretical and Mathematical Physics*, 193(2):1680–1693, 2017.

[159] Natalia Bebiano and João Da Providência. Classes of non-hermitian operators with real eigenvalues. *The Electronic Journal of Linear Algebra*, 21:98–109, 2010.

[160] Mark S Swanson. Transition elements for a non-hermitian quadratic hamiltonian. *Journal of Mathematical Physics*, 45(2):585–601, 2004.

[161] Andreas Fring and Miled H. Y. Moussa. Non-hermitian swanson model with a time-dependent metric. *Phys. Rev. A*, 94:042128, Oct 2016.

[162] Fabio Bagarello, Francesco Gargano, and Salvatore Spagnolo. Two-dimensional non commutative swanson model and its bi-coherent states. *Geometric Methods in Physics, XXXVI*, pages 9–19, 2019.

[163] H. Bateman. On dissipative systems and related variational principles. *Phys. Rev.*, 38:815–819, Aug 1931.

[164] E Celeghini, M Rasetti, and G Vitiello. Quantum dissipation. *Annals of Physics*, 215(1):156–170, 1992.

[165] H. Dekker. Quantization of the linearly damped harmonic oscillator. *Phys. Rev. A*, 16:2126–2134, Nov 1977.

[166] Hans Dekker. Classical and quantum mechanics of the damped harmonic oscillator. *Physics Reports*, 80(1):1–110, 1981.

[167] Herman Feshbach and Yoel Tikochinsky. Quantization of the damped harmonic oscillator. *Transactions of the New York Academy of Sciences*, 38(1 Series II):44–53, 1977.

[168] Chung-In Um, Kyu-Hwang Yeon, and Thomas F George. The quantum damped harmonic oscillator. *Physics Reports*, 362(2-3):63–192, 2002.

[169] Mario Cesar Baldiotti, R Fresneda, and Dmitri Maximovitch Gitman. Quantization of the damped harmonic oscillator revisited. *Physics Letters A*, 375(15):1630–1636, 2011.

[170] Bin Kang Cheng. Extended feynman formula for damped harmonic oscillator with time-dependent perturbative force. *Physics Letters A*, 110(7-8):347–350, 1985.

[171] VK Chandrasekar, M Senthilvelan, and M Lakshmanan. On the lagrangian and hamiltonian description of the damped linear harmonic oscillator. *Journal of mathematical physics*, 48(3):032701, 2007.

[172] S Twareque Ali, Fabio Bagarello, and Jean Pierre Gazeau. Modified landau levels, damped harmonic oscillator, and two-dimensional pseudo-bosons. *Journal of mathematical physics*, 51(12):123502, 2010.

[173] Fabio Bagarello. Dissipation evidence for the quantum damped harmonic oscillator via pseudo-bosons. *Theoretical and Mathematical Physics*, 171(1):497–504, 2012.

[174] Shinichi Deguchi, Yuki Fujiwara, and Kunihiko Nakano. Two quantization approaches to the bateman oscillator model. *Annals of Physics*, 403:34–46, 2019.

[175] F Bagarello and A Fring. Generalized bogoliubov transformations versus d-pseudo-bosons. *Journal of Mathematical Physics*, 56(10):103508, 2015.

[176] Carl M. Bender, Mariagiovanna Gianfreda, Şahin K. Özdemir, Bo Peng, and Lan Yang. Twofold transition in $\mathcal{PT}$-symmetric coupled oscillators. *Phys. Rev. A*, 88:062111, Dec 2013.

[177] Fabio Bagarello and Andreas Fring. Non-self-adjoint model of a two-dimensional noncommutative space with an unbound metric. *Phys. Rev. A*, 88:042119, Oct 2013.

[178] Fabio Bagarello, Francesco Gargano, and Federico Roccati. A no-go result for the quantum damped harmonic oscillator. *Physics Letters A*, 383(24):2836–2838, 2019.

[179] Piero Caldirola. Forze non conservative nella meccanica quantistica. *Il Nuovo Cimento (1924-1942)*, 18(9):393–400, 1941.

[180] E Kanai. On the quantization of the dissipative systems. *Progress of Theoretical Physics*, 3(4):440–442, 1948.

[181] G. Crespo, A. N. Proto, A. Plastino, and D. Otero. Information-theory approach to the variable-mass harmonic oscillator. *Phys. Rev. A*, 42:3608–3617, Sep 1990.

[182] Fabio Bagarello. Weak pseudo-bosons. *Journal of Physics A: Mathematical and Theoretical*, 53(13):135201, 2020.

[183] Fabio Bagarello. Pseudo-bosons and bi-coherent states out of $\mathcal{L}(\mathbb{R}^2)$. In *Journal of Physics: Conference Series*, volume 2038, page 012001. IOP Publishing, 2021.

[184] Hashim A Yamani and Zouhair Mouayn. Supersymmetry of tridiagonal hamiltonians. *Journal of Physics A: Mathematical and Theoretical*, 47(26):265203, 2014.

[185] M Agaoglou, M Fečkan, M Pospíšil, VM Rothos, and H Susanto. Gain–loss-driven travelling waves in pt-symmetric nonlinear metamaterials. *Wave Motion*, 76:9–18, 2018.

[186] Jean-Pierre Antoine and Camillo Trapani. Partial inner product spaces, metric operators and generalized hermiticity. *Journal of Physics A: Mathematical and Theoretical*, 46(2):025204, 2012.

[187] P. Siegl and D. Krejčiřík. On the metric operator for the imaginary cubic oscillator. *Phys. Rev. D*, 86:121702, Dec 2012.

[188] D Krejčiřík, Petr Siegl, Milos Tater, and Joe Viola. Pseudospectra in non-hermitian quantum mechanics. *Journal of mathematical physics*, 56(10):103513, 2015.

[189] Fabio Bagarello, Francesco Gargano, and Salvatore Spagnolo. Bi-squeezed states arising from pseudo-bosons. *Journal of Physics A: Mathematical and Theoretical*, 51(45):455204, 2018.

[190] F Bagarello, F Gargano, S Spagnolo, and S Triolo. Coordinate representation for non-hermitian position and momentum operators. *Proceedings of the Royal Society A: Mathematical, Physical and Engineering Sciences*, 473(2205):20170434, 2017.

[191] Fabio Bagarello and Miloslav Znojil. Nonlinear pseudo-bosons versus hidden hermiticity. *Journal of Physics A: Mathematical and Theoretical*, 44(41):415305, 2011.

[192] Ole Christensen et al. *An introduction to frames and Riesz bases*, volume 7. Springer, 2003.

[193] Shi-Hai Dong. *Factorization method in quantum mechanics*, volume 150. Springer Science & Business Media, 2007.

[194] F. Bagarello. From self-adjoint to non-self-adjoint harmonic oscillators: Physical consequences and mathematical pitfalls. *Phys. Rev. A*, 88:032120, Sep 2013.

[195] Fabio Bagarello. Examples of pseudo-bosons in quantum mechanics. *Physics Letters A*, 374(37):3823–3827, 2010.

[196] Jean-Pierre Gazeau. *Coherent States in Quantum Optics*. Berlin: Wiley-VCH, 2009.

[197] Didier Robert and Monique Combescure. *Coherent states and applications in mathematical physics*. Springer, 2012.

[198] Syed Twareque Ali, Jean-Pierre Antoine, Jean-Pierre Gazeau, et al. *Coherent states, wavelets and their generalizations*, volume 1. Springer, 2000.

# Acknowledgments

Ci sono moltissime persone che vorrei ringraziare per questi tre anni e spero di non dimenticare nessuno.

Prima di tutto vorrei ringraziare il mio advisor Francesco Ciccarello. La cura per i dettagli, la dedizione, l'attenzione per l'essenziale, la capacità di sintesi, solo alcune delle cose che ho avuto l'opportunità di apprendere grazie a lui in questi anni. "Non c'era messo", come si dice. Ringrazio il mio co-advisor Fabio Bagarello, la sua tenacia e passione sono state e sono per me insegnamenti dal valore inestimabile. Ringrazio Massimo Palma. Quando ho avuto bisogno di parlare di questioni importanti ho sempre trovato aperta la sua porta. Un suo pollice in su in chat vale più di mille parole.

Vorrei ringraziare Salvatore Lorenzo. Per i preziosi consigli che sa dare e per le ore passate insieme davanti a Mathematica (tutto quello che so è un sottoinsieme proprio di quello che sa lui). Vorrei anche ringraziare Angelo Carollo. La sua attitudine un po' più matematica è stata spesso per me un ponte utile per arrivare a comprendere concetti che, ahimè, da matematico testone non avrei mai capito. Vorrei ringraziare tutto il gruppo di fisica, per il tempo trascorso insieme e per quello che ho imparato da loro: Bernardo Spagnolo, Davide Valenti, Umberto De Giovannini, Dario Cilluffo (tanto lardo), Luca Leonforte, Luca Innocenti, Roberto Grimaudo, Dario Chisholm, Claudio Pellitteri.

Ringrazio Francesco Gargano (non si è mai visto...) per il supporto ricevuto in questi anni. Insieme al prof. Bagarello abbiamo veramente lavorato (e mangiato) bene. Ringrazio le persone che ho incontrato a ingegneria: Salvatore Triolo, Marco Pavone e Salvatore Spagnolo (che meriterebbe una pagina intera di ringraziamenti...).

Una delle bellezze di questo lavoro è la possibilità di collaborare con persone in ogni parte del mondo e di ogni tipo. Vorrei ringraziare in particolare quelle con cui ho collaborato più attivamente: Giuseppe Calajò, Matteo Brunelli e Gabriel Landi.

Vorrei ringraziare anche Francesco Barra, una nuova compagnia inaspettata in questi ultimi mesi di dottorato. Ringrazio il coordinatore Giuseppe Lazzara per la sua rapidità e prontezza nel comprendere delicate questioni. Vorrei ringraziare anche il dott. Priolo dell'ufficio dottorati per la sua professionalità e puntualità nel risolvere questioni complesse.

I would like to thank Prof. Savannah Garmon and Prof. Miloslav Znojil for having carefully read my work, the valuable advice and their helpful and encouraging comments.

Infine, vorrei ringraziare la mia famiglia: mia mamma Lia e mia zia Alessandra. Non in generale (quello lo sanno e non credo bastino parole). Piuttosto per il loro contributo a questo traguardo. Se sono arrivato fino a qui, se ho potuto studiare per arrivare fino a qui, se ho potuto seguire la mia passione, è in grandissima parte grazie al vostro sostegno, materiale e morale. Mi avete fornito di tutti gli strumenti necessari (tranne la matematica, quella mi sa che ve la devo insegnare io...) per seguire i miei desideri. Senza questo tassello questo non sarebbe possibile.

"Domani parto"

Federico Roccati